PHOTODEGRADATION OF (E)- AND (Z)-ENDOXIFEN: KINETICS, BY-PRODUCTS IDENTIFICATION AND TOXICITY ASSESSMENT

A Thesis
Submitted to the Graduate Faculty
of the
North Dakota State University
of Agriculture and Applied Science

By

Marina Arino Martin

In Partial Fulfillment of the Requirements
for the Degree of
MASTER OF SCIENCE

Major Program:
Environmental and Conservational Sciences

February 2018

Fargo, North Dakota

North Dakota State University
Graduate School

Title

Photodegradation of (E)- and (Z)-Endoxifen in Water by UV-light and Natural Sunlight: Kinetics, Photodegradation By-product, Toxicity Assessment, and Acute Toxicity Study.

By

Marina Arino Martin

The Supervisory Committee certifies that this ***disquisition*** complies with North Dakota State University's regulations and meets the accepted standards for the degree of

MASTER OF SCIENCE

SUPERVISORY COMMITTEE:

Eakalak Khan
Chair

John McEvoy

Thomas DeSutter

Approved:

April 13, 2018
Date

Craig Stockwell
Department Chair

ABSTRACT

Endoxifen is an effective metabolite of tamoxifen, a commonly used chemotherapy drug, and has been detected at the final effluent of a municipal wastewater treatment plant (WWTP). Its presence in the environment could bring negative effects to aquatic lives. This research investigated the use of ultraviolet radiation (253.7 nm) and natural sunlight to photodegrade endoxifen in water and wastewater, the generation of photodegradation by-products (PBPs) and their toxicity. Endoxifen concentration in water was reduced by 99.1% after 35 seconds of UV light generating two toxic PBPs. Experiments in wastewater at UV light doses used for disinfection resulted in reduction of endoxifen by 30 to 71%. Endoxifen concentration in wastewater was reduced by at least 83% after 150 minutes of solar radiation generating eight PBPs. Seven of these PBPs are potentially more toxic than endoxifen itself. Therefore, highly toxic PBPs are potentially generated at WWTPs if endoxifen is present in wastewater.

ACKNOWLEDGMENTS

I would like to thank my advisor Dr. Eakalak Khan for his patience, guidance, and advices during my research at North Dakota State University (NDSU). Without his support and his constant encouragement this research thesis and many other success throughout my graduate study would not have been possible. I am also thankful to Dr. Jayaraman Sivaguru for his invaluable advice and discussion about photodegradation analyses and molecular identification. I would like to take this opportunity to thank Dr. Achintya Bezbaruah for providing me an opportunity to be part of his Graduate Teaching Assistant team. I would like to acknowledge my committee members, Dr. John McEvoy and Dr. Thomas DeSutter, for their continuous support and precious guidance. I am highly obliged to my friends and colleagues for their enormous help along my way as a graduate student.

For my research funding, I would like to thank the Civil and Environmental Engineering Department, the Environmental and Conservational Sciences program, the North Dakota Water Research Institute Fellowship and the Center of Excellence for Hazardous Substance Management, Chulalongkorn University.

I am eternally grateful to my parents and my sister for their continuously encouragement, love, and unconditional support. They all kept me going through the challenging moments as a graduate student. Last, but by no means the least, I would like to thank my husband Daniel Sanchez for his love, understanding, and most of all for never stopping to believe in me.

DEDICATION

To my parents, Jose Maria and Ana Maria, my sister Laura and my husband Daniel Sanchez.

TABLE OF CONTENTS

LIST OF TABLES

LIST OF FIGURES

LIST OF APPENDIX TABLES

LIST OF APPENDIX FIGURES

CHAPTER 1. INTRODUCTION

1.1. Background

During the last decade, the presence of cytostatic drugs in the environment has been a growing concern worldwide. Cytostatic drugs are a group of chemotherapy drugs used to inhibit the proliferation of carcinogenic cells. The abundance of these chemotherapy drugs in the environment is related to their frequency of consumption (Johnson et al., 2013). According to the American Association Cancer Research (2015), breast cancer is the major cancer type among women globally. Among different types of breast cancer, positive endocrine (ER+) breast cancer accounts for 60-70% of all cases (Jager et al., 2012). Patients with ER+ breast cancer commonly receive selective estrogen receptor modulators (SERMs) as chemotherapy treatment (Peng et al., 2009) . SERMs block estrogen receptors in carcinogenic cells, inhibiting their proliferation (Negreira et al., 2015). By definition, SERMs are chemotherapy treatments cataloged as cytostatic drugs.

In the last 40 years, tamoxifen has been the most widely used chemotherapy drug to treat and prevent ER+ breast cancer (Hoskins et al., 2009; Johnson et al., 2004; Negreira et al., 2015). Furthermore, it is used as a preventive treatment for women with high-risk of breast cancer (Fisher et al., 2005). The effectiveness of tamoxifen for patients diagnosed with breast cancer relies on an ability of the liver to actively metabolize the drug by cytochrome P450 enzymes to endoxifen (Zhang et al., 2015). The major metabolite resulting from tamoxifen conversion is the *trans* isomer Z-endoxifen, or commonly called endoxifen (Jaremko et al., 2010). However, (Z)-endoxifen easily suffer *cis* isomerization to (E)-endoxifen (Elkins et al., 2014). Although both isomers present antiestrogenic activity, (Z)-endoxifen is considered the isomer responsible for the inhibition of breast cancer cell proliferation due to its higher antiestrogenic ability (Jaremko et al., 2010).

Despite the fact endoxifen is an effective treatment for breast cancer, it presents possible consequences on the environment (Goverment of Canada, 2015). Endoxifen is not completely metabolized in human body and is actively excreted (Kisanga et al., 2005). As a result, endoxifen is released to the water environment via wastewater treatment plants (WWTPs) (Negreira et al., 2014). Data on the actual concentrations of endoxifen in the environment is limited. Several studies reported the presence of tamoxifen in the level of ng L^{-1} to μg L^{-1} in surface water and wastewater (Ashton et al., 2004; Coetsier et al., 2009; Goverment of Canada, 2015; Lara-Martín et al., 2014; Roberts and Thomas, 2006; Thomas and Hilton, 2004). Studies reporting endoxifen concentration in water are even fewer than tamoxifen, probably due to the recent discovery of endoxifen pharmaceutical activity. However, tamoxifen and endoxifen present a similar chemical and molecular structure, which suggests a similar fate. Endoxifen has been detected in hospital effluents and wastewater, but there is no data on endoxifen concentration in the environment (Evgenidou et al., 2015).

Although the presence of endoxifen in water bodies could bring negative effects to the environment, there has been only one study on this issue (Borgatta et al., 2015). Similar to other pharmaceutical compounds (PhCs), endoxifen is considered an environmental micropollutant (Evgenidou et al., 2015). However, toxicology studies have been focused mainly on tamoxifen. The antiestrogenic activity of tamoxifen produces negative effects when it is present in the environment, affecting the fish reproduction and physiology (Maradonna et al., 2009). Because endoxifen is 30-100 times more potent than tamoxifen (Jager et al., 2012) and presents antiestrogenic activity (Goverment of Canada, 2015; Johnson et al., 2004), it is important to determine the acute toxicity of endoxifen in water and its potential effect on aquatic lives.

Regardless of the lack of information about the toxicity of endoxifen, as a pharmaceutical compound, there is a need to eliminate it from water and wastewater.

Several techniques can be applied in wastewater treatment plants to eliminate endoxifen. Among these techniques, photodegradation with UV light (253.7 nm) has demonstrated to be a highly efficient method to eliminate PhCs in wastewater (Challis et al., 2014). Previous laboratory bench-scale studies using low-pressure (LP) mercury lamps emitting UV light at 253.7 nm reported an efficient elimination of PhCs in water (Pereira et al., 2007; Prados-Joya et al., 2011; Rivas et al., 2010). The elimination of PhCs by UV light should produce photodegradation by-products (PBPs) that are less toxic than their parents compounds (Larson and Befenbaum, 1988). However, the identification and the toxicity assessment of potential PBPs need to be investigated before actual applications of the process. LP mercury lamps (253.7 nm) are also commonly used in UV disinfection process at WWTPs. However, the UV light doses applied at WWTPs are lower than those applied for photodegradation. Because the use of UV light as a disinfection process at WWTPs has gained more attention during the last decade (Guo et al., 2009), it might be interesting to determine the photodegradability of endoxifen in wastewater at light doses similar to those applied at WWTPs.

Another cost-effective technique commonly used in WWTPs to enhance the elimination of organic compounds is the discharge of the final effluent into lagoon systems (Gros et al., 2015; Li et al., 2013) where photodegradation by natural sunlight irradiation is one of the key removal processes for organic micropollutants such as PhCs (Garcia-Rodríguez et al., 2014). A previous study by Wang and Wang (2016) demonstrated that endocrine disrupting compounds absorb solar radiation due its molecular structure. Therefore, photodegradability of endoxifen by natural sunlight needs to be investigated in order to consider solar radiation as a potential cost-effective

treatment to eliminate (E)- and (Z)-endoxifen from wastewater. Photodegradation by natural sunlight is one of the main transformation processes occurring in natural water bodies (Koumaki et al., 2015). In order to understand the fate of (E)-and (Z)-endoxifen in wastewater and receiving surface water, it is important to identify the generation of potential PBPs and their toxicity when endoxifen is exposed to natural sunlight.

1.2. Research objectives

The proposed research has the following objectives:

- To investigate the suitability of LP mercury lamps emitting UV light at 253.7 nm to remove (E)- and (Z)-endoxifen from water
- To determine the effects of pH, light intensity and initial (E)- and (Z)-endoxifen concentrations on the photodegradation kinetics and efficiency
- To examine the role of hydroxyl radicals on the photodegradation of (E)- and (Z)-endoxifen
- To determine the photodegradability of (E)- and (Z)-endoxifen at UV light doses similar to those applied at WWTPs.
- To investigate the ability of UV light to mineralize (E)- and (Z)-endoxifen.
- To examine the suitability of natural sunlight to photodegrade (E)- and (Z)-endoxifen in water, wastewater, and receiving surface water.
- To identify the main PBPs of (E)- and (Z)-endoxifen
- To assess the toxicity of PBPs in the aquatic environment.
- To determine the acute toxicity of (E)- and (Z)-endoxifen in water with *Daphnia magna* as a test organism.

1.3. Hypotheses

The proposed research has the following hypotheses:

- (E)- and (Z)-endoxifen are photodegradable by UV light at 253.7 nm and natural sunlight.
- Photodegradation kinetics and efficiency of (E)- and (Z)-endoxifen by UV light at 253.7 nm are affected by pH, light intensity and initial concentrations of (E)- and (Z)-endoxifen.
- Photodegradation with UV light at 253.7 nm results in minimal mineralization of (E)- and (Z)-endoxifen.
- (E)- and (Z)-endoxifen are not or minimally photodegraded by UV light at doses commonly used for disinfection in WWTPs.
- Photodegradation of (E)- and (Z)-endoxifen by UV light and natural sunlight results in PBPs that are less toxic than the parent compounds.
- (E)-and (Z)-endoxifen are toxic to *Daphnia magna* at the level of μg L^{-1} in water.

1.4. Scope of study

Photodegradability of (E)- and (Z)-endoxifen by UV light (253.7 nm) in water is investigated. The effects of pH between 5 and 9, light intensity between 28 and 224 W s^{-1} cm^{-2}, and initial concentrations of (E)- and (Z)-endoxifen between 0.5 and 2 μg mL^{-1} on photodegradation kinetics are examined. The role of hydroxyl radical during photodegradation reaction is determined by the addition of isopropyl alcohol (1%) and benzoic acid (50 mg L^{-1}) as hydroxyl radical quenchers. Photodegradation of (E)- and (Z)-endoxifen by UV light (253.7 nm) is investigated at light doses used for disinfection in WWTPs such as 16, 30 and 97 mJ cm^{-2}. Photodegradability of (E)- and (Z)-endoxifen in water exposed to natural sunlight is also

investigated. The formations of PBPs of (E)- and (Z)-endoxifen are identified by ultra-high performance-tandem mass spectrometry (UHPLC-MS/MS). The potential toxicity of PBPs in the aquatic environment is assessed by modeling using the Toxicity Estimator Software Tool (TEST) developed by USEPA (2016). The acute toxicity of (E)-and (Z)-endoxifen in water was investigated using an arthropod, *Daphnia magna*, as a test organism.

1.5. Anticipated results and benefits

The research results will elucidate the abilities of UV light (253.7 nm) and sunlight to degrade (E)- and (Z)-endoxifen. Identification of potential (E)- and (Z)-endoxifen by-products and the estimation of their toxicity in the aquatic environment will demonstrate the suitability of UV light (253.7 nm) and sunlight as (E)- and (Z)-endoxifen treatment processes. An effective treatment technique for (E)- and (Z)-endoxifen would be useful in reducing their release to the aquatic environment and in turn potential toxicological effects on aquatic lives or even humans. Identification of the acute toxicity of (E)- and (Z)-endoxifen in water will lead to a better understanding of the potential environmental effect that endoxifen could cause. Elucidating the fate of (E)- and (Z)-endoxifen in wastewater and receiving surface water will lead to a better understanding on potential sources of the compounds and their PBPs in the aquatic environment.

CHAPTER 2. LITERATURE REVIEW

2.1. General background

Tamoxifen is the most widely used chemotherapy drug to treat and prevent ER+ breast cancer (Hoskins et al., 2009; Johnson et al., 2004; Negreira et al., 2015). Tamoxifen inhibits the tumor growth through its affinity to bind to estrogen receptor in cells, inhibiting cancer cells proliferation (Helland et al., 2015; Negreira et al., 2015). In addition, the ability of tamoxifen to mimic the endocrine system has also shown effective results for infertility treatment, gynecomastia, and bipolar disorder (Steiner et al., 2005). However, in order to be effective, tamoxifen needs to be metabolized by cytochrome P450 enzymes (CYP2D6 and CYP3A4/5) present in the human liver (Fauq et al., 2010). There are two routes for the generation of the active metabolite, endoxifen; tamoxifen undergoes demethylation to form N-desmethyl tamoxifen and followed by hydroxylation, or hydroxylation to 4-hydroxy-tamoxifen and then demethylation (Figure 1) (Ahmad et al., 2010; Zhang et al., 2015). Endoxifen is mainly formed through hydroxylation of N-desmethyl-tamoxifen and to a lesser extent by through demethylation of 4-hydroxy-tamoxifen (Figure 1).

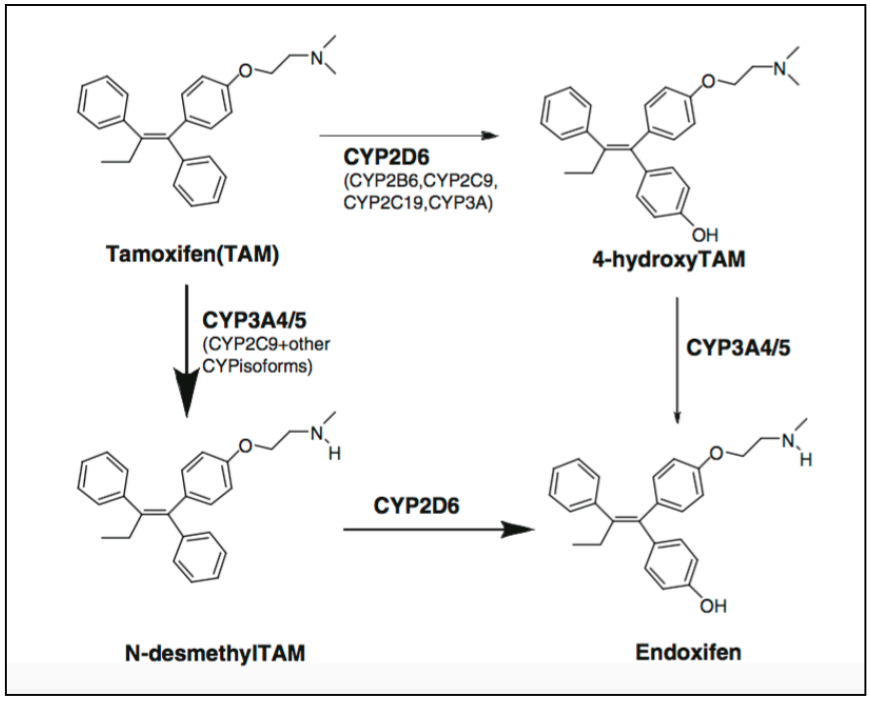

Figure 1. Metabolism of tamoxifen to the active metabolite endoxifen through cytochrome P450 enzyme (Ahmad et al., 2010).

Endoxifen is the metabolite responsible for treatment effectiveness (Goverment of Canada, 2015). Besse et al. (2012) stated that endoxifen is 30 to100 times more potent and active than the parent compound. Accordingly, the anti-estrogenic ability of endoxifen is 30 to 100 folds greater than tamoxifen, but its anti-estrogenic activity relies on its ability to target and degrade estrogen receptor (Wu et al., 2009). The enzymatic transformation of tamoxifen to endoxifen is crucial for effective results (Helland et al., 2015), but a significant number of women present genetic polymorphism of CYP2D6 (Ahmad et al., 2010), resulting in the inability to metabolize tamoxifen to endoxifen. In addition, the concomitant administration of serotonin reuptake inhibitor, a complementary treatment to avoid hot flushes as a side effect of tamoxifen in 45% of patients, inhibits the activity of CYP2D6 (Ahmad et al., 2010; Binkhorst et al., 2011). As a consequence, several patients under tamoxifen treatment are not able to obtain optimal results (Ahmad et al., 2010). Because endoxifen shows independence from CYP2D6 action, it has been administered

directly to patients and has shown promising results (Ahmad et al., 2010). According to the Mayo Foundation for Medical Education and Research (2014), a clinical trial in phase I has shown that endoxifen presents an anti-tumor activity and is safe for patients. A clinical trial phase II is being conducted by the National Cancer Institute with an estimated completion date in May 2017 (National Institute of Health, 2015). Based on these clinical trials, endoxifen is a promising therapeutic agent to treat ER+ breast cancer (Ahmad et al., 2010).

Endoxifen, directly administered or as tamoxifen metabolite, does not suffer posterior metabolization in the human body (Negreira et al., 2014). As a result, endoxifen and unmetabolized tamoxifen are both actively excreted by patients (Negreira et al., 2014). A study by Kisanga et al. (2005) showed that patients under oral chemotherapy treatment of radio-labeled tamoxifen excreted 63% of the drug to municipal sewage during the following 10 days. The excreted tamoxifen was exclusively detected in feces while endoxifen was excreted via urine (Kisanga et al., 2005).

The excreted tamoxifen and endoxifen end up in WWTPs and consequently in surface waters receiving the WWTP effluent discharge (Borgatta et al., 2015). Several studies have detected tamoxifen in wastewater influent and effluent and surface water at a concentration range from 4 ng L^{-1} to 369 ng L^{-1} (Ashton et al., 2004; Coetsier et al., 2009; Goverment of Canada, 2015; Lara-Martín et al., 2014; Roberts and Thomas, 2006; Thomas and Hilton, 2004). However, the actual concentration of endoxifen in wastewater and natural water bodies has been poorly documented (Borgatta et al., 2015). The lack of technology and the know-how to measure endoxifen in laboratories are handicaps in order to determine its concentration in wastewater and surface water (Heath et al., 2016; Kovalova et al., 2012). Ferrando-Climent et al. (2013) detected

but did not quantify endoxifen in two hospital wastewater samples, while a study by Negreira et al. (2014) reported a concentration of 96 ng L^{-1} of endoxifen in a wastewater effluent sample.

2.2. Endoxifen detection methods

Micellar liquid chromatographic procedure, liquid chromatography-mass spectrometry (LC-MS), and ultra-high performance liquid chromatography tandem mass spectrometry (UHPLC-MS/MS) have been commonly used to detect and quantify tamoxifen and endoxifen in human plasma, blood, and scalp hair (Antunes et al., 2015; Aranda et al., 2011; Binkhorst et al., 2011; Drooger et al., 2015; Heath et al., 2016). However, these methods require expensive equipment limiting routine analyses (Binkhorst et al., 2011). A more economical method used to identify and quantify endoxifen in human blood samples was liquid chromatography with a fluorescence detector (LC-FLD) (Aranda et al., 2011). The ability of tamoxifen to form a fluorescence phenanthrene nucleo within its structure after UV irradiation suggest a similar behavior for endoxifen (Mendenhall et al., 1978). The potential formation of a phenanthrene nucleo after irradiation of endoxifen with UV light makes LC-diode array detector (DAD) a suitable method to detect and quantify endoxifen in blood (Aranda et al., 2011). However, samples needed irradiation for 20 minutes with UV light, making it a lengthy process (Aranda et al., 2011).

Negreira et al. (2014) quantified endoxifen for the first time in wastewater samples. An automated on line solid-phase extraction-liquid chromatography-tandem mass spectrometry (SPE-LC-MS/MS) was used to determine several cytostatic drugs in wastewater samples. Endoxifen was detected only in one water sample at a concentration of 96 ng L^{-1} while tamoxifen was the most frequently detected drug in all samples with values ranging from 102-181 ng L^{-1}. These concentrations mimic the concentrations present in blood of administered patients. The concentration ratio of tamoxifen and endoxifen in blood of patients under tamoxifen treatment is

about 2:1 (Helland et al., 2015). Therefore, the concentration of endoxifen obtained by Negreira et al. (2014) was close to the expected concentration (96 ng L^{-1} is approximately half of 181 ng L^{-1}). However, endoxifen was found in only one sample which does not allow a statistical analysis. This single detection can be explained because the method was developed to detect a large number of drugs instead of focusing exclusively on endoxifen. Therefore, the method by Negreira et al. (2014) must be refined in order to obtain better results for endoxifen detection.

A cost-effective method able to detect and quantify analytes in the presence of other compounds is high performance liquid chromatography coupled with DAD (HPLC-DAD) (Teunissen et al., 2010). This method allows the identification of peak purity by spectra comparison (Pragst et al., 2004). Therefore, HPLC-DAD is a potential method to identify endoxifen in wastewater and natural water samples where other compounds are present. Furthermore, the identification and separation of endoxifen isomers through HPLC-DAD were previously reported by Elkins et al. (2014). Successful separation and resolution of (E)- and (Z)-endoxifen were observed during isomer characterization using a phenyl-hexyl column. Therefore, HPLC-DAD could be a technology to determine the concentrations of endoxifen isomers in wastewater and receiving water bodies which are required to develop proper environmental risk assessments (Ferrando-Climent et al., 2013).

2.3. Toxicity of endoxifen

The available information to develop an environmental risk assessment of endoxifen is very limited. Potential effects of endoxifen in aquatic organisms have been poorly studied (Borgatta et al., 2015). However, several studies have focused on the ecological effect of tamoxifen (Government of Canada, 2015). Tamoxifen, as other endocrine disruptor compounds, has shown significant alteration in the sex ratio of exposed zebrafish (*Danio rerio*) at a low critical toxicity

value (CTV) of 510 ng L^{-1} (Knacker et al., 2010; Liu et al., 2010; Singh, 2013; van der Ven et al., 2007) and modifications of gonadotropin expression in frogs at a concentration of 3.2 µg L^{-1}(Urbatzka et al., 2007). A study by Borgatta et al. (2015) showed a reproductive decline and mortality of *Daphnia pulex* exposed to tamoxifen metabolites, including endoxifen. The study showed an increase of sensitivity during the second generation, resulting in a significant decline of the population growth. Further long-term studies are needed in order to determine the chronic toxicity of endoxifen to aquatic organisms. Furthermore, the actual aquatic Predicted No Effect Concentration (PNEC) of tamoxifen is 51 pg mL^{-1}, and it is considered applicable to endoxifen due to the lack of toxicology studies focused on endoxifen (Goverment of Canada, 2015). This suggested same PNEC is questionable because endoxifen is a 100-fold more potent antiestrogen than tamoxifen. Similar chemical and physical properties of endoxifen and tamoxifen suggest a similar fate (Borgatta et al., 2015) and therefore the potential release of endoxifen into the water environment presents a potential harm to aquatic lives (Government of Canada, 2015).

2.4. Chemical and physical properties of endoxifen

Endoxifen (Phenol, 4-(1-(4-(2-(methylamino)ethoxy)phenyl)-2-phenyl-1-butenyl)) is a relatively new polyaromatic hydrocarbon with registered CAS number 110025-28-0, crystalline solid with an off-white to pink solid color (TRC, 2016). The molecular weight is 373.48738 g/mol with a molecular formula $C_{25}H_{27}NO_2$. Three different isomers have been identified for endoxifen: (E)-endoxifen, (Z)-endoxifen (endoxifen) and (Z´)-endoxifen (Figure 2) (Jaremko et al., 2010). The major metabolite resulting from tamoxifen conversion is (Z)-endoxifen, or commonly called endoxifen, which presents 30 to 100-fold greater activity than tamoxifen. In the event of N-desmethyl-tamoxifen (Z-ND-Tam) hydroxylation at the para-benzene ring, the resulting metabolite is (Z')-endoxifen without anti-estrogenic activity reported (Jaremko et al., 2010). (E)-

endoxifen (*cis*-isomer) is formed by non-enzymatic conversion of Z-endoxifen due to protonation and further deprotonation of the ethylene core by the electro-donating phenolic group (Jaremko et al., 2010). The (E)-isomer presents less estrogenic activity than (Z)-endoxifen and its concentration in human plasma is lower (Jaremko et al., 2010). However, the presence of (E)-endoxifen in the environment could also bring detrimental effects due to its estrogenic activity.

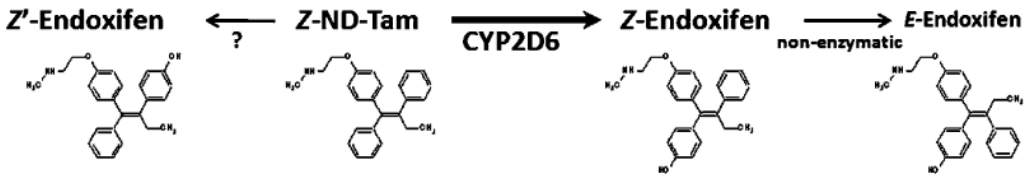

Figure 2. Isomerization of endoxifen (Jaremko et al., 2010).

The modeled physical and chemical properties of endoxifen that are relevant to its environmental fate are presented in Table 1 (Government of Canada, 2015). Briefly, the modeled vapor pressure is very low while its Henry's law constant is high (Government of Canada, 2015). These values suggest a minimal volatilization when endoxifen is released to water. The high modeled octanol-water partition coefficient of endoxifen suggests that it is potentially bioacumulate in aquatic life. However, further experimental analyses are needed in order to corroborate the values obtained by modeling. According to Government of Canada (2015), modeled data for degradation of endoxifen in water showed a half-life value greater or equal to 182 days. This value suggests that endoxifen is potentially a persistent organic pollutant in water. Therefore, these physical and chemical properties of endoxifen together with its potential toxicity in the aquatic environment, bring an urgent need to find effective techniques to eliminate endoxifen from water.

Table 1. Physical and chemical properties of endoxifen

Property	Type	Value	Temperature (°C)
Melting point (ºC)	Model	212.4	
Boiling point (ºC)	Model	501.85	
Vapor pressure (Pa)	Model	4.32×10^{-9}	25
Henry's law constant ($Pa \cdot m^3/mol$)	Model	2.16×10^{-9}	25
Log K_{ow} (dimensionless)	Model	5.61	
Log K_{oc} (dimensionless)	Model	6.56	
Water solubility ($mg\ L^{-1}$)	Model (estimated from K_{ow})	2.79	25
Water solubility ($mg\ L^{-1}$)	Model (estimated from fragments)	2.19	25
pKa (dimensionless)	Model	10.36 (acid) 9.4 (base)	
Log D (dimensionless)	Model	3.74	

*Source: Government of Canada, 2015
Abbreviations:
Kow: Octanol-water partition coefficient
Koc: Organic carbon-water partition coefficient
pKa: Acid dissociation constant
D: Distribution coefficient taking into account the presence of ionic species; represents a net amount of the neutral and ionic forms expected to partition into the lipid or organic carbon phases at a given pH

2.5. Potential treatment methods for endoxifen in water

Several studies reported the uses of advanced treatment processes to eliminate PhCs in water (Heberer, 2002; Heberer et al., 2002; Hu et al., 2017). However, information about removal of cytostatic drugs is limited and there have been no studies on treatment of endoxifen in water (Franquet-Griell et al., 2017).

2.5.1. Photodegradation of endoxifen by UV light

The use of direct UV photolysis to remove xenobiotic compounds from water is a cost-effective method that does not require the addition of hazardous chemicals making it an environmental friendly process (Zhang et al., 2017). Although UV photolysis is an effective treatment method, it may not be enough to eliminate certain xenobiotic compounds. For treatment of these compounds, a combination of advanced oxidants (sometimes with a catalyst) such as UV + hydrogen peroxide, UV + ozone, and UV + persulfate (Shemer et al., 2006). However, the elimination of xenobiotic compounds by direct photolysis is a chemical-free technology that does not influence the aesthetical quality of the treated water (Zhang et al., 2017). Compared with other oxidation processes, the use of UV light is expected to produce less toxic by-products (Fatta-Kassinos et al., 2011; Zhang et al., 2017). Photodegradation with UV light has shown to be an effective treatment method to remove PhCs from water (Challis et al., 2014). The presence of aromatic rings and conjugated π bonds in the molecule structure of some PhCs results in a great absorption of UV-C light (100-280 nm). The absorption of UV-C light by the molecule itself led to the degradation of PhCs (Challis et al., 2014). Endoxifen has three aromatic rings and a conjugated π bond, its photodegradation by UV light irradiation is a potential effective treatment method.

The direct photolysis of PhCs depends on the absorption spectra of the molecule (Trawiński and Skibiński, 2017). PhCs usually have a maximum absorbance of light at wavelengths below 280 nm (Mathon et al., 2016). Likewise, endoxifen has a light absorbance region between 220 and 340 nm with a maximum absorption around 240 nm (Teunissen et al., 2010). This maximum absorption wavelength suggests that UV-C (100-280 nm) light is potentially an effective light source to photodegrade endoxifen through direct photolysis. The wavelength produced by UV lamps is directly related to the mercury vapor pressure present inside the lamp (USEPA, 2003). Low pressure (LP) and medium pressure (MP) mercury UV lamps are the most common types of UV lamps used for UV photodegradation in water (Pereira et al., 2007). As shown in Figure 3, LP lamps emit a mono-chromatic wavelength at 253.7 nm while MP lamps emit a broad spectrum of UV light in a wavelength range of 205 to above 500 nm (USEPA, 2003).

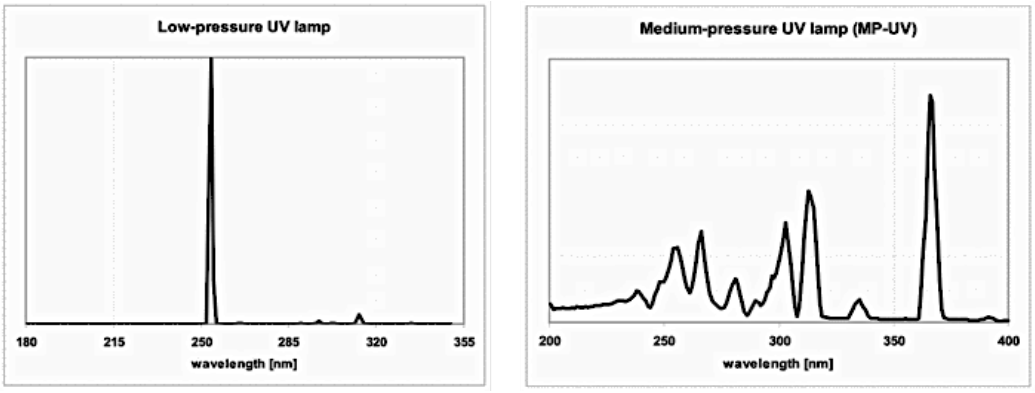

Figure 3. Wavelength spectrum for LP lamps and MP (bestUV, 2011).

In addition to the light energy source, several factors could influence the photodegradation of endoxifen in water. The pH of solution, the emission light intensity, the initial concentration, and quantum yield are important parameters to consider for photodegradation (Pereira et al., 2007; Udom et al., 2014). Quantum yield is the ratio of photodegraded molecules per photon absorbed

(Trawiński and Skibiński, 2017). If quantum yield is constant, photolysis rate of endoxifen will depend only on the number of photons absorbed by the molecule (Tønnesen, 2004). However, the presence of organic and inorganic molecules in water such as those in wastewater samples could vary the photolysis rate of endoxifen (Trawiński and Skibiński, 2017).

WWTPs with UV light as a disinfection process commonly use LP lamps as UV light source. LP lamps have demonstrated their ability to degrade PhCs efficiently in wastewater samples through direct photolysis using a light dose of 100 mJ cm^{-2} (Oppenländer, 2003; Pereira et al., 2007). However, light doses used during WWTPs disinfection process are lower than those used to photodegrade a specific target compound. Little is known about the fate of endoxifen in WWTPs with UV light as a disinfection process.

2.5.2. Photodegradation of endoxifen by natural sunlight

The use of lagoon systems at WWTPs has also demonstrated to be an effective treatment method to remove organic compounds from wastewater (Gros et al., 2015). WWTPs with lagoon system discharge the effluent to wide and shallow ponds where treated wastewater is exposed to natural sunlight and microbial degradation for long retention times ranging from 7 to 20 days (Hoque et al., 2014). Among the different degradation mechanisms occurring in lagoon systems, photodegradation by natural sunlight irradiation has been as a key removal process for organic micropollutants (Garcia-Rodríguez et al., 2014). Organic micropollutants are sometimes resistant to bacterial biodegradation and their elimination at WWTPs is associated with abiotic processes such as photodegradation (Andreozzi et al., 2003; Luo et al., 2014; Radjenović et al., 2009; Yamamoto et al., 2009). Photodegradation by natural sunlight radiation is a potential treatment method to eliminate emerging organic micropollutants commonly found in wastewater (Wang et al., 2017). However, environmental conditions highly influence photodegradation efficiency due

to seasonal variations on sunlight duration and light intensity (Gruchlik et al., 2018). Koumaki et al. (2015), demonstrated that the calculated half-life of naproxen in summer increased by 34% in winter due to low sunlight intensity during the winter period in Athens, Greece. As shown in Figure 4, the intensity of sunlight radiation varies for summer and winter at latitudes of the earth where a notable difference of climate is observed between the summer and winter seasons such as Greece (Koumaki et al., 2015). This environmental variability explains why most of the studies focused on sunlight photodegradation of organic micropollutants have been performed under controlled artificial sunlight (Andreozzi et al., 2003; Boreen et al., 2004; Clara et al., 2011; Lam and Mabury, 2005; Lin and Reinhard, 2005; Rivera-Utrilla et al., 2013).

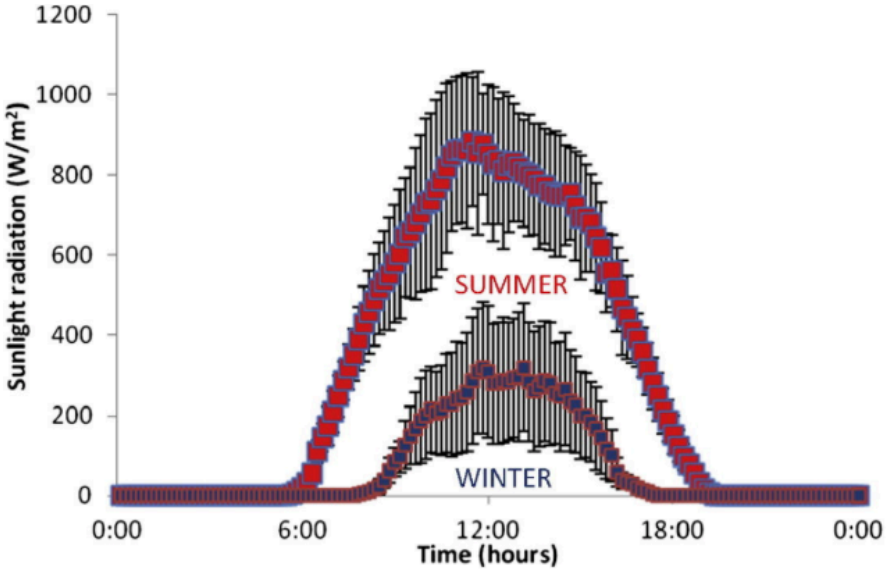

Figure 4. Average of daily sunlight radiation (W/cm^2) in summer and winter seasons in Athens, Greece (Koumaki et al., 2015).

Among the few studies on photodegradation by natural sunlight, the photodegradation of endocrine disrupting compounds has been poorly documented (Gruchlik et al., 2018). However, it is well known that endocrine disrupting compounds absorb solar radiation due its molecular structure. Wang et al. (2017) demonstrated the ability of natural sunlight irradiation to remove 2,4-

dichlorophenoxyacetic acid, an endocrine disrupting compound commonly found in wastewater. However, there have been no studies on endoxifen photodegradation by natural sunlight either in wastewater or water. Because photodegradation by natural sunlight is one of the main transformation processes occurring in water bodies (Koumaki et al., 2015), it is important to determine the fate of endoxifen and the potential PBPs formed during its photodegradation by natural sunlight when wastewater and receiving water are exposed to sunlight.

2.6. Fate of endoxifen in WWTPs

The detection of endoxifen in wastewater effluents questions the treatment efficiency of WWTPs. There has been only one study on endoxifen removal process in WWTPs. Negreira et al. (2015) showed how chlorination process in ultrapure water and wastewater results in an ineffective degradation of endoxifen. Thirteen chlorinated by-products of endoxifen were formed after two minutes of reaction (Negreira et al., 2015). The toxicity assessment of the resultant disinfection by-products (DBPs) showed a low concentration for the predicted LC_{50} value for crustacean and fish categorizing them as hazardous to the aquatic environment. Therefore, the inefficient degradation of endoxifen and the production of hazardous DBPs during wastewater disinfection process bring an urgent need for further research particularly on endoxifen removal.

The use of UV light as a disinfection process at WWTPs has gained more attraction (Guo et al., 2009). It should produce less toxic DPBs than disinfection through chlorination process (Larson and Befenbaum, 1988). However, the light doses used at WWTPs are low compare to those applied for photodegradation. According to EPA, (2002), small WWTPs (3.8 to 76 m^3 day^{-1}) that use UV light (253.7 nm) for disinfection need a minimum UV light dose of 16 mJ cm^{-2} in order to meet the standard fecal coliform for secondary effluent (200 CFU per 100 mL). WWTPs with filtered nitrified secondary effluents use a minimal UV light dose of 30 mJ cm^{-2} (Shin et al.,

2001) while conventional WWTPs with activated sludge process use a minimal UV light dose of 97 mJ cm^{-2} (Darby et al., 1993). Although these light intensities are low, it might be interesting to determine if endoxifen photodegradation by UV disinfection takes place in WWTPs. Identifying the fate of endoxifen in WWTPs will led to a better understanding of endoxifen removal and release to receiving waters.

CHAPTER 3. MATERIALS AND METHODS

3.1. Materials

3.1.1. Chemicals

A mixture of (E/Z)-endoxifen (1:1, w/w) was purchased from AdooQ Bioscience (Irvine, CA, USA). (Z)-endoxifen isomer was purchased from MedChem Express (Monmouth Junction, NJ, USA). Water, acetonitrile, methanol, and benzoic acid all of them HPLC-grade, and sulfuric acid and eriochrome red 3B azo dye, both reagent grade, were supplied by VWR (Chicago, IL, USA). Iron(III) sulfate, potassium oxalate monohydrate, sodium acetate trihydrate, hydroxylamine hydrochloride and 1,10-phenanthroline, all of them analytical grade, and HPLC-grade ammonium formate (>99.99%) were purchased from Sigma-Aldrich (St Louis, MO, USA).

3.2. Experimental framework

Figure 5 summarizes the experimental framework.

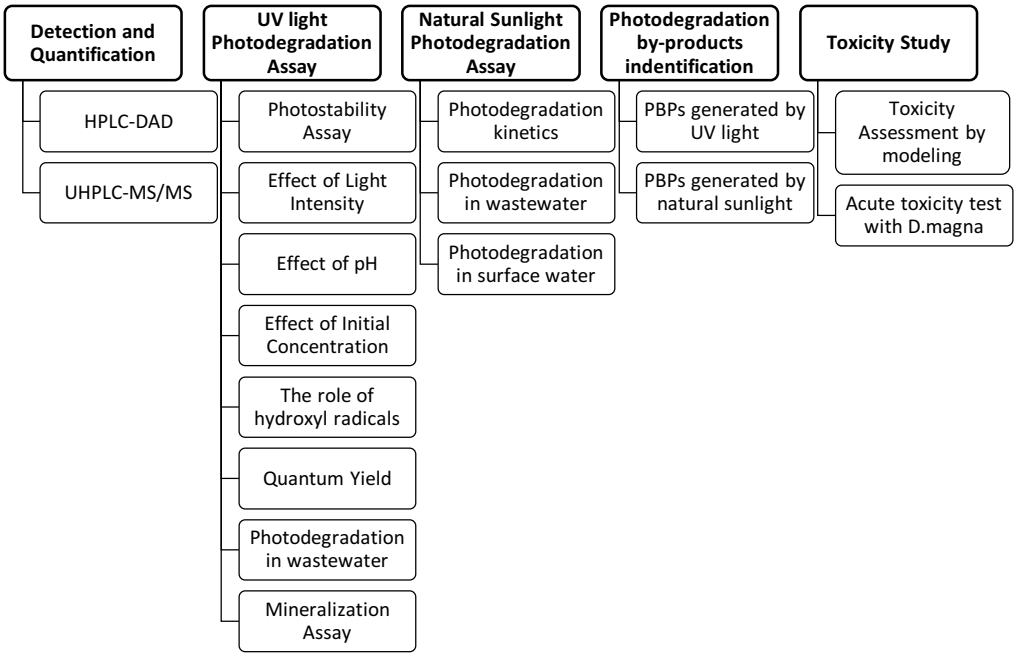

Figure 5. Experimental framework

3.3. Methods

3.3.1. Preparations of (E)- and (Z)-endoxifen stock solutions

Stock solutions of (E)- and (Z)-endoxifen were prepared in a mixture of water and methanol (10:1, v/v) at 1 mg ml^{-1} and kept at -20°C. Standard samples for analytical calibration were obtained by diluting the stock solution in HPLC water to desired concentrations. For photodegradation experiments, water samples directly spiked with (E)-and (Z)-endoxifen were prepared daily.

3.3.2. Detection and quantification of endoxifen and its photodegradation by-products

3.3.2.1 Detection and quantification of endoxifen by HPLC-DAD

The concentrations of (E)- and (Z)-endoxifen in the water samples were analyzed using a HPLC (AGILENT® 1620 Poroshell 120 Phenyl-Hexyl Column 2.7 μm, 4.6 mm × 100 mm, 60±0.8°C) with a DAD. The isocratic mobile phase was a mixture of HPLC-grade acetonitrile and ultrapure water (50:50 v/v) containing 10 mM ammonium formate (pH 3.4). The isocratic mobile flow was 0.3 mL min^{-1} with a constant injection volume of 50 μL. An absorbance 3D plot analysis showed the optimum absorbance wavelength of (E)- and (Z)-endoxifen at a wavelength of 244 nm (Appendix A, Figure A.1). The described HPLC-DAD method was validated according to the International Council of Harmonization (ICH) guidelines for selectivity, linearity, sensitivity, accuracy, and precision (ICH, 2005) (Results in Appendix A). The data was processed by LC Chemstation software.

3.3.2.1.1. Selectivity

Blank water and wastewater samples and spiked with (E)- and (Z)-endoxifen at 2 μg mL^{-1} were analyzed for peak detection by HPLC-DAD. The absence of co-elution impurities was determined by comparing the resultant chromatograms (Appendix A, Figure A.2). Selectivity was

confirmed by successfully separating the analytes from possible impurities found in water and wastewater samples.

3.3.2.1.2. (E)- and (Z)-endoxifen retention times

The identifications of (E)- and (Z)-endoxifen isomers retention times were determined by spiking water samples with only (Z)-endoxifen isomer at 1 μg mL^{-1} and analyzed for retention time by HPLC-DAD. According to (Elkins et al., 2014), the major observed peak at the resultant chromatogram was (Z)-endoxifen while the minor peak was (E)-endoxifen (Appendix A, Figure A.3). Eighteen water samples spiked with a mixture of (E)- and (Z)-endoxifen at 1 μg mL^{-1} were analyzed in triplicate by HPLC-DAD. Chromatogram peaks with retention times of 9.24±0.3 minutes and 10.03±0.4 minutes corresponded to (E)- and (Z)-endoxifen, respectively.

3.3.2.1.3. Linearity and sensitivity

Nine standard samples for analytical calibration were prepared by combining aliquots of the stock solution with the proper volume of water to obtain standard samples with (E)- and (Z)-endoxifen (1:1, w/w) concentrations in the range of 25 to 500 ng ml^{-1} per isomer. The calibration was performed in triplicate. The resultant chromatograph peak areas were correlated with the known concentration using a linear regression analysis (significance level p = 0.95) (Appendix A, Figure A.4). Coefficient of determination (R^2) was calculated for (E)- and (Z)-endoxifen isomers and was greater than 0.997 for both isomers (Appendix A, Table A.1). The limit of detection (LOD) and limit of quantification (LOQ) were calculated based on the slopes and the standard deviation of the response using the following equations (ICH, 2005):

$$LOD = \frac{3.3\sigma}{S} \quad (1)$$

$$LOQ = \frac{10\sigma}{S} \quad (2)$$

Where: σ = standard deviation of the response; and S= slope of the calibration curve.

3.3.2.1.4. Accuracy and precision

Quality control (QC) samples were prepared for within-day and inter-day assays by combining aliquots of the stock solution with the proper volume of water to obtain three standard samples with the following concentrations of (E)- and (Z)-endoxifen: 100 ng mL^{-1} for the quality control low (QCL), 350 ng mL^{-1} for the quality control medium (QCM), and 700 ng mL^{-1} for quality control high (QCH). Five replicates of each QC sample were prepared individually to analyze the precision and accuracy of the HPLC-DAD method. Within-day assay was calculated by injecting five times each QC sample during the same day and inter-day assay was calculated by injecting each QC sample for five consecutive days. The accuracy was presented as percent coefficient of variation (CV, %) while precision was calculated as percent deviation of the sample consistency (RSD) (Appendix A, Table A.2). The method was considered accurate and precise when CV and RSD values were below 15%.

3.3.2.2. Photodegradation by-products identification by UHPLC-MS/MS

The molecular structure of PBPs were identified using UHPLC-MS/MS (ACQUITY UPLC® BEH C18 column 17 µm, 100 mm × 2.1 mm, 25°C) with a mixture of acetonitrile and 10 mM ammonium formate solution (1:1, v/v), both HPLC-grade, as a mobile phase. The isocratic flow rate was 0.26 mL min^{-1} and the sample injection volume was 5 µL. The mass range analyzed was between 50 and 1000 Da. The assessment of mass measurement error (Δm) in ppm was performed for detected compounds. Total analytical run was 5 minutes with retention times of 1.67±0.04 minutes and 1.79±0.05 minutes for (E)- and (Z)-endoxifen, respectively (Appendix D, Figure D.2). (E)- and (Z)-endoxifen were observed at the ion-m/z = 374.21 with Δm within less than 3.74 ppm (Appendix D, Figure D.3). Chromatography peaks showing different ion-*m/z* values and retention times than (E)- and (Z)-endoxifen were determined as potential PBPs. These PBPs

were analyzed with Tandem Quadrupole Mass spectrometry (MS/MS) with an electrospray ionization (ESI) source and operated at a positive mode (Collison energy = 27 V). Data and potential molecular composition were analyzed through MassLynk V4.1 SCN627 software.

3.3.3. Photodegradation with UV light

3.3.3.1. Experimental setup and procedure

Laboratory-scale photodegradation experiments were performed in a RPR-200 Rayonet™ photoreactor (Southern New England Ultraviolet Company, Brandfort, UK), equipped with a cooling fan to keep the photoreactor temperature at 23-25°C (Figure 6). The photoreactor was equipped with sixteen 14W low-pressure mercury lamps emitting UV light at 253.7 nm. The emitted light intensity (14 W/lamp) was determined by the lamp manufacturer (Southern New England Ultraviolet Company, n.d.). The light intensity was regulated by controlling the number of lamps in the photoreactor. Photodegradation experiments were performed using 10 mL quartz test tubes (ACE Glass incorporate, Vineland, NJ, USA) filled with 5 mL of the sample. The pH was adjusted with either 1 M HCl or 1 M NaOH. The quartz tubes were placed vertically at a fixed distance of 3.5 inches from the lamp in a rotary merry-go-round at 5 rpm. Sample aliquots were collected in 2 mL HPLC amber vial (VWR, Chicago, IL, USA) with time and analyzed for endoxifen and PBPs using HPLC-DAD and/or UHPLC-MS/MS.

According to Elkins et al. (2014), (Z)-endoxifen isomer suffer *trans* isomerization to (E)-endoxifen isomer under certain conditions. In this study, the direct dilution of (Z)-endoxifen in water results in an immediate *trans* isomerization to (E)-endoxifen. Likewise, (E)-endoxifen in aqueous solution suffered an immediate *cis* isomerization to (Z)-endoxifen. (E)- and (Z)-endoxifen present estrogenic activity in water but the third isomer (Z')-endoxifen has no estrogenic activity reported and is not a potential risk to the environment (Jaremko et al., 2010). Therefore,

photodegradation experiments were conducted using a mixture of (E)- and (Z)-endoxifen (1:1, w/w).

Figure 6. RPR-200 Rayonet™ photoreactor (Source: Southern New England Ultraviolet Company, Brandfort, UK).

3.3.3.2. Method standardization

Procedures for photodegradation of (E)- and (Z)-endoxifen by UV light (253.7 nm) in a Rayonet photochamber were standardized with eriochrome red 3B azo dye decoloration as described by Elmorsi et al. (2010). In order to simulate the incident photonic flux of 87.6 μEin L^{-1} used by Elmorsi et al. (2010), a HPLC water sample containing eriochrome red 3B azo dye at 22.32 mg L^{-1} (pH 3 and 24.3°C) were irradiated in triplicate by UV light at an emission light intensity of 56 W s^{-1} cm^{-2} for 18 seconds. One milliliter aliquots were collected with time and decolorization of the dye were quantitatively measured though a spectrophotometer (Cari 7000, Agilent, Santa clara, CA, USA.) based on a decrease in absorbance at a wavelength of 492 nm. Control samples (dark condition) were run in parallel for 18 seconds.

3.3.3.3. Optimization of photodegradation kinetics and efficiency

3.3.3.3.1 Effect of UV light intensity

Photodegradation kinetics and efficiency of (E)- and (Z)-endoxifen were tested at the following UV light intensities in triplicate: 28 W s^{-1} cm^{-2} (2 lamps), 56 W s^{-1} cm^{-2} (4 lamps), 112 W s^{-1} cm^{-2} (8 lamps), 168 W s^{-1} cm^{-2} (12 lamps), and 224 W s^{-1} cm^{-2} (16 lamps). Water samples directly spiked with a mixture of (E)- and (Z)-endoxifen (1:1, w/w) at 2 μg mL^{-1} were exposed to UV light (253.7 nm). The water samples were irradiated for 80 seconds at 28 W s^{-1} cm^{-2}, 60 seconds at 56 W s^{-1} cm^{-2}, 45 seconds at 112 W s^{-1} cm^{-2}, and 30 seconds at 168 and 224 W s^{-1} cm^{-2}. At certain time intervals, 1 mL aliquots were collected and analyzed for endoxifen concentration by HPLC-DAD. Controls samples in dark condition ran in parallel for 80 seconds.

3.3.3.3.2. Effect of initial pH

Water samples directly spiked with a mixture of (E)- and (Z)-endoxifen (1:1, w/w) at 2 μg mL^{-1} were irradiated in triplicate at a constant UV light intensity of 28 W s^{-1} cm^{-2} for 80 seconds. Initial pH of the samples was varied at 5, 6, 7, 8, and 9. The pH adjustment was performed by using 1 M HCl or 1 M NaOH. One milliliter aliquots were collected every 10 seconds and analyzed for (E)- and (Z)-endoxifen concentrations by HPLC-DAD. The first order rate constant (k) was calculated for each isomer. The pH after the irradiation was also recorded.

3.3.3.3.3. Effect of initial concentration

Effect of initial concentrations of (E)- and (Z)-endoxifen (0.5, 1, and 2 μg mL^{-1}) on the photodegradation kinetic and efficiency was tested in triplicate. Water samples directly spiked with the desired concentrations of (E)- and (Z)-endoxifen were irradiated at a constant UV light intensity of 224 W s^{-1} cm^{-2} for 30 seconds. One milliliter aliquots were collected every 5 seconds and analyzed for (E)- and (Z)-concentration by HPLC-DAD.

3.3.3.3.4. Effect of light source

Photodegradation of (E)- and (Z)-endoxifen was tested under three different light sources in triplicate: sun light (May 31, 2017, 1:00 PM, Fargo, ND, USA, GPS coordinate: 46.895128, -96.801131), indoor light (F15T8/CW 15 W T8 cool white fluorescent bulb), and UV light (253.7 nm and emission light intensity of 224 W s^{-1} cm^{-2}). Ten milliliter quartz test tubes filled with 5 mL of water directly spiked with (E)- and (Z)-endoxifen at 2 μg mL^{-1} and pH 7 were irradiated for 1 minute. Controls were run in the dark in parallel. One milliliter aliquots of water samples exposed to UV light were collected every 5 seconds while aliquots of water samples exposed to sunlight and indoor lamp were collected every 15 seconds. The collected samples were analyzed for (E)- and (Z)-endoxifen using HPLC-DAD.

3.3.3.4. The role of hydroxyl radicals

The oxidation of (E)- and (Z)-endoxifen by hydroxyl radicals generated during UV photodegradation was investigated. Isopropyl alcohol (IPA) and benzoic acid (BA) were added to water samples to quench hydroxyl radicals generated by UV light (253.7 nm) (Jo et al., 2017; Wu et al., 2015). Water samples with IPA (1%, v/v), with BA (50 mg L^{-1}), and without IPA and BA, all of them directly spiked with (E)- and (Z)-endoxifen at 2 μg mL^{-1} were irradiated by UV light (253.7 nm) at a constant light intensity of 224 W s^{-1} cm^{-2} for 30 seconds. The experiment was conducted in triplicate. Controls (dark condition) were included. One milliliter aliquots were collected with time and analyzed for (E)- and (Z)-endoxifen concentrations by HPLC-DAD.

3.3.3.5. Molar extinction coefficient of (E/Z)-endoxifen

The molar extinction coefficient (ε) of (E/Z)-endoxifen was determined at a wavelenght of 253.7 nm using a UV-Vis spectophotometer (Cari 7000, Agilent, Santa clara, CA, USA.) Aborbance (253.7 nm) was measured in triplicate for water samples directly spiked with (E/Z)-

endoxifen at the following concentrations: 0.375, 0.7, 1.4, 2.8 an 5 μg mL^{-1}. The observed absorbance values were plotted versus (E/Z)-endoxifen concentrations and the resultant slope (0.1097 mM^{-1} cm^{-1}) revealed the molar extinction coefficient of (E/Z)-endoxifen (Appendix C, Figure C.1). The molar extintion coefficient is a indispensable parameter to calculate quantum yield (Φ) in order to determine the photolysis efficiency (Jin et al., 2017).

3.3.3.6. Quantum yield, incident light intensity and light dose

Quantum yield (Φ) was calculated by the ferroxilate actinometer method (Bolton et al., 2011). Briefly, iron(III) sulfate solution (0.2 M) was prepared in H_2SO_4 solution (2 N) and storage in the dark. Ferroxilate solution (6 mM) for the determination of quantum yield was prepared in a 1,000-mL volumetric flask containing 800 mL deionized water added with 15.2 mL of potassium oxalate solution (1.2 M) and 35 mL of H_2SO_4 solution (2 N). The solution was mixed well and 15.23 mL of the previously prepared iron(III) sulfate solution was added. Ferroxilate samples were prepared in the dark to avoid photolysis of the ferroxilate.The iron(III) percentage for the ferroxilate solution (21.72%) was calculated using the Beer-Lambert law equation:

$$A = C \varepsilon l \quad (3)$$

Where: A = absorbance of the iron (III) sulfate solution at 302 nm; C = concentration of iron (III) (M); ε = molar extintion coefficient of iron (III) (2,196 M^{-1} cm^{-1} at 25°C); and l = path lenght (cm^{-1}).

Photoreaction of the ferroxilate solution was performed exactly as the photodegradation experiemnts of (E)- and (Z)-endoxifen. The ferroxilate solutions were irradiated in triplicate at four emission light intensities (56, 112, 168, and 224 W s^{-1} cm^{-2}) for 60 seconds. After that, one mililiter aliquots were adeed to 10-mL volumetric flasks containing 164 mg of sodium acetate trihydrate and 0.4 mg of 1,10-phenantroline. Dionized water was adeed to the 10 mL mark and the

flasks were kept in the dark for 1 hour. The solution was then transfered into a quartz cuvette and the absorbance at 502 nm was read (Appendix C, Figure C.2). Unirradiated samples (controls in the dark) were included). The mole of Fe^{2+} formed in the ferroxilate solutions was determined spectrophophotometrically by using the following equation:

$$\text{moles of } Fe^{2+} = \frac{[A_{510}(\text{sample}) - A_{510}(\text{blank})] \times V_1 \times V_2}{\varepsilon\ Fe^{2+}\text{-o-phenantroline} \times 1{,}000 \times V_3} \quad (4)$$

Where: A = absorbance (510 nm); V_1 = volume of the complexation solution (10 mL); V_2 = volume collected from the irradiated sample (1 mL); ε Fe^{2+}-o-phenantroline = molar extintion coefficient of Fe^{2+}-o-phenantroline complex (11,110 M^{-1} cm^{-1}); and V_3 = volume of the irradiated sample (5 mL)

Photon irradiance (E_p) (Einstein^{-1} cm^{-2} min^{-1}) at each emission light intensity was calculated using the following equation:

$$E_p = \frac{\text{moles } Fe^{2+}}{\Phi Fe^{2+}_{(254nm)} \times \text{Area} \times t} \quad (5)$$

Where: $\Phi Fe^{2+}_{(254\ nm)}$ = 1.25 (mol Einstein^{-1}); Area = quartz test tube area (2.54 cm^2); and t = irradiation time (1 min).

Photon irradiance gave information about the number of photons reaching the water sample in mol Einstein^{-1}. The application of the appropriated conversions units (1 Einstein $_{(254\ nm)}$ = 47,0954.74 W s^{-1}) allowed the calculation of the incident light intensity (mW s^{-1} cm^{-2}), and light dose (mJ cm^{-2}) was calculated using the following formula:

Light dose = Incident light intensity × Irradiation time

Quantum yield (Φ) (mole Einstein^{-1}) at each emission light intensity was calculated using the following formula:

$$\Phi = \frac{k}{2.303 E_p \times \varepsilon_{(253.7nm)}} \quad (6)$$

Where: k = first order reaction of (E)- and (Z)-endoxifen (M min^{-1}); E_p = photon irradiance (Einstein^{-1} cm^{-2} min^{-1}); and $\varepsilon_{(254nm)}$ = molar extinction coefficient of (E)- and (Z)-endoxifen at 257.3 nm (0.1097 mM^{-1} cm^{-1}).

3.3.3.7. Photodegradation experiments in wastewater

Photodegradation experiments of (E)- and (Z)-endoxifen were performed in secondary treated (high purity oxygen activated sludge and moving bed bioreactor) wastewater samples collected from the Moorhead WWTP, MN, USA. The wastewater sample was filtered through a 0.45 μm pore-size cellulose acetate membrane filter (Whatman, Pittsburgh, PA, USA). Total organic carbon (TOC) of the wastewater was determined using a UV/persulfate oxidation TOC analyzer (Phoenix 8000, Tekmar Dohrmann, OH, USA). Nitrite and nitrate concentrations were analyzed using the nitrite TNT840 plus vial test and nitrate TNT835 plus vial test, respectively (HACH, Loveland, CO, USA).

Two experiments were conducted with wastewater samples using UV light, one to determine the photodegradation kinetics of (E)- and (Z)-endoxifen in wastewater and the other to simulate photodegradation of (E)- and (Z)-endoxifen at light doses used in WWTPs disinfection process. For both experiments, wastewater was directly spiked with (E)- and (Z)-endoxifen isomers at 1 μg mL^{-1} and control samples were run parallel in the dark to determine the presence of side reactions that could reduce the concentration of (E)- and (Z)-endoxifen in the sample. To determine the photodegradation kinetics of (E)- and (Z)-endoxifen, wastewater samples were irradiated in triplicate with an emission light intensity of 56 W s^{-1} cm^{-2} for 45 seconds. One

milliliter aliquots were collected with time and analyzed for (E)- and (Z)-endoxifen concentrations by HPLC-DAD.

For the second experiment, wastewater samples were irradiated at a UV light intensity of 56 W s^{-1} cm^{-2} (Incident light intensity = 2.77 mW s^{-1} cm^{-2}) for 6, 11, and 35 seconds in order to simulate the minimal UV light doses applied at WWTPs of 16, 30 and 97 mJ cm^{-2} respectively. One milliliter aliquots were collected at the specified time points and analyzed for (E)- and (Z)-endoxifen concentrations by HPLC-DAD. The potential molecular structures of observed PBPs at 35 seconds were identified by UHPLC-MS/MS following the previously described method.

3.3.3.8. Mineralization of (E)- and (Z)-endoxifen by UV light

Mineralization of (E)- and (Z)-endoxifen was examined in a HPLC water sample directly spiked with a mixture of (E)- and (Z)-endoxifen (1:1, w/w) at 2 µg mL^{-1} and exposed to UV light (253.7 nm) at 224 W s^{-1} cm^{-2} for 60 and 120 minutes. Two aliquots of one and forty milliliters were collected with time. The one milliliter aliquots were directly injected to UHPLC-MS/MS in order to determine the presence of endoxifen and/or its PBPs. With the aim to detect neutral and small molecular weight molecules the aforementioned UHPLC-MS/MS detection method (Section 3.3.2.2) was slightly modified. The following gradient program was employed to improve detection: 1 minute, 100% mobile phase A (10 mM ammonium formate); 3 minutes, 50% mobile phase A and 50% mobile phase B (acetonitrile and 10 mM ammonium formate). The total analytical run was 7 minutes with retention times of 5.11 minutes and 5.34 minutes for (E)- and (Z)-endoxifen, respectively. The forty milliliters aliquots were analyzed for total organic carbon (TOC) through an UV/persulfate oxidation TOC analyzer (Phoenix 8000, Tekmar Dohrmann, OH, USA). The experiment was conducted in triplicate and dark control samples were run in parallel.

3.3.4. Photodegradation with natural sunlight

3.3.4.1 Experimental setup and procedure

Photodegradation experiments with natural sunlight were performed using 30 mL quartz test tubes (ACE Glass incorporate, Vineland, NJ, USA) filled with 20 mL of water sample spiked with a mixture of (E)- and (Z)-endoxifen (1:1, w/w). The pH was adjusted to 7 with either 1 M HCl or 1 M NaOH. The quartz tubes were placed vertically and exposed to natural sunlight in a sunny day for 180 minutes. Sunlight intensity was measured every 30 minutes using a digital light meter (Goer Tex Digital Luxmeter Illuminance Meter, Goer Tex electronic, Sunnyvale, California). One milliliter aliquots were collected with time in a 2 mL HPLC amber vials (VWR, Chicago, IL, USA) and analyzed for endoxifen and PBPs using HPLC-DAD and/or UHPLC-MS/MS.

3.3.4.2. Photodegradation kinetics and efficiency

Photodegradation kinetic of (E)- and (Z)-endoxifen were tested in HPLC water samples spiked with a mixture of (E)- and (Z)-endoxifen at 2 $\mu g\ mL^{-1}$ for each isomer. The water samples were exposed to natural sunlight (September 27, 2017, 9:00 AM, Fargo, ND, USA, GPS coordinate: 46.895122, -96.800208) for 180 minutes. At defined time intervals, sample aliquots were collected and directly analyzed for endoxifen concentration and the presence of PBPs using HPLC-DAD and/or UHPLC-MS/MS.

3.3.4.3. Photodegradation experiments in wastewater and surface water samples

Photodegradation of (E)- and (Z)-endoxifen was tested in secondary treated wastewater samples (high purity oxygen activated sludge and moving bed bioreactor processes) collected from the Moorhead WWTP, MN, USA and in surface water samples collected at the discharging point of the Moorhead WWTP in the Red River, MN, USA, (GPS Coordinate: 46.890486, -96.771859).

Both samples were filtered through a 0.45 μm pore-size cellulose acetate membrane filter (Whatman, Pittsburgh, PA, USA) and analyzed for TOC, nitrite, and nitrate as previously described for photodegradation experiments with UV light in wastewater samples (section 3.2.4.5).

The collected water samples were directly spiked with (E)- and (Z)-endoxifen isomers at 2 μg mL^{-1} and exposed to natural sunlight (October 7, 2017, 11:00 AM, Fargo, ND, USA, GPS Coordinates: 46.895373, -96.800200) for 180 minutes. One milliliter aliquots were collected with time and analyzed for (E)- and (Z)-endoxifen concentrations by HPLC-DAD. The presence of PBPs was determined by UHPLC-MS/MS as previously described. The experiments were conducted in triplicate and control samples (dark condition) were run in parallel.

3.3.5. Toxicity assessment

The toxicity of (E)-endoxifen, (Z)-endoxifen, and the potential PBPs were assessed using the Toxicity Estimator Software Tool (TEST) developed by (USEPA, 2016). TEST is a mathematical model that predicts the biological activity of analytes based on their molecular structures through Quantitative Structure Activity Relationships (QSAR) analyses (USEPA, 2016). The consensus method was selected because it provides the average of five QSAR methodologies giving the best toxicology approach. Among the different toxicology analysis offered by TEST, the calculation of the 50 % Lethal Concentration (LC_{50}) acute end-points of the crustacean *Daphnia magna* (48 h) and the fish fathead minnow (96 h) were selected as recommended by Negreira et al. (2015) as suitable species for an aquatic toxicity assessment.

3.3.6. Acute toxicity test

The acute toxicity of endoxifen was determined by the calculation of the acute end-points of *Daphnia magna* after 48 h incubation in a water solution spiked with a mixture of endoxifen isomers. The tested concentrations were determined based on prior modelling results of *D.magna*

acute end-points (LC_{50}) (obtained from the previously described toxicity assessment experiment). Five different concentrations of the isomeric endoxifen mixture were tested in triplicate: 11.60, 5.80, 2.90, 1.45, and 0.73 μg mL^{-1}. The toxicity test was carried out at the Prairie Waters Education Research Center, Valley City State University (Valley city, ND, USA). Briefly, 200 mL of water enriched with $MgSO_4$ (60 mg L^{-1}), $NaHCO_3$ (96 mg L^{-1}), KCl (4 mg L^{-1}) and $CaSO_4$ (60 mg L^{-1}) at pH 7 were spiked with the corresponding concentration of endoxifen isomers and placed in a beaker for 48 hours. Eight *D. magna* arthropods were added to each flask and the mortality was recorded every 24 hours. Control samples of enriched water without endoxifen were run in parallel.

3.3.7. Statistical analysis

Statistical analysis of data was performed by the analysis of variance (ANOVA) using Minitab 1.7. The significance of the independent variables (light intensity, pH, initial endoxifen concentration, and IPA addition) was evaluated for (E)- and (Z)-photodegradation rate in water with a 95% level of confidence using the Tukey test. The significance criterion is $p < 0.05$.

CHAPTER 4. RESULTS AND DISCUSSION

4.1. Photodegradation with UV light

4.1.1. Photodegradation standardization method

Eriochrome red 3B azo dye solution were lightly photodegraded by direct photolysis and resulted in dye decolorization of less than 4% after irradiation with UV light (253.7 nm) in a Rayonet photochamber with an incident photonic flux of 87.6 μE L^{-1} (Figure 7). Similar results were reported by Elmorsi et al. (2010) where a hardly photodegradation of eriochrome 3B azo dye was also observed after its irradiation with UV light (253.7 nm and incident photonic flux of 1.46 μE L^{-1} m^{-1}) for 60 minutes (Figure 8). Therefore, the proposed UV light bench scale procedure used to determine (E)- and (Z)-endoxifen photodegradation was standardized with a previous study demonstrating the validity of the data generated by this assay.

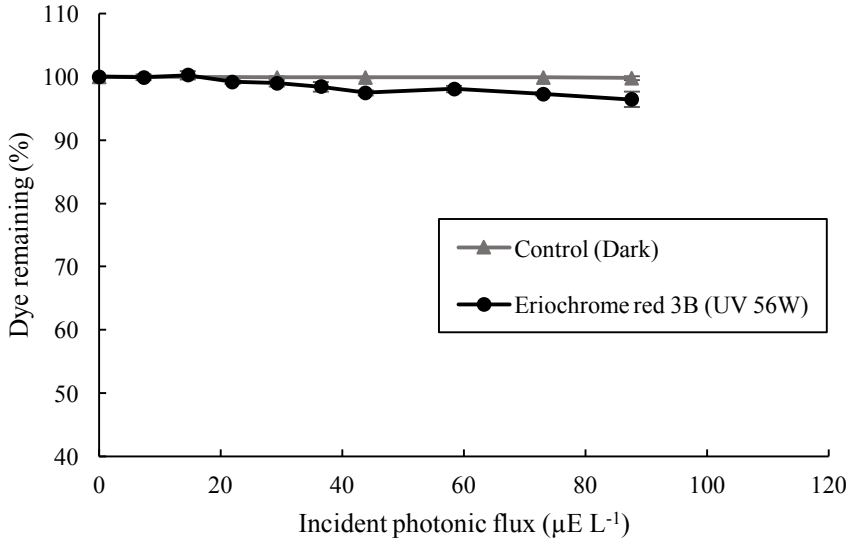

Figure 7. Photodegradation of eriochrome red 3B azo dye in a HPLC water solution at 22.32 mg L^{-1} (pH 3 and 24.3°C) by UV light (253.7 nm) at 56 W cm^{-1} s^{-1} in a Rayonet photochamber.

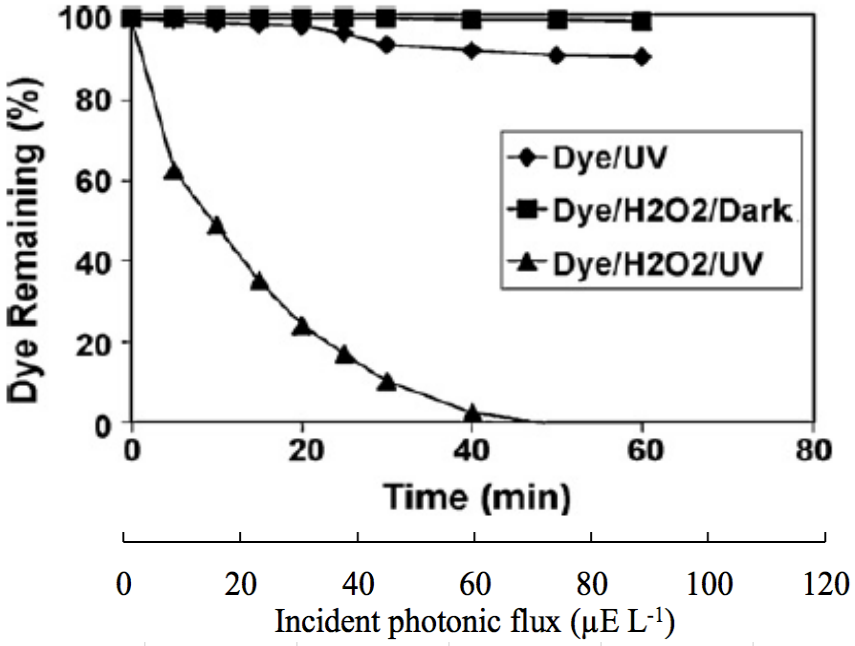

Figure 8. Photodegradation of Eriochrome red 3B azo dye in a water solution at 22.32 mg L^{-1} (pH 3 and 24.3°C) by direct photolysis with UV light (253.7 nm) (Elmorsi et al., 2010).

4.1.2. Optimization of photodegradation kinetics and efficiency

4.1.2.1. Effect of light intensity on endoxifen photodegradation

Linear regression analyses of (E)- and (Z)-endoxifen photodegradation data at five different light intensities (28, 56, 112, 168, and 224 W s^{-1} cm^{-2}) revealed that both endoxifen isomers followed a first order kinetic model (Figures 9 and 10). The R^2 of the fitness of the model were greater than 0.97 at all light intensities for first order reaction while zero and second order fits had the same or lower R^2 (Appendix B, Table B.1). The photodegradation rate constants (k) of (E)- and (Z)-endoxifen isomers for the first order kinetic model and the emission light intensities were linearly related (R^2 > 0.949 and 0.935 for (E)- and (Z)-endoxifen, respectively) (Appendix B, Figure B.1). ANOVA results also indicated that the effect of light intensity on the photodegradation rate was significant (p = 0.0001 for (E)- and (Z)-endoxifen). The maximun emission light intensity of 224 W s^{-1} cm^{-2} provided the highest photodegradation rates of (E)- and

(Z)-endoxifen isomers with k values of 77.1±5.4 μM s^{-1} and 82.5± 5.6 μM s^{-1}, respectively. Previous studies focused on phenol photodegradation reported that the greater the UV light intensity, the greater the number of photons present in the water sample to carry on first order photodegradation reactions (Chiou and Juang, 2007; Udom et al., 2014). Likewise, the photodegradation rates of (E)- and (Z)-endoxifen were greater as the emission light intensity increased.

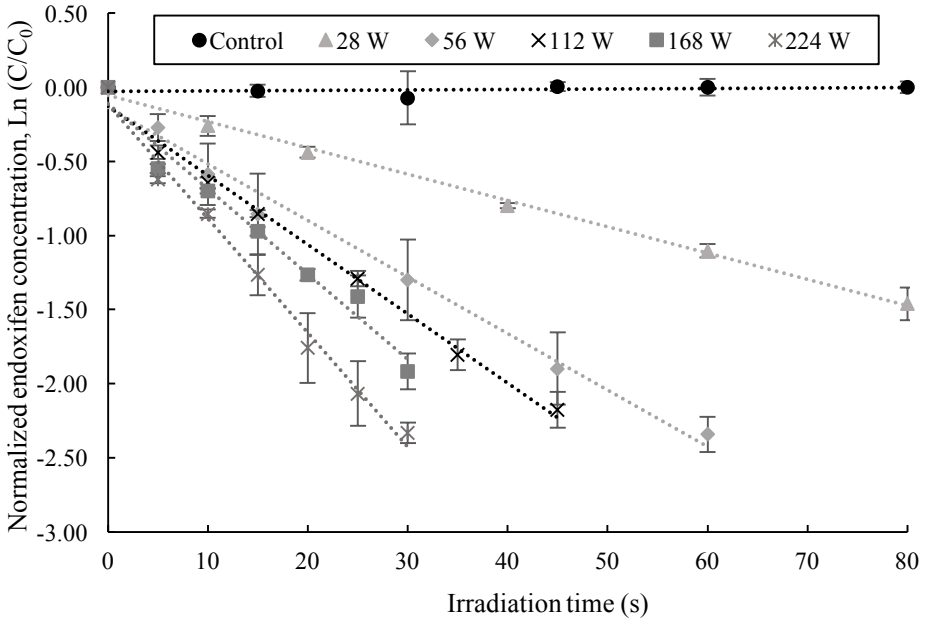

Figure 9. Kinetics of photodegradation (E)-endoxifen in aqueous solution at 2 μg ml^{-1} (pH 7 and 22.4 °C) and at five different emission light intensities (28, 56, 112, 168, and 224 W s^{-1} cm^{-2}) and first-order fit.

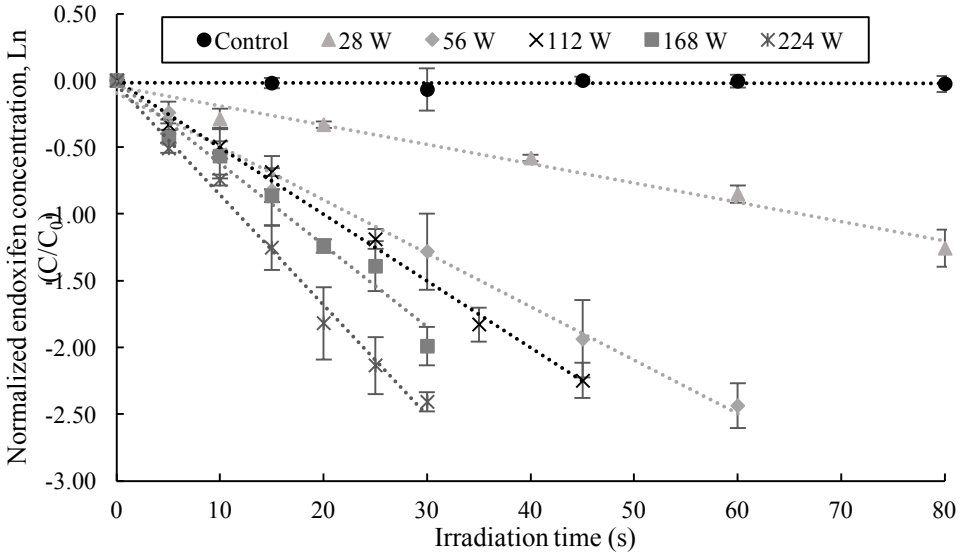

Figure 10. Kinetics of photodegradation (Z)-endoxifen in aqueous solution at 2 µg ml^{-1} (pH 7 and 22.4 °C) and at five different emission light intensities (28, 56, 112, 168, and 224 W s^{-1} cm^{-2}) and first-order fit.

4.1.2.2. Effects of pH on endoxifen photodegradation

The influence of pH on the photodegradation rate constant (k) was investigated in a pH range of 5-9 and at a constant emission light intensity of 28 W s^{-1} cm^{-2}. The results are summarized in Figure 11 where the calculated k value for each tested pH was plotted against its corresponding pH value. The maximum k value for (E)- and (Z)-endoxifen isomers were 16.61 and 15.36 µM s^{-1} at pH 7 and 9, respectively. The differences between the maximum and minimum k values for (E)- and (Z)-endoxifen isomers were 2.06 and 2.39 µM s^{-1}, respectively. These results suggest that the photodegradation of (E)- and (Z)-endoxifen isomers in water is not pH dependent. A statistical analysis (ANOVA) confirms that the photodegradation rate is independent of the pH tested ($p = 0.950$ for (E)-endoxifen and $p = 0.884$ for (Z)-endoxifen). The neutral pH of 7 was selected as the working pH because it presents the maximum k value for (E)-endoxifen and the k value that is slightly lower than the maximum value for (Z)-endoxifen (0.83 µM s^{-1} difference).

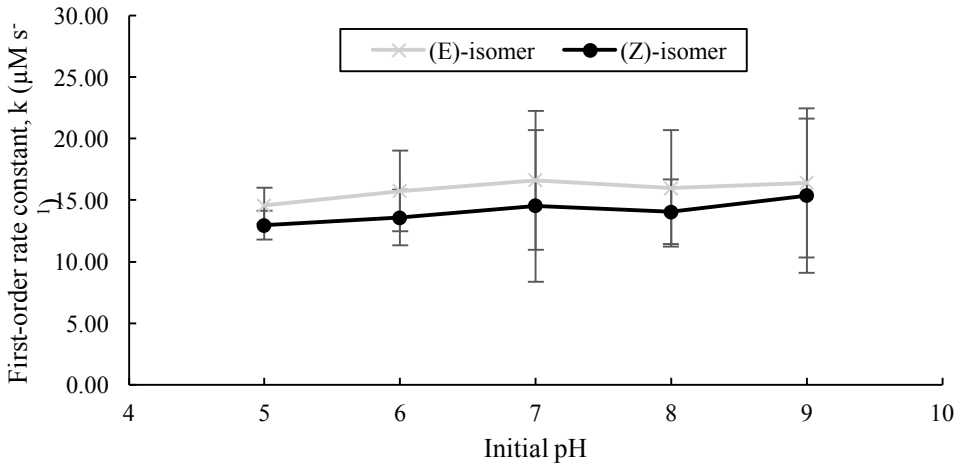

Figure 11. Effect of pH on photodegradation first-order rate constant (k) for aqueous solution with 2 μg mL^{-1} of (E)- and (Z)-endoxifen isomers at an emission light intensity of 28 W s^{-1} cm^{-2} (22.4°C).

Changes in pH before and after 80 seconds of photodegradation reaction (with an emission light intensity of 28 W s^{-1} cm^{-2}) were calculated in the water samples (Appendix B, Figure B.2). pH decreased in all the cases except for the initial pH of 5. This acidification could be due to the presence of a hydroxyaromatic group in the molecular structure of endoxifen. It is well known that hydroxyaromatic compounds present a different pK_a value during the lowest excitation state due to their acid-based property (Jin et al., 2017; Lawrence et al., 1991). Greater pK_a values during the lowest excited state result in a deprotonation of the hydroxyl group. Therefore, the acidification of the low acidic (pH 6), neutral (pH 7), and alkaline (pH 8 and 9) solutions could be explained by the deprotonation of (E)- and (Z)-endoxifen isomers during the lowest excited state due to the presence of a phenol group in their molecular structures. Further analyses need to be conducted in order to determine the pK_a of (E)- and (Z)-endoxifen at their lower excitation state during photodegradation.

4.1.2.3. Effect of initial endoxifen concentration on endoxifen photodegradation

The role of the initial concentrations of (E)- and (Z)-endoxifen (500, 1,000, and 2,000 ng mL^{-1}) on the photodegradation reaction was investigated at a constant light intensity of 224 W s^{-1} cm^{-2}. The higher concentration tested in this study was selected based on the solubility of (E)- and (Z)-endoxifen in water (maximum of 2,000 ng mL^{-1}). The photodegradation rate constants (k) were calculated for each isomer. The reaction rate constants (k) for (E)- and (Z)-endoxifen exhibit positive linear relationships with their initial concentrations ($R^2 > 0.99$) (Appendix B, Figure B.3). The photodegradation rate was dependent on initial concentrations of (E)- and (Z)-endoxifen ($p < 0.0001$ for (E)- and (Z)-endoxifen). The percentage photodegradation of (E)- and (Z)-endoxifen notably decreased by 59 and 57% respectively when the concentration was reduced from 2 to 0.5 mg L^{-1}. Previous studies reported a similar correlation between k (pseudo first order) and the initial concentration of an aromatic compound (oxytetracycline, chrysene, benzo[a]pyrene, phenanthrene, and acenaphthene) during photodegradation (Jin et al., 2017; Miller and Olejnik, 2001). Weller (1961) used the molecular photosensitization of aromatic compounds to explain the positive linear relationship between k and initial concentration of target compound. However, the fluorescence emission of (E)- and (Z)-endoxifen (Appendix A, Figure A.5) is not in the same range as their absorption spectra (Appendix A, Figure A.1). Therefore, photosensitization is not a possible explanation for these results. Another theory is that thermodynamic collision occurs along with photolysis (Jin et al., 2017). In this study, two photo-excited endoxifen molecules collided, triggering the thermodynamic collision reaction. Therefore, the number of excited molecules is directly proportional to the concentration of endoxifen in the ground state. Hence, the photolysis of (E)- and (Z)-endoxifen is not only due to the light energy, but molecular collision could also play an important role.

4.1.2.4. Effect of light source on endoxifen photodegradation

As shown in Figures 12 and 13, the concentrations of (E)- and (Z)-endoxifen isomers remained constant with time after 60 seconds of indoor and sunlight irradiation. Effective photodegradation of (E)- and (Z)-endoxifen isomers was observed when the water samples were exposed to UV light (253.7 nm). After 35 seconds of UV light exposure, the concentrations of (E) and (Z)-endoxifen isomers were below the lower limit of detection ($LOD_{(E)\text{-endoxifen}}$ = 12.66 ng mL^{-1}; $LOD_{(Z)\text{-endoxifen}}$=12.12 ng mL^{-1}). Therefore, the concentrations of both isomers, (E)- and (Z)-endoxifen, were reduced by at least 99.1% after 35 seconds of UV light exposure at 224 W s^{-1} cm^{-2}. These results showed the suitability of UV light to effectively photodegrade (E)- and (Z)-endoxifen isomers in HPLC water.

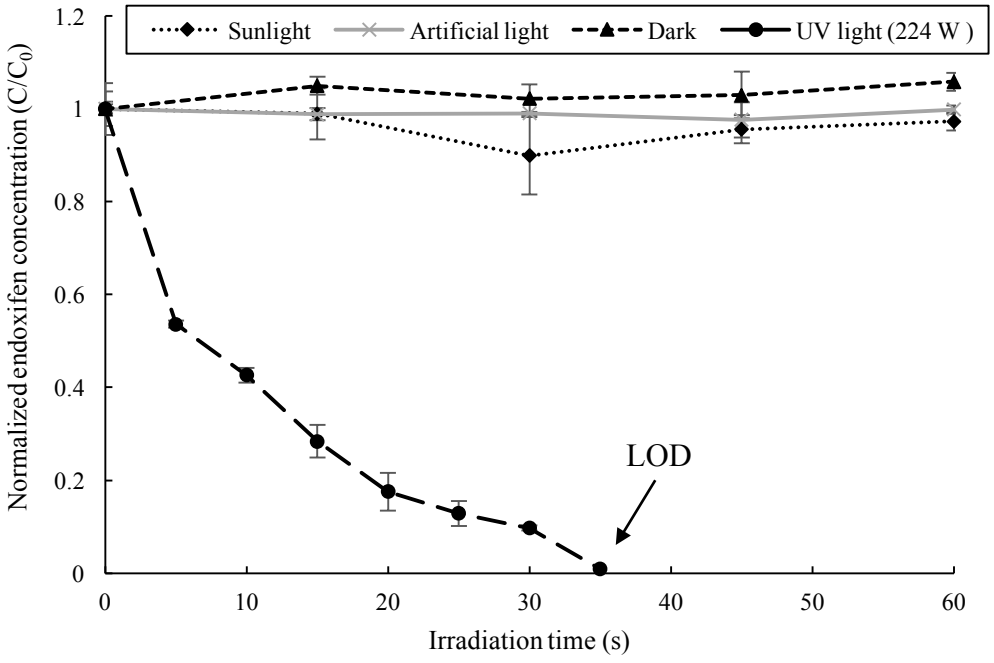

Figure 12. Effect of light source on photodegradation of (E)-endoxifen in aqueous solution at 2 µg mL^{-1}. (E)-endoxifen was undetectable at 35 seconds of irradiation with UV light (224 W s^{-1} cm^{-2}, pH 7, and 22.4°C) (LOD(E)-endoxifen = 12.66 ng mL^{-1}).

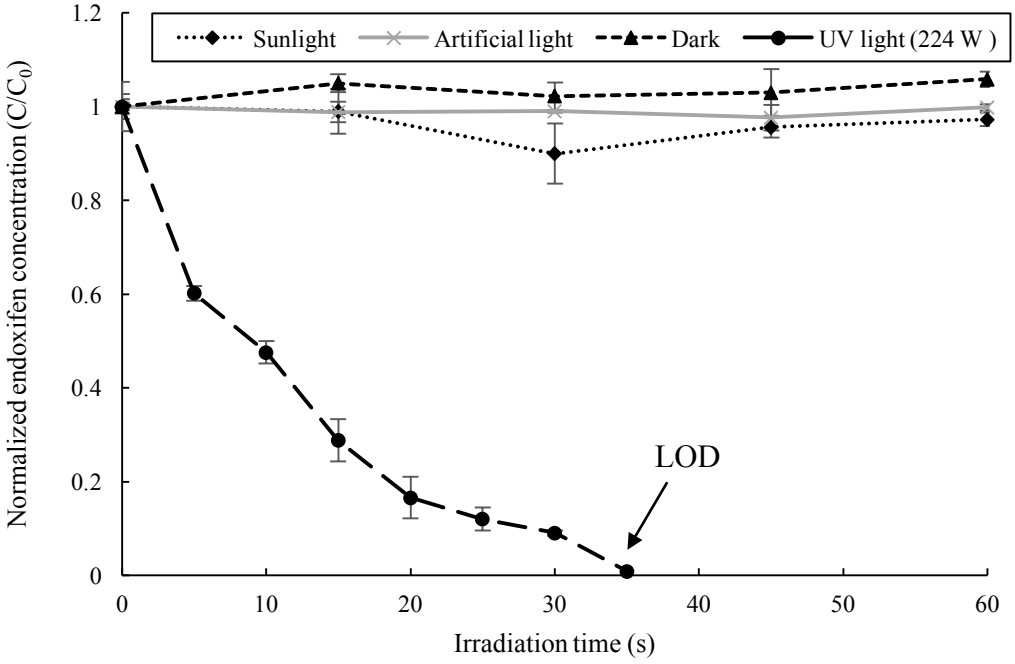

Figure 13. Effect of light source on photodegradation of (Z)-endoxifen aqueous solution at 2 µg mL^{-1}. (Z)-endoxifen was undetectable at 35 seconds of irradiation with UV light (224 W s^{-1} cm^{-2}, pH 7, and 22.4°C) (LOD(Z)-endoxifen = 12.12 ng mL^{-1}).

4.1.3. The role of hydroxyl radicals

HPLC water was used as solvent for (E)- and (Z)-endoxifen isomers during UV photodegradation reactions at 254 nm. According to Dobrović et al. (2017), vacuum ultraviolet (VUV) process with UV light at 185 nm in water generates •OH free radicals which can oxidize organic molecules. The formation of •OH from water irradiated with UV light at 254 nm was unlikely. To confirm that, the contribution of •OH to photodegradation of (E)- and (Z)-endoxifen was examined. IPA (1%) and BA (50 mg L^{-1}) were used as •OH scavengers during the photodegradation. The samples spiked with and without IPA or BA showed similar reaction courses (Figures 14 and 15) but ANOVA results showed that (E)- and (Z)-endoxifen

photodegradation is dependent on the addition of IPA or BA ($p = 0.003$ for both (E)- and (Z)-endoxifen).

The samples with IPA had k values of 60.1±0.6 and 65.3±1.3 μM s^{-1} and the samples with BA had k values of 118.2±9.2 and 122.5±2.6 μM s^{-1} for (E)- and (Z)-endoxifen, respectively. However, the water samples without IPA (1%) or BA (50 mg L^{-1}) resulted in k values of 84.6±6.5 and 89.9±6.6 μM s^{-1} for (E)- and (Z)-endoxifen, respectively. If (E)- and (Z)-endoxifen photodegradation was enhanced by the presence of $^{\bullet}OH$ in the solution, lower k values were expected for (E)-and (Z)-endoxifen photodegradation with the addition of $^{\bullet}OH$ scanvergers. However, the additions of BA and IPA resulted in statistically different k values. The presence of BA in the solution enhanced the photodegradation reaction while IPA reduced the photodegradation reaction kinetic of (E)- and (Z)-endoxifen. This difference in photodegradation efficiencies between $^{\bullet}OH$ quenchers was previously reported by Wu et al. (2015), in a study focusing on chlorine/UV degradation of a common azo dye named C.I. reactive red 2 (RR2) in water. In this study, the addition of BA also resulted in higher removal efficiency of RR2 than others $^{\bullet}OH$ quencher. Therefore, the addition of IPA or BA itself seems to affect the photodegradation reaction rate of (E)- and (Z)-endoxifen rather than $^{\bullet}OH$ radicals. A previous study on the photodegradation of low-brominated diphenyl ether in water reported similar results for IPA and attributed to the effect of IPA addition (dual solvent of IPA and HPLC water versus single solvent of HPLC water) rather than $^{\bullet}OH$ contribution (Wang et al., 2015). That is also likely the case for the observed (E)- and (Z)-endoxifen photodegradation results.

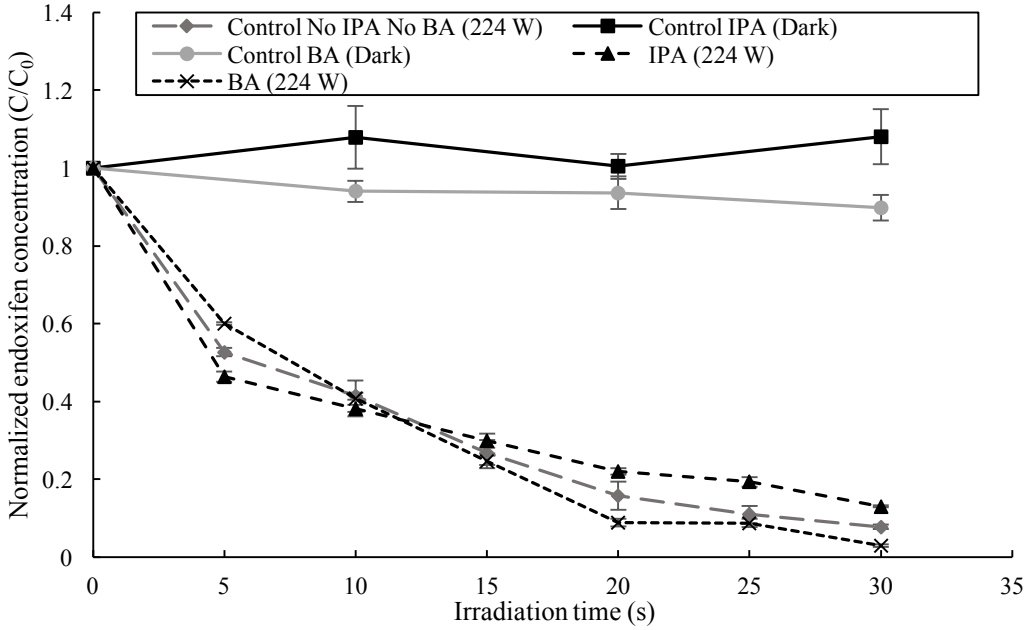

Figure 14. Effects of IPA (1%) and BA (50 mg L^{-1}) on normalized (E)-endoxifen concentration (C/C_0) in aqueous solution at 2 µg mL^{-1} during photodegradation reaction at a UV light intensity of 224 W s^{-1} cm^{-2} (pH 7 and 22.4°C).

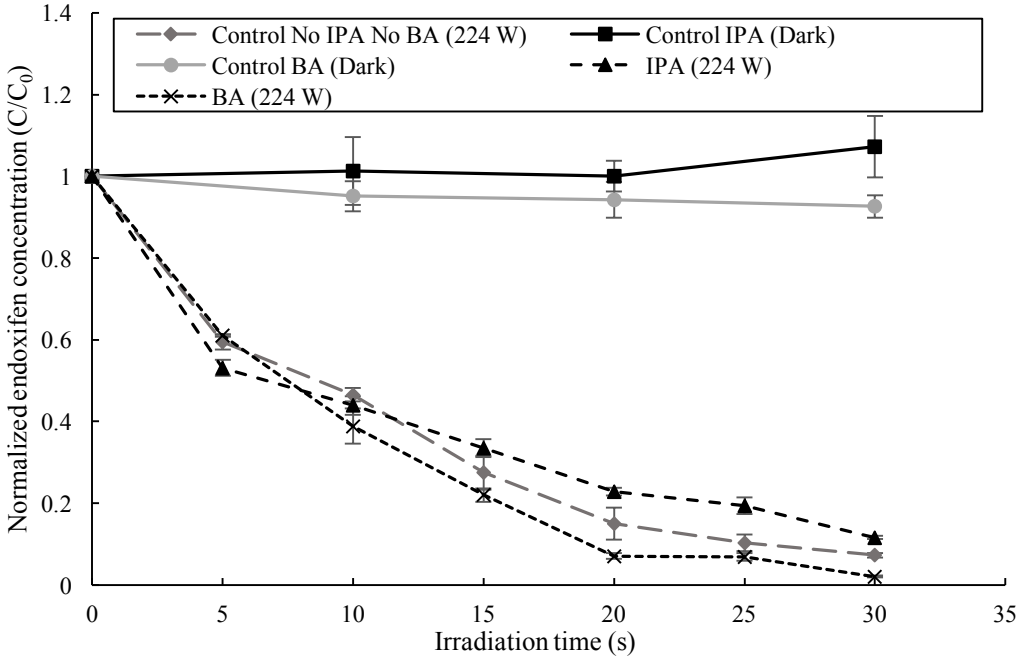

Figure 15. Effects of IPA (1%) and BA (50mg L^{-1}) on normalized (Z)-endoxifen concentration (C/C_0) in aqueous solution at 2 µg mL^{-1} during photodegradation reaction at a UV light intensity of 224 W s^{-1} cm^{-2} (pH 7 and 22.4°C).

4.1.4. Quantum yield and emission light intensity

Quantum yield (Φ) of endoxifen photoreaction was calculated at four emission light intensities (56, 112, 168, and 224 W s^{-1} cm^{-2}). Photon irradiance (E_p) (Einstein cm^{-2} min^{-1}), moles of Fe^{2+} formed in the iron (III) sulfate solution, and the k values of (E)- and (Z)-endoxifen were previously calculated for each emission light intensity (Table 2). In order to determine the quantum yield for the first order kinetic photodegradation reaction of (E/Z)-endoxifen, the molar extinction coefficient (ε) of (E/Z)-endoxifen at 253.7 nm was calculated (Appendix C, Figure C.1). Equation 6 in subsection 3.3.3.6 was then used to calculate the quantum yield.

The quantum yield values decreased as the emission light intensity increased (Figure 16). These results suggest that photon absorbance by (E)- and (Z)-endoxifen was more efficient at lower light intensities. This inverse relationship between emission light intensity and quantum yield was previously observed in photoreaction studies (Chowdhury et al., 2017; Fujishima et al., 2000). (E)- and (Z)-endoxifen were photodegraded more efficiently at low emission light intensities.

There is a need to calculate the incident light intensity in the sample as the emission light intensity is attenuated by several factors such as lamp aging, lamp bulb wall temperature, lamp operating frequency, quartz sleeve absorption, and distance between sample and light source. As expected, the emission light intensities were at least three orders of magnitude higher than the incident light intensities (Table 3). The information provided by the manufacturer of the lamps specified an incident light intensity of 16 mWs^{-1} cm^{-2} in samples placed 2 inches from the brand new lamps using an emission light intensity of 35 W s^{-1} cm^{-2} (Southern New England Ultraviolet Company, n.d.). Therefore, the calculated light intensities in this study at the four-selected emission light intensities were reasonable values compared to the information from the manufacturer. The incident light intensities allow the calculation of light doses applied to the water

samples by multiplying by the irradiation time (s). The light doses during the photodegradation of (E)- and (Z)-endoxifen are shown in Table 3. As expected, lower irradiation intensities need longer irradiation time to achieve a targeted light dose. However, the incident light intensity at the lower emission intensity (56 W s^{-1} cm^{-2}) was remarkably low. This result suggests that light energy dissipation was even higher when lower emission energies were applied to the water samples in the photoreactor.

Table 2. Moles of Fe^{2+} formed in Iron (III) sulfate solution after one minute of UV light irradiation, photon irradiance (Einstein min^{-1} cm^{-2}), and the first order reaction rate constants of (E)- and (Z)-endoxifen isomers at four emission light intensities (56, 112, 168, and 224 W s^{-1} cm^{-2}).

Emission Light Intensity (W s^{-1} cm^{-2})	**Fe^{2+} (μM)**	**E_p (Einstein min^{-1} cm^{-2})**	**k (mM m^{-1})**	
			(E)-endoxifen	**(Z)-endoxifen**
56	1.12	0.35×10^{-6}	2.29±0.10	2.40±0.17
112	3.26	1.03×10^{-6}	2.80±0.15	3.00±0.17
168	5.65	1.78×10^{-6}	3.45±0.22	3.67±0.29
224	6.90	2.17×10^{-6}	4.62 ±0.33	4.95±0.33

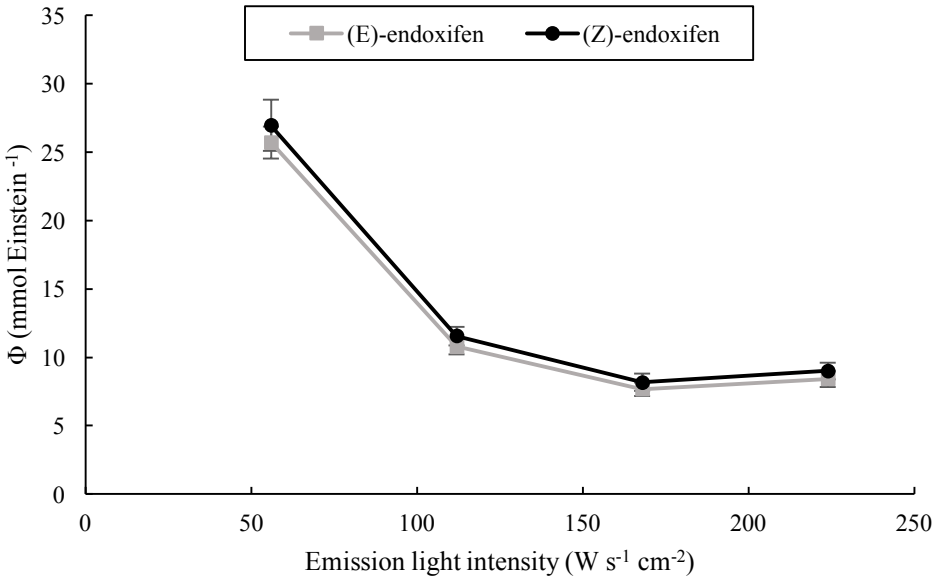

Figure 16. The effect of the emission light intensity (W s^{-1} cm^{-2}) on the quantum yield value (mmol $Einstein^{-1}$) for (E)- and (Z)-endoxifen isomers.

Table 3. Incident light intensity (mW s^{-1} cm^{-2}), exposure time (s), and light doses (mJ cm^{-2}) at four emission light intensities (56, 112, 168, and 224 W s^{-1} cm^{-2}).

Emission light intensity (W s^{-1} cm^{-2})	**Incident light intensity (mW s^{-1} cm^{-2})**	**Irradiation time (s)**	**Light dose (mJ cm^{-2})**
56	2.77	60	166.2
112	8.07	45	363.15
168	14	30	420
224	17.1	30	513

4.1.5. Detection and identification of photodegradation by-products

4.1.5.1. Detection of photodegradation by-products by HPLC-DAD

The chromatogram peak areas corresponding to (E)- and (Z)- endoxifen isomers decreased with time until they became undetectable ($LOD_{(E)\text{-endoxifen}}$ = 12.66 ng mL^{-1}; $LOD_{(Z)\text{-endoxifen}}$=12.12 ng mL^{-1}) after 35 seconds of UV light exposure at 224 W s^{-1} cm^{-2} (Appendix D, Figure D.1). However, a new chromatogram peak with a retention time of 11.43 minutes was observed as (E)-

and (Z)-endoxifen isomers were degraded. After 30 seconds of photodegradation, the new peak presented a total chromatogram percentage area of 82%. The presence of this new peak suggested the formation of at least one photodegradation by-product.

4.1.5.2. Identification of photodegradation by-products by UHPLC-MS/MS

A water sample containing (E)- and (Z)-endoxifen isomers was exposed to UV light (253.7 nm) for 35 seconds to reproduce the photodegradation by-product previously observed by HPLC-DAD. The irradiated water sample was then injected to UPLC-MS/MS in order to identify the molecular weight of the photodegradation by-product. However, instead of only one peak, three new peaks were observed (Figure 17). The first peak (PB1a) and the second peak (PB1b) had the same ion-*m/z* value (372.19) (Appendix D, Figure D.4). This ion-*m/z* value indicated an aromatization of (E) and (Z)-endoxifen isomers forming a phenanthrene nucleo (by the elimination of two hydrogen (H^+) and the formation of one molecular bond between two benzene rings) (Table 4).

The elimination of two hydrogens (H^+) through endoxifen aromatization could explain the recorded ion-*m/z* value of PB1a and PB1b. A previous study on the detection of endoxifen by HPLC with a fluorescence detector reported the formation of a photocycled derivate with a phenanthrene nucleo after the irradiation of endoxifen by UV light (Aranda et al., 2011). According to Miller and Olejnik (2001), irradiated polyaromatic hydrocarbons (PAHs) undergo chemical changes during their excited state after photon absorption. The most probable way for these PAHs to return to their ground state is through energy dissipation by proton transfer. Likewise, deprotonation of (E)- and (Z)-endoxifen forming a phenanthrene nucleo by molecular changes during their excited state is the most probable explanation for the observed ion-*m/z* values. Furthermore, the minimal difference in ppm (<10) between the expected ion-*m/z* mass and the

theoretical ion-*m/z* mass of the proposed molecular structure for PB1a and PB1b support the suggested aromatization of (E)- and (Z)-endoxifen after 35 seconds of UV irradiation. This aromatization of endoxifen was also proposed by Negreira et al. (2015) during chlorination analyses by the addition of two chlorine (Cl^-) to the phenol group followed by an oxidative carbon-carbon coupling that results in a chlorinated phenanthrene nucleo (Figure 31).

The third peak (3) observed with a retention time of 2.03 minutes (PB2) showed an ion-*m/z* value of 314.21 (Appendix D, Figure D.4). This ion-*m/z* value observed at 35 seconds was similar to the observed ion-*m/z* value of (E)- and (Z)-endoxifen isomers at time 0 chromatogram (Appendix D, Figure D.3). However, the retention time of PB2 was different than the retention times observed for (E)- and (Z)- endoxifen isomers at time 0 (Appendix D, Figure D.2). Therefore, the presence of this new peak (PB2) with the same ion-*m/z* value as (E)- and (Z)-endoxifen isomers but different retention time suggests the presence of a new photodegradation by-product with the same molecular weight as (E)- and (Z)-endoxifen isomers. The hydrogenation by the addition of two H^+ to the phenanthrene nucleo formed during the aromatization of endoxifen could explain the obtained ion-*m/z* value of PB2. However, the determination of the molecular structure of PB2 was challenging due the presence of only one peak instead of two peaks.

PB1 showed two peaks corresponding to the aromatization of (E)- and (Z)-endoxifen isomers resulting in two well differentiated photodegradation by-products. The observation of only one peak for PB2 suggests that either only one of the two endoxifen isomers underwent hydrogenation to PB2 or the two peaks overlapped. However, PB2 was not considered as the main photodegradation by-product due to a small percentage of the chromatogram peak area.

Table 4 shows the two possible molecular structures of PB2 depending on whether the hydrogenation occurred in the (E)-endoxifen isomer or the (Z)-endoxifen isomer. The proposed

molecular structures of PB1(a, b) and PB2 were analyzed through UPLC-MS/MS. In order to identify the formed product ions after the fragmentation of (E/Z)-endoxifen and PB2 through MS/MS, the ion-*m/z* value of 374.21 was selected and fragmented with a cone voltage of 27 eV.

(E)- and (Z)-endoxifen present similar formed product ions as PB2 but the ion-*m/z* = 223.1140 and the ion-*m/z* = 194.0757 were not observed in the PB2 MS/MS spectrum (Appendix D, Figure D.5). The proposed molecular structure of PB2 contain a phenanthrene nucleo that could hinder the cleavage of PB2 to generate the fragment ion-*m/z* values of 223.1140 and 194.0757. The proposed molecular structures of PB1(a, b), also present a phenanthrene nucleo as a molecular core. MS/MS spectra for PB1(a, b) showed no fragmentation within the phenanthrene nucleo (Appendix D, Figure D.6).

Finally, two more peaks (3 and 4) were observed in the chromatogram (Figure 17). These two peaks had the same retention times and ion-*m/z* values as the peaks observed in the initial chromatogram before the photodegradation reaction (Appendix D, Figures D.2 and D.3). Therefore, these two peaks represented remaining (E)- and (Z)-endoxifen isomers present in the water sample after 35 seconds of photodegradation reaction that were undetectable by HPLC-DAD. The observation of (E)- and (Z)-endoxifen isomers after 35 seconds of photodegradation using UPLC-MS/MS could be explained by the higher sensitivity of MS/MS than DAD techniques. Kopec et al. (2013) compared MS and DAD detector during a quantitative analysis and showed that MS detector was 37 times more sensitive than DAD detector.

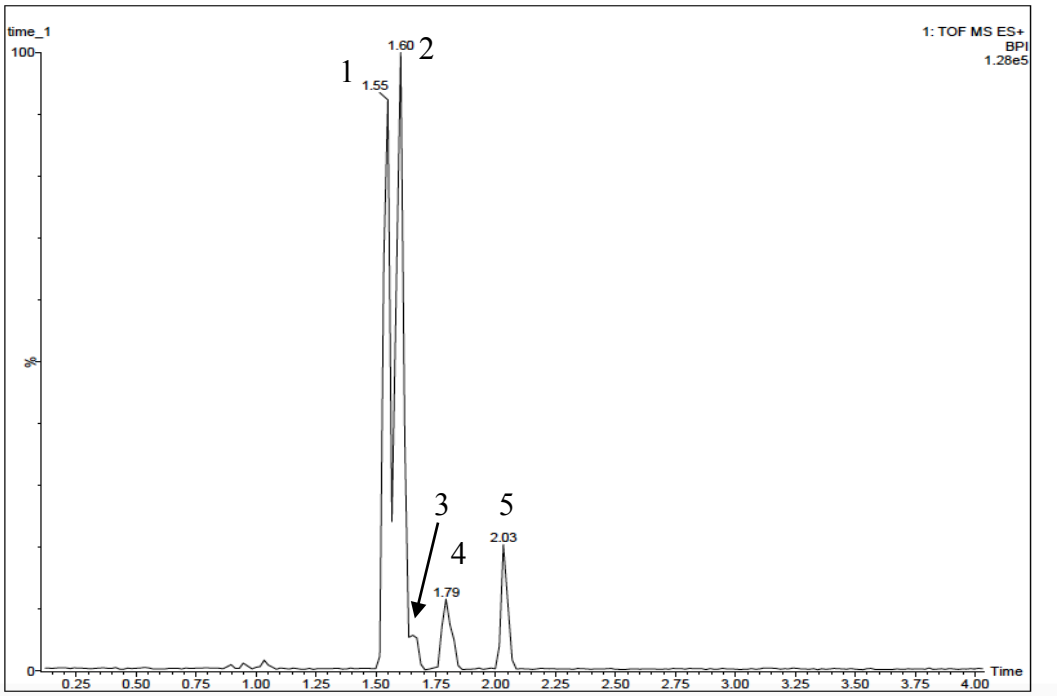

Figure 17. UHPLC-MS chromatogram of aqueous solution of (E)- and (Z)-endoxifen (1 µg ml-^{1} each, pH 7, and 22.4°C) after 35 seconds of irradiation with a UV light intensity of 224 W s^{-1} cm^{-2}: PB1a and PB1b (1 and 2); (E)-endoxifen (3); (Z)-endoxifen (4); and PB2 (5).

Table 4. Molecular mass and proposed molecular structures of (E)- and (Z)-endoxifen photodegradation by-products.

Compound	Predicted Molecular Structure	Rt	Molecular Formula ($M+H^+$)	Expected ion-*m/z*	Theoretical ion-*m/z*	|ppm|
(E)-endoxifen	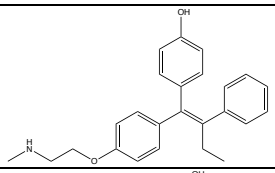	1.65	$C_{25}H_{27}NO_2$	374.2120	374.2106	3.74
(Z)-endoxifen	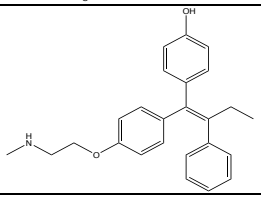	1.78	$C_{25}H_{27}NO_2$	374.2120	374.2107	3.47
PB1a	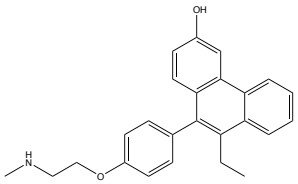	1.55	$C_{25}H_{25}NO_2$	372.1919	372.1949	8.06
PB1b	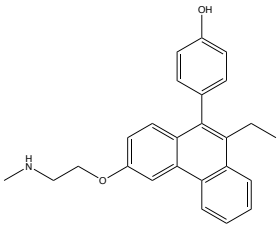	1.60	$C_{25}H_{25}NO_2$	372.1919	372.1949	8.06
PB2	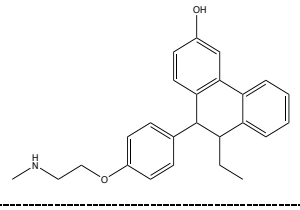	2.03	$C_{25}H_{27}NO_2$	374.2120	374.2109	2.94

4.1.6. Mineralization of (E)- and (Z)-endoxifen by UV light

Mineralization by UV light (253.7 nm) of endoxifen is the most desirable outcome. A mineralization experiment was conducted using a HPLC water sample spiked with (E)- and (Z)-endoxifen (1:1, w/w) at 2 μg mL^{-1} irradiated with UV light at 244 W s^{-1} cm^{-2} for 120 minutes. As shown in Figure 18, the chromatograms obtained by UHPLC analysis suggest that endoxifen and its PBPs were photodegraded to neutral and/or small molecular weight molecules that cannot be ionized by MS detector neither at the positive or negative mode. Two small new peaks (peaks 3 and 4) were observed after 60 and 120 minutes of photodegradation reaction but their ion-*m/z* values (250.18 and 365.28 for peaks 3 and 4 respectively) suggest that these molecular weights were not related to (E)- and (Z)-endoxifen (Figure 19). The TOC analysis revealed that (E)- and (Z)-endoxifen were mineralized 33.6 % and 73.4 % after 60 and 120 minutes of UV light radiation at 244 W cm^{-1} s^{-1}, respectively (Figure 20). Mineralization of aromatic compounds by direct photolysis with UV light (253.7 nm) was previously reported by Yazdanbakhsh et al. (2018). The authors reported the ability of UV light to mineralize 2,4,6-trichlorophenol through direct absorbance of UV light by the molecule breaking the aromatic ring to small molecules such as carboxylic acids which can be easily converted to CO_2 and H_2O. That is also likely the case for the observed (E)- and (Z)-endoxifen mineralization.

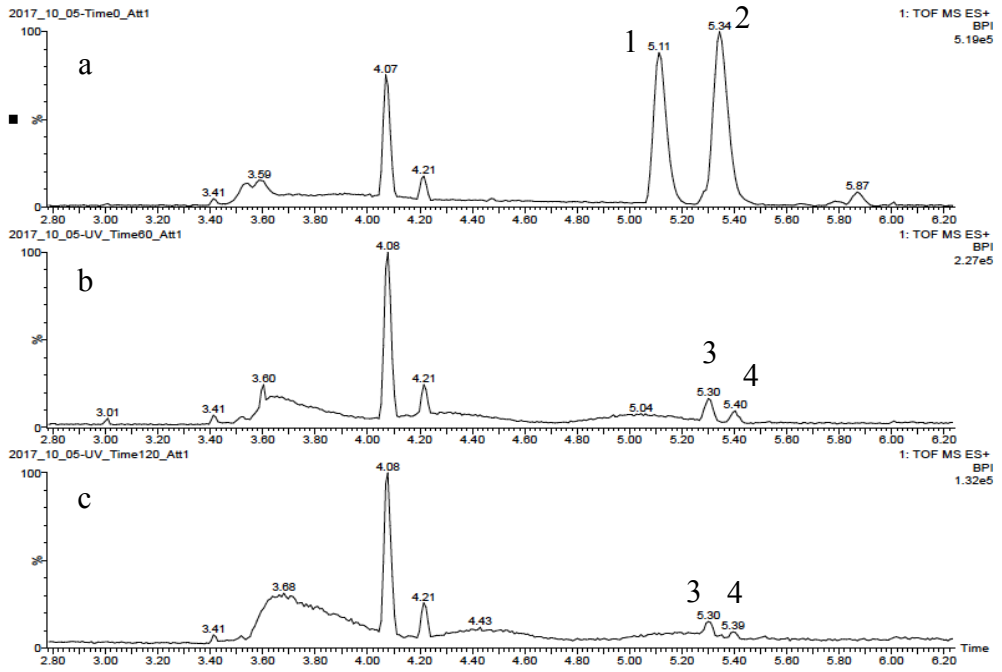

Figure 18. UHPLC-MS chromatogram of aqueous solution of (E)-endoxifen (1; RT = 5.11 min) and (Z)-endoxifen (2, RT = 5.34 min) (2µg mL^{-1}, pH 7 and 24.3°C) by UV light at 244 W s^{-1} cm^{-2}: (a) before photodegradation reaction; (b) after 60 minutes of photodegradation reaction; (c) after 120 minutes of photodegradation reaction

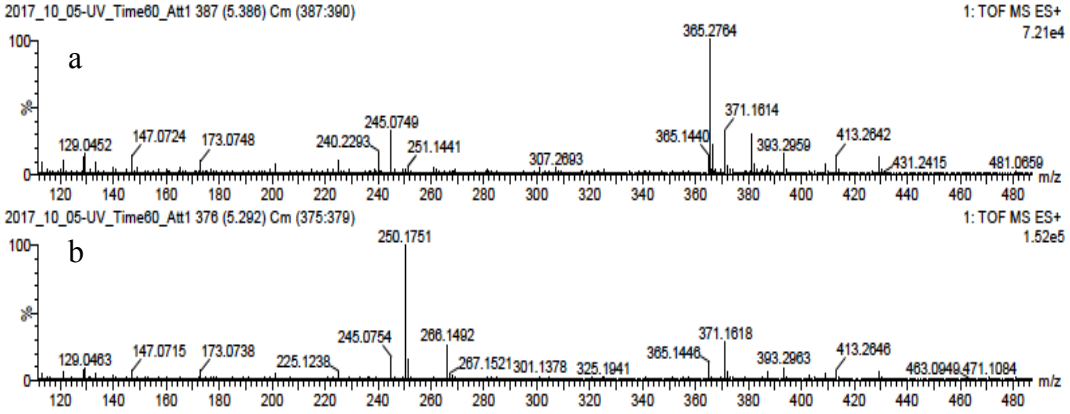

Figure 19. Mass spectrometry of peak 4 (a) and peak 3 (b) observed in an aqueous solution spiked with (E)- and (Z)-endoxifen (2 µg mL^{-1}, pH 7, and 24.3°C) after 60 minutes of irradiation with UV light at 244 W s^{-1} cm^{-2}.

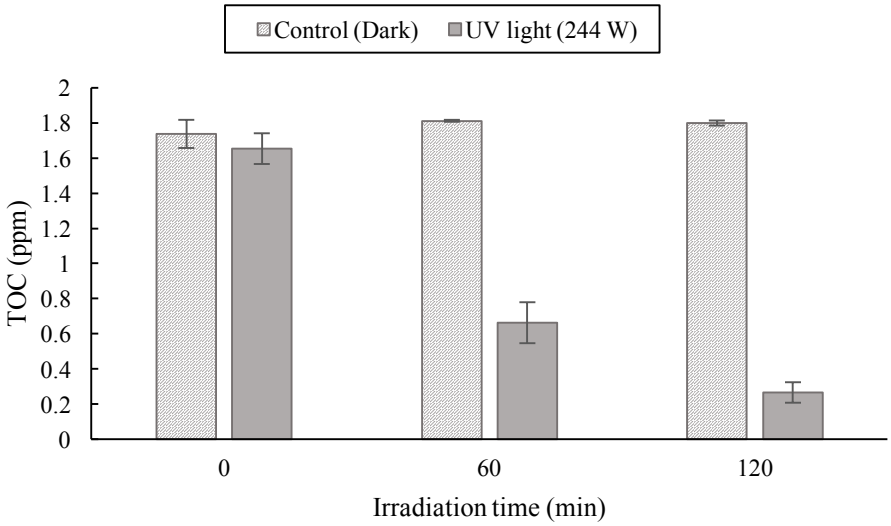

Figure 20. TOC analysis of aqueous solution containing a mixture of (E)- and (Z)-endoxifen at 2 μg mL^{-1} (pH 7 and 24.3°C) before photodegradation reaction and after 60 and 120 minutes of photodegradation reaction with UV light at 244 W cm^{-1} s^{-1}.

4.1.7. Photodegradation of (E)- and (Z)-endoxifen in wastewater by UV light

Photodegradation of (E)- and (Z)-endoxifen was tested in wastewater samples collected from the secondary effluent of a WWTP spiked with (E)- and (Z)-endoxifen at 1 μg mL^{-1}. The photodegradation reaction of (E)- and (Z)-endoxifen in wastewater followed a second order model with $R^2 > 0.99$ and reaction rate constants (k) of 72.9 and 75.9 μM s^{-1}, respectively (Appendix D, Figure D.8). Based on R^2 of the fittings, second order model is a more suitable choice than zero and first order models (Appendix D, Table D.1). Using the same emission light intensity (56 W s^{-1} cm^{-2}), the photodegradation reaction rate constants (k) of (E)- and (Z)-endoxifen in the wastewater samples were almost twice greater than the reaction rate constants in the HPLC water samples. This large difference in k values could be explained by different photochemical processes in wastewater and HPLC water.

The photodegradation of (E)- and (Z)-endoxifen in water samples occurred through direct photolysis by the direct absorption of UV light that resulted in a chemical transformation of the molecular structures of (E)- and (Z)-endoxifen. However, the presence of other molecules in the wastewater sample that also absorbed UV light could induce the chemical transformation of (E)- and (Z)-endoxifen through indirect or sensitized photolysis. Therefore, photodegradation of (E)- and (Z)-endoxifen in wastewater occurred likely through two different mechanisms (direct and indirect photolysis) resulting in higher k values. The indirect photolysis of (E)- and (Z)-endoxifen in wastewater samples also explains the difference in the photodegradation kinetics (first order in water and second order in wastewater).

In order to determine if (E)- and (Z)-endoxifen photodegradation would take place during UV light disinfection at WWTPs, wastewater samples spiked with (E)- and (Z)-endoxifen were irradiated with light doses similar to those applied at WWTPs (Figure 21). The initial concentrations of (E)- and (Z)-endoxifen in wastewater were reduced by 30 and 31% after receiving the minimal UV light dose for disinfection established by the USEPA (2016) of 16 mJ cm^{-2}. WWTPs with filtered nitrified secondary effluents normally apply a minimal UV light dose of 30 mJ cm^{-2} (Shin et al., 2001). The irradiation of (E)- and (Z)-endoxifen in wastewater with a light dose of 30 mJ cm^{-2} resulted in a reduction of the concentrations by 44.3 and 45.7%, respectively. Moreover, the use of higher light dose of 97 mJ cm^{-2} which is not uncommon for conventional WWTPs (Darby et al., 1993) reduced (E)- and (Z)-endoxifen by 71.2 and 72.4%, respectively. Therefore, (E)- and (Z)-endoxifen if present in secondary treated wastewater would be photodegraded by UV disinfection process. As in HPLC water, this photodegradation reaction could form PB1(a, b) and PB2 which are more toxic than the parent compounds.

In order to determine the presence of PB1(a, b) and PB2 in the wastewater sample after the photodegradation of (E)- and (Z)-endoxifen isomers, UPLC-MS/MS analyses were performed before and 35 seconds after irradiation at a light intensity of 56 W s^{-1} cm^{-2} (Figure 22). The chromatogram of the wastewater sample before irradiation with UV light (Figure 22.b) has two main peaks (Rt = 1.71 and 1.83 minutes) with the same ion-*m/z* values as endoxifen (ion-*m/z* = 374.21) (Appendix D, Figure D.7). The absence of these two peaks in the initial chromatogram (Figure 22.a) before (E)- and (Z)-endoxifen were spiked suggests that these two peaks were (E)- and (Z)-endoxifen isomers. The chromatogram after 35 seconds of irradiation has four main peaks (Figure 22.c). Two of the peaks (Rt = 1.57 and 1.64 minutes) had the same ion-*m/z* value as PB1(a, b) (ion-m/z = 372.19) (Figure 23). Further MS/MS analyses revealed that these two peaks represented PB1(a, b) (Appendix D, Figure D.9).

The other two peaks in the chromatogram after 35 seconds of irradiation showed similar retention times (Rt = 1.71 and 1.84 minutes) and the same ion-*m/z* values (ion-*m/z* = 374.21) as the peaks observed in the initial chromatogram before the photodegradation reaction (Appendix D, Figure D.7). These two peaks were from undegraded (E)- and (Z)-endoxifen isomers in the wastewater sample. Therefore, the photodegradation of (E)- and (Z)-endoxifen in WWTPs potentially led to the generation of the toxic PB1(a, b). However, the initial concentration of (E)- and (Z)-endoxifen used in this study (1 μg mL^{-1}) was higher than the expected concentration in wastewater (ppb). The positive correlation observed between initial endoxifen concentration and the first-order photodegradation rate suggests that lower concentrations of (E)- and (Z)- endoxifen in wastewater could lead to lower photodegradation rates. However, photodegradation of (E)- and (Z)-endoxifen in the wastewater samples followed a second order model possibly due to photosensitization by inorganic and other organic compounds in wastewater. This

photosensitization led to greater photodegradation rates suggesting that (E)- and (Z)-endoxifen could be photodegraded in wastewater even at low concentrations. Further work on the development of precise quantification methods for endoxifen with LOD and LOQ below the expected concentrations in wastewater (ppb level) is needed. With better quantification methods, the photodegradability of (E)- and (Z)- endoxifen at concentrations similar to those expected in wastewater can be elucidated.

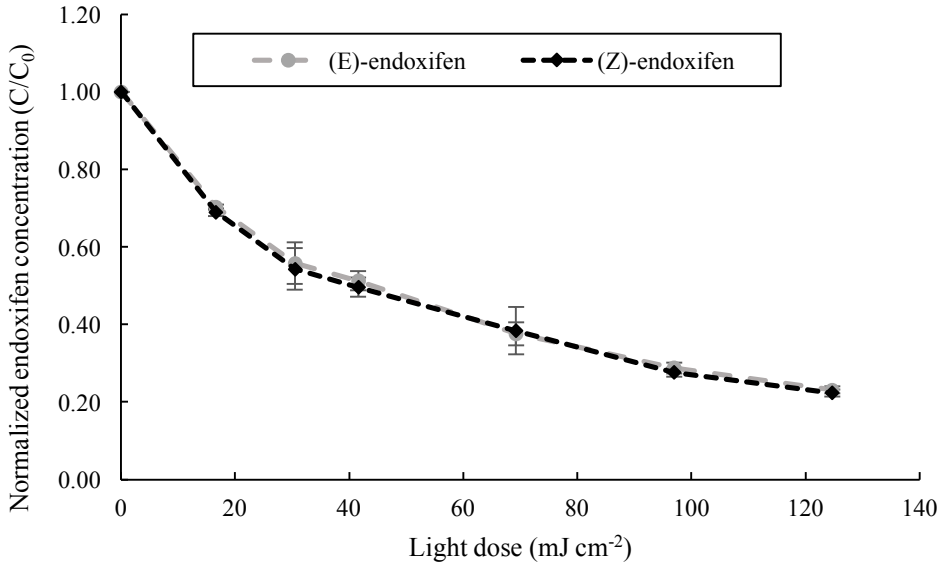

Figure 21. Effect of light dose (mJ cm^{-2}) on (E)- and (Z)-endoxifen concentrations in a wastewater sample (pH 7.59, NO_2^- = 0.032 mg L^{-1}, NO_3^- = 0.010 mg L^{-1}, TOC = 19.17 mg L^{-1}, and 22.4°C) irradiated with an emission light intensity of 56 W s^{-1} cm^{-2}.

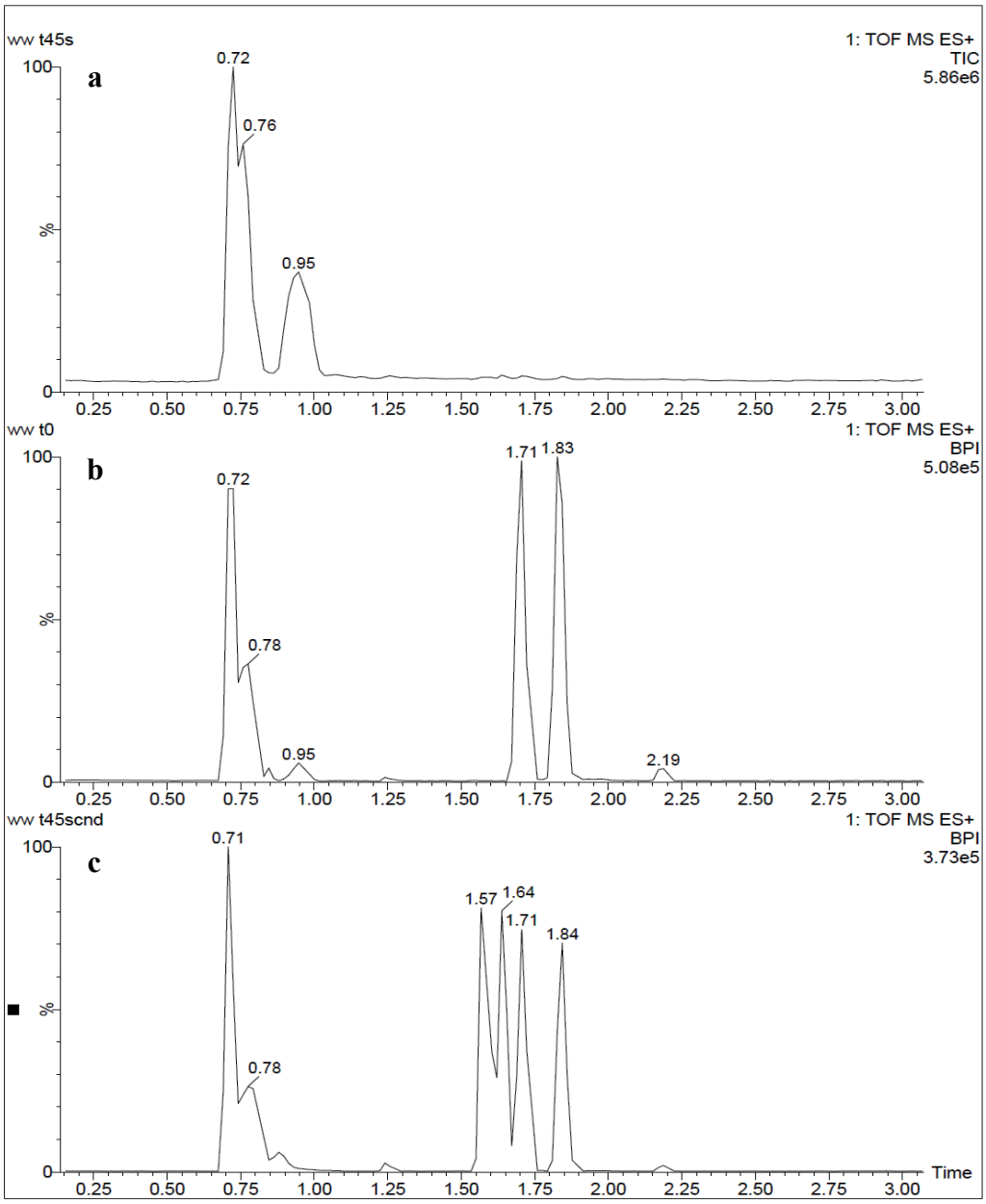

Figure 22. UHPLC-MS/MS chromatogram of (E)- and (Z)-endoxifen in wastewater (1 µg ml^{-1}) and PBPs (Photodegradation conditions: pH 7.59, NO_2^- = 0.032 mg L^{-1}, NO_3^- = 0.010 mg L^{-1}, TOC = 19.17 mg L^{-1}, 22.4°C, and UV light intensity of 56 W s^{-1} cm^{-2}): (a) wastewater sample with no (E)- and (Z)-endoxifen; (b) wastewater sample spiked with (E)- and (Z)-endoxifen before irradiation; (c) wastewater sample spiked with (E)- and (Z)-endoxifen and irradiated for 35 seconds.

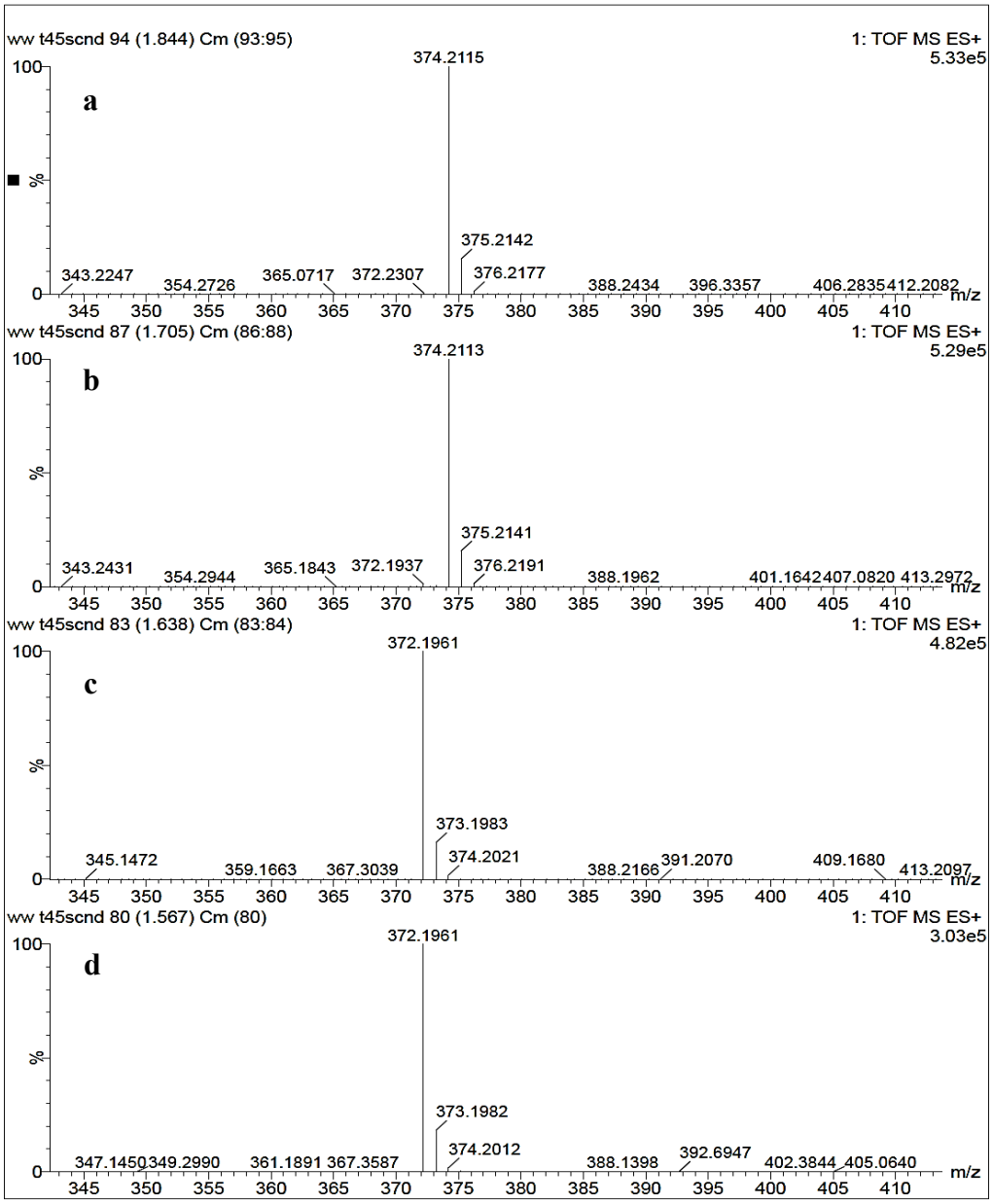

Figure 23. Mass spectrometry of the wastewater sample spiked with (E)- and (Z)-endoxifen (1 µg ml^{-1}) after 35 seconds of irradiation with UV light (pH 7.59, NO_2^- = 0.032 mg L^{-1}, NO_3^- = 0.010 mg L^{-1}, TOC = 19.17 mg L^{-1}, 22.4°C, light intensity = 56 W s^{-1} cm^{-2}): (a) (Z)-endoxifen (Rt = 1.84 minutes, ion-m/z = 374.2115); (b) (E)-endoxifen (Rt = 1.71 minutes, ion-m/z = 374.2113); (c) PB1b (Rt = 1.64 minutes, ion-m/z = 372.1961); (d) PB1a (Rt = 1.57 minutes, ion-m/z = 372.1961).

4.2. Photodegradation with natural sunlight

4.2.1. Photodegradation kinetics and efficiency

With the aim to determine the ability of natural solar radiation to photodegrade endoxifen by direct photolysis, photodegradability of (E)- and (Z)-endoxifen was investigated using HPLC water spiked with a mixture of (E)- and (Z)-endoxifen (1:1, w/w) at 2 μg mL^{-1}. (E)- and (Z)-endoxifen were photodegraded by 90 and 93% after 180 minutes of natural sunlight radiation (84,000-100,000 lux). Linear regression analysis revealed that the degradation of both isomers followed a zero order kinetic model (Figure 24) with $R^2 > 0.96$ for zero order reaction while the first and second order fits had lower R^2 (Appendix E, Table E.1). The photodegradation rate constants (k) of (E)- and (Z)-endoxifen for the zero order kinetic model were 5.0±0.1 μM min^{-1} and 5.2±0.1 μM min^{-1}, respectively.

The photodegradation rate constants (k) calculated for the natural sunlight experiment were considerably lower than that obtained with UV light (253.7 nm) experiments. This difference in rate constants could be explained by the proximity between the maximum absorbance wavelength of (E)-and (Z)-endoxifen (244 nm) with the wavelength emitted by UV light (253.7 nm), whereas the sun emits light at wavelengths ranging from 290 nm to 800 nm (Mumbo et al., 2017; Zepp and Cline, 1977). A previous study by Gros et al. (2015) reported the ability of natural sunlight to photodegraded the antidepressant amisulpride by 90% after 9 hours of sunlight irradiation in pure water. The study also reported a lower photodegradation rate of amisulpride when the experiment was performed on wastewater samples ($t_{1/2}$ 2.79 h for pure water versus $t_{1/2}$ 4.20 h for wastewater). Therefore, it would be interesting to determine the photodegradability of (E)- and (Z)-endoxifen in wastewater and receiving surface water samples exposed to natural sunlight.

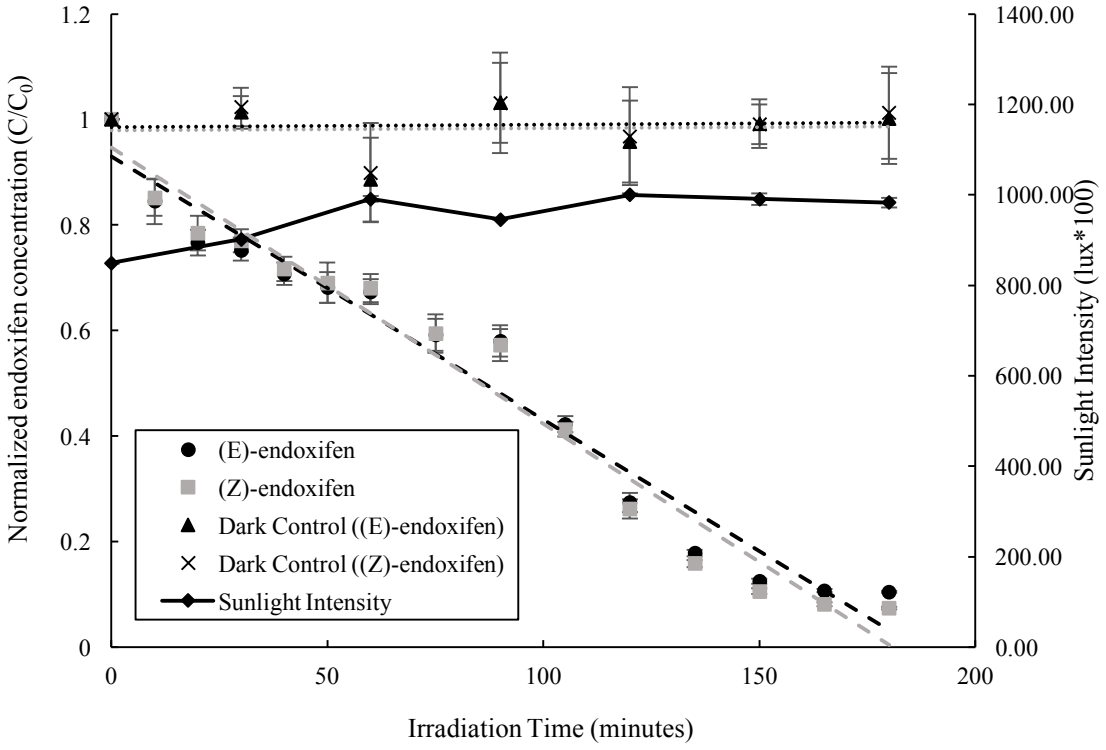

Figure 24. Kinetics of photodegradation of (E)- and (Z)-endoxifen in aqueous solution at 2 µg mL^{-1} (pH 7 and 23.4ºC) irradiated with natural sunlight (84,900-100,000 lux) with zero order fit.

4.2.2. Photodegradation experiments with wastewater and surface water

Photodegradation by natural sunlight is a promising technique to eliminate pharmaceutical compounds in WWTPs with lagoon systems (Gros et al., 2015). In the present study, photodegradation of (E)- and (Z)-endoxifen was examined using wastewater and receiving surface water samples spiked with a mixture of the isomers (1:1, w/w) at 2 µg mL^{-1} and exposed to natural sunlight (90,367-97,133 lux) for 180 minutes. (E)- and (Z)-endoxifen in wastewater samples were photodegraded 85 and 83%, respectively, whereas, in surface water samples, they were both photodegraded 61% after 150 minutes of radiation. (E)- and (Z)-endoxifen photodegradation followed the first and zero order kinetic models for wastewater and surface water samples,

respectively. The R^2 of the fitness of the model were greater than 0.96 for first order reaction in wastewater experiments while zero and second order fits had lower R^2 (Appendix E, Table E.2). Receiving surface water samples showed R^2 greater than 0.85 for zero order reaction while lower R^2 values were observed for first and second order fits.

Less efficient photodegradation of (E)- and (Z)-endoxifen in wastewater and receiving surface water samples compared to pure water suggests that their photodegradation of was highly influenced by the presence of other compounds in the samples. Similar results were reported by a study of Yassine et al. (2018) in which higher photodegradation rates were observed in pure water than in surface water samples for two oral anticoagulants, dabigatran and apixaban. Yassine et al. (2018) related the decrease in photodegradation rate to the presence of natural hydroxyl radical ($^{\bullet}$OH) scavenger in surface water. However, in the present study, with the results on $^{\bullet}$OH scavenger (Section 4.1.3) suggest that photodegradation of (E)- and (Z)-endoxifen was not impacted by the presence of $^{\bullet}$OH free radicals in water. Cory et al. (2015), demonstrated that dissolved organic matter in water streams absorbs UV and visible light of the solar spectrum resulting in an attenuation of the light that penetrated the water. Likewise, dissolved organic matter commonly present in wastewater and receiving surface water could absorbs sunlight reducing the flux of photons reaching the molecules of (E)- and (Z)-endoxifen in water. However, the opposite effect was observed with UV light experiments (section 4.1.9) where photodegradation rates of (E)-and (Z)-endoxifen were higher in wastewater samples due to photosensitizing process by other molecules present in the samples.

It is well known that dissolved organic matter could play an important role as a photosensitizer in natural water bodies (Guerard and Chin, 2012). However, the composition of DOM profoundly affects the photodegradation fate of contaminants acting as a photosensitizer or

as a photoinhibitor (Challis et al., 2014). Guerard and Chin (2012) reported that DOM from two different sources resulted in the opposite effects during the photodegradation of the antibiotic sulfadimethoxine. In this study, wastewater and surface water samples for UV light and sunlight experiments were collected from the same sources but at different time. Therefore, the composition of the DOM could attribute to the observed performance differences between UV light and sunlight photodegradation in wastewater. These results lead to a conclusion that (E)-and (Z)-endoxifen are highly photodegradable by natural sunlight if they are present in wastewater and/or receiving surface water samples. Therefore, it is imperative to identify endoxifen PBPs generated by sunlight radiation.

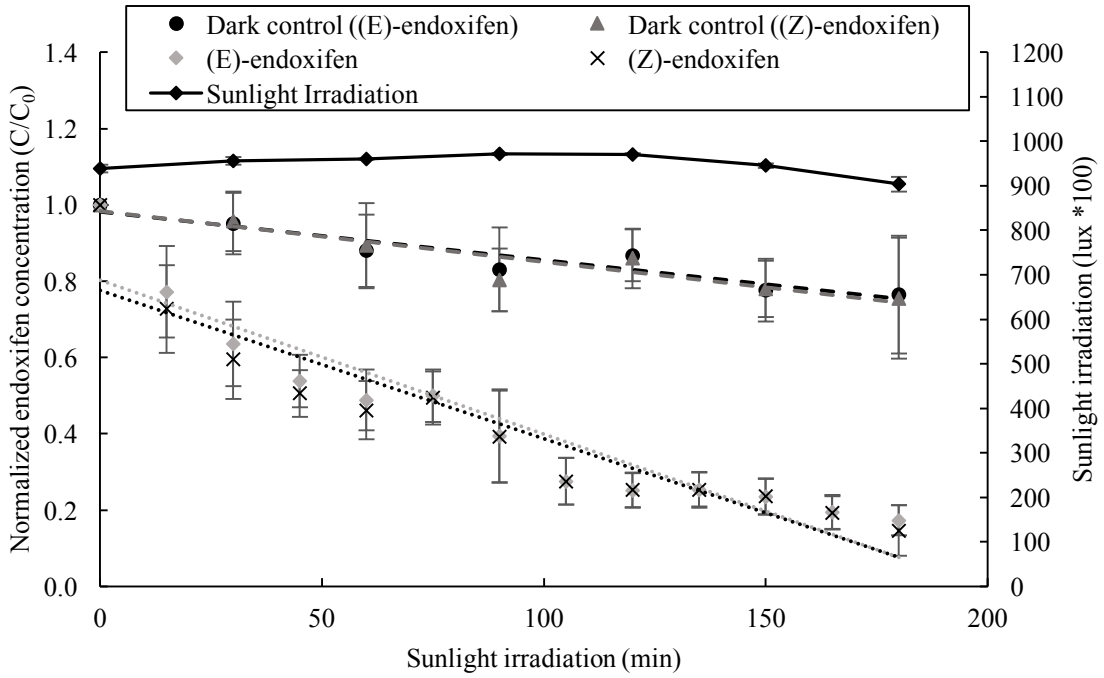

Figure 25. Kinetics of photodegradation of (E)- and (Z)-endoxifen in wastewater at 2 µg mL^{-1} (Photodegradation conditions: pH 6.81, NO_2^- = 0.06 mg L^{-1}, NO_3^- = 1.65 mg L^{-1}, TOC = 20.18 mg L^{-1}, and 8.3°C) irradiated with natural sunlight.

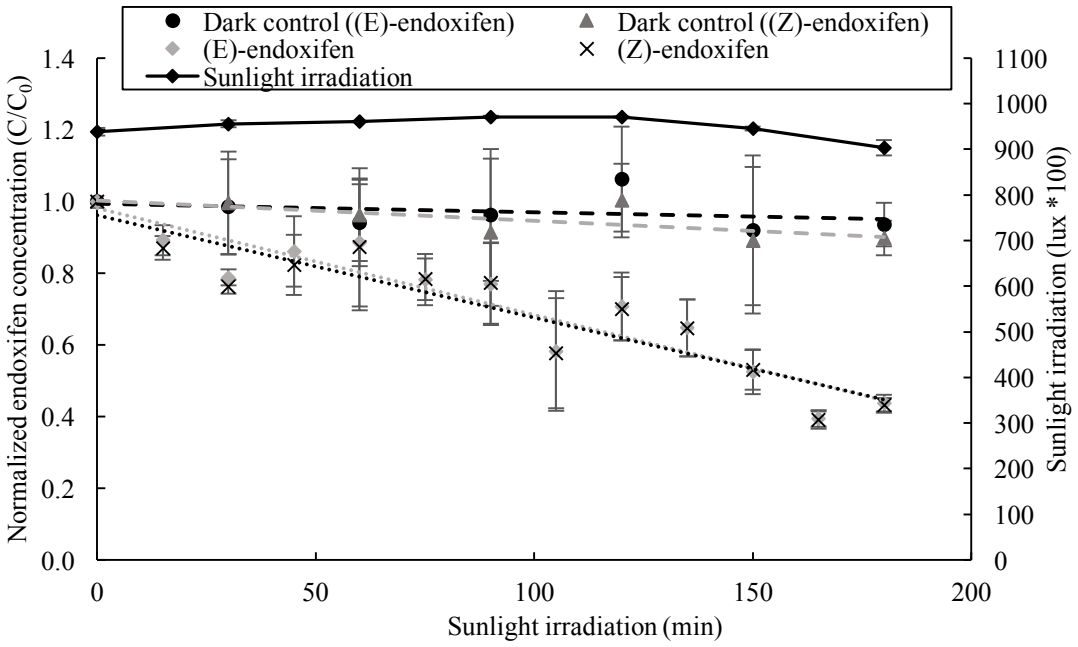

Figure 26. Kinetics of photodegradation of (E)- and (Z)-endoxifen in surface river water at 2 µg mL^{-1} (Photodegradation conditions: pH 7.97, NO_2^- = 0.09 mg L^{-1}, NO_3^- = 5.56 mg L^{-1}, TOC = 9.18 mg L^{-1}, and 8.3°C) irradiated with natural sunlight (90,367-97,133 lux).

4.2.3. Photodegradation by-products of (E)- and (Z)-endoxifen by natural sunlight photodegradation

A HPLC water sample containing (E)- and (Z)-endoxifen isomers at 2 µg mL^{-1} (1:1, w/w) was exposed to natural sunlight for 9 hours in order to determine the generation of PBPs (September 27, 2017,9:00 PAM, Fargo, ND, USA, GPS coordinate: 46.895122, -96.800208). Aliquots were collected with time and directly injected to UHPLC-MS/MS in order to identify their molecular weights and the formed products ions (cone voltage of 27eV). Eleven new peaks (peaks 3 to 13) were observed in the course of the sunlight photodegradation (Figure 27). The first (1) and the second (2) peaks observed in the chromatogram prior sunlight photodegradation (Figure 27a) with retention times of 1.70 and 1.82 minutes suggest that these two peaks were (E)- and (Z)-endoxifen respectively. As shown in Table 5, the ion-*m/z* value (374.21) and the retention

time were the same than those observed for (E)- and (Z)-endoxifen in previous UV light experiments (Table 4). In addition, further MS/MS analyses of these two PBPs with a cone voltage of 27eV confirmed that the first and the second peaks were (E)- and (Z)-endoxifen.

The third (3) and the fourth (4) observed peaks after 2 hours of photodegradation (Figure 27b) with retention times of 1.57 and 1.63 minutes, respectively, presented the same ion-*m/z* values (372.19) and the same formed products ions as the previously identified PB1a and PB1b (Table 4 and Appendix E, Table E.3). Likewise, the fifth (5) and the sixth (6) peaks observed after 6 hours of photodegradation (Figure 27d) with retention times of 1.91 and 2.15 minutes, respectively, present the same ion-*m/z* values (374.21) and the same formed products ions as the previously identified PB2a and PB2b (Table 4 and Appendix E, Table E.3). These results suggest that photodegradation of (E)- and (Z)-endoxifen with natural sunlight initially follows a photodegradation pathway similar to that observed with UV light. However, seven more peaks were observed after 3, 6 and 9 hours of natural sunlight photodegradation (Figure 27c to 27e). The seventh peak (PB3a, b) observed after 3 hours of photodegradation reaction (Figure 27c) with a retention time of 0.96 minutes presents ion-*m/z* of 404.19 suggesting a double hydroxylation of the previously formed PB1a and/or PB1b. Furthermore, dehydroxylation of PB3a and/or PB3b after 6 hours of photodegradation reaction potentially resulted in a new observed peak (8) with a retention time of 1.13 minutes and ion-*m/z* value of 388.19 (PB4a, b). Demethylation of PB4a and/or PB4b could explain the observed ninth peak (9) after 6 hours photodegradation with a retention time of 1.40 minutes and ion-*m/z* of 374.17 (PB5a, b).

The tenth and eleventh peaks (PB6a and PB6b) observed after 6 hours of photodegradation (Figure 27d) with retention times of 1.50 and 1.56 minutes respectively, present the same ion-*m/z* value (360.19) and the same formed products ion suggesting that they are isomers generated from

demethylation of PB2a and PB2b (Appendix E, Table E.3). Further hydroxylation of PB6(a,b) by two hydroxyl groups potentially resulted in the generation of a new PBP observed after 6 hours of photodegradation with a retention time of 1.21 minutes and ion-*m/z* of 378.17 (peak 12; PB7a, b). After 9 hours of sunlight photodegradation, a new peak (13) was observed (Figure 27e) with a retention time of 1.75 minutes and ion-*m/z* of 196.08 (PB8). HPLC-MS/MS analysis of PB8 through formed products ions suggest the presence of a hydroxylated phenantrene nucleo (Appendix E, Table E.3).

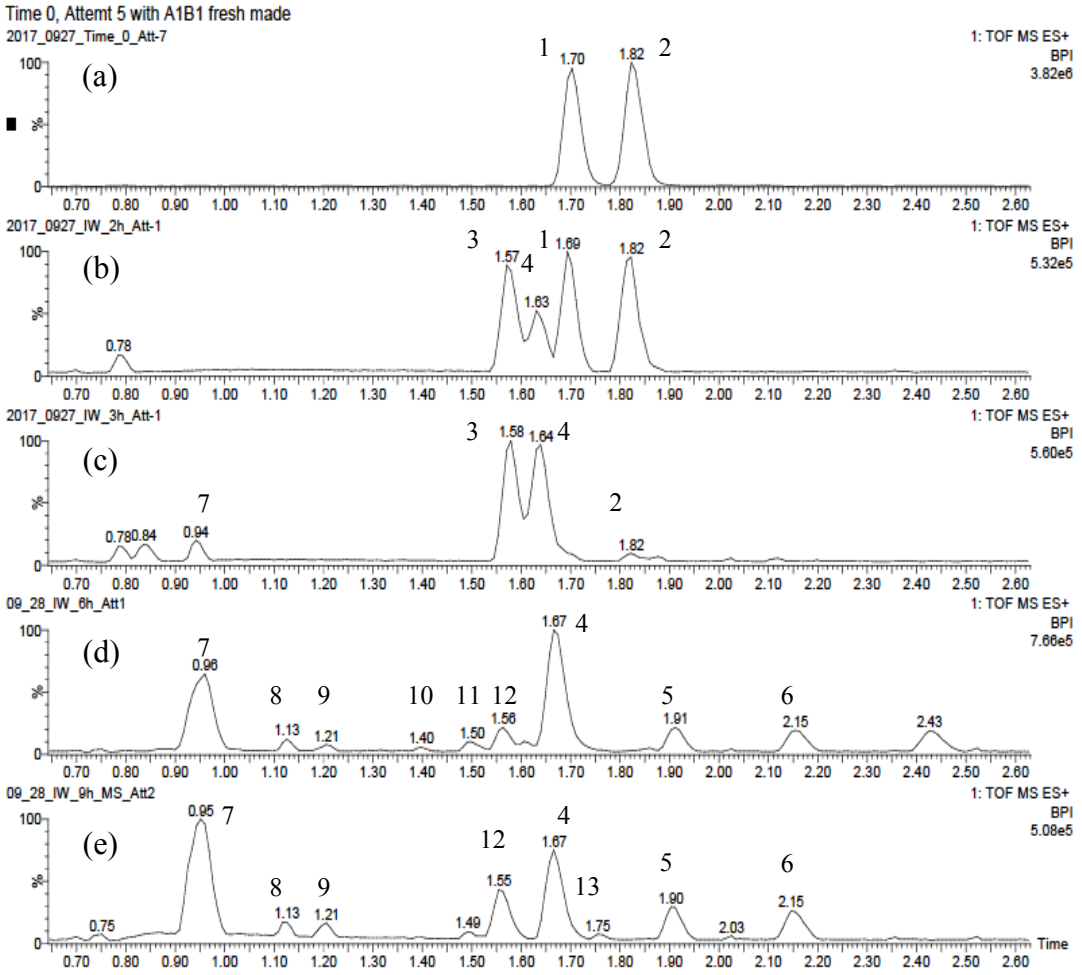

Figure 27. UHPLC-MS chromatogram of aqueous solution of (E)-endoxifen (1; RT = 1.70 minutes), (Z)-endoxifen (2, RT = 1.82 minutes) (2 µg mL^{-1}, pH 7 and 23.4°C and natural sunlight irradiation) and the detection of 8 photodegradation by-products (peaks 3-13): (a) before photodegradation reaction; (b) after 2 hours of photodegradation reaction; (c) after 3 hours of photodegradation reaction; (d) after 6 hours of photodegradation reaction; (e) after 9 hours of photodegradation reaction.

Table 5. Proposed molecular structures and molecular weights of the eight PBPs generated through natural sunlight photodegradation of (E)- and (Z)-endoxifen.

Compound	Predicted Molecular Structure	Rt	Molecular Formula ($M+H^+$)	Expected ion-*m/z*	Theoretical ion-*m/z*	|ppm|
(E)-endoxifen	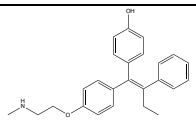	1.69	$C_{25}H_{27}NO_2$	374.2120	374.2110	2.67
(Z)-endoxifen	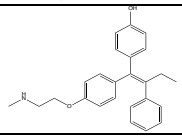	1.81	$C_{25}H_{27}NO_2$	374.2120	374.2111	2.41
PB1a	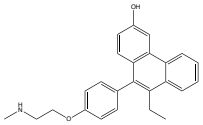	1.56	$C_{25}H_{25}NO_2$	372.1919	372.1953	9.14
PB1b	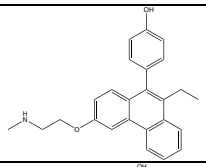	1.67	$C_{25}H_{25}NO_2$	372.1919	372.1954	9.46
PB2a	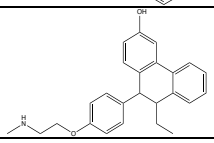	1.91	$C_{25}H_{27}NO_2$	374.2120	374.2112	2.14
PB2b	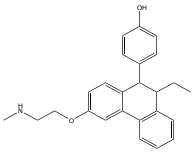	2.15	$C_{25}H_{27}NO_2$	374.2120	374.2111	2.41
PB3 (a, b)	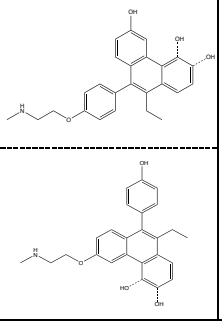	0.96	$C_{25}H_{25}NO_4$	404.1862	404.1856	1.48

Table 5. Proposed molecular structures and molecular weights of the eight PBPs generated through natural sunlight photodegradation of (E)- and (Z)-endoxifen (continued).

Compound	Predicted Molecular Structure	Rt	Molecular Formula ($M+H^+$)	Expected ion-*m/z*	Theoretical ion-*m/z*	|ppm|
PB4 (a, b)	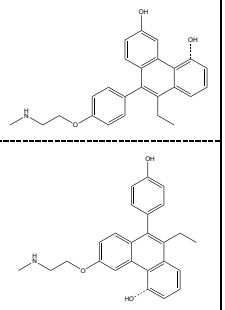	1.14	$C_{25}H_{25}NO_3$	388.1913	388.1904	2.32
PB5 (a, b)	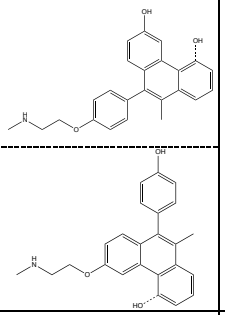	1.40	$C_{24}H_{23}NO_3$	374.1756	374.1742	3.74
PB6a	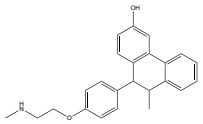	1.56	$C_{24}H_{25}NO_2$	360.1964	360.1951	3.61
PB6b	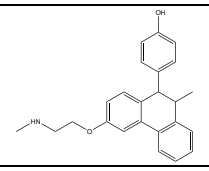		$C_{24}H_{25}NO_2$	360.1964	360.1929	9.72
PB7 (a, b)	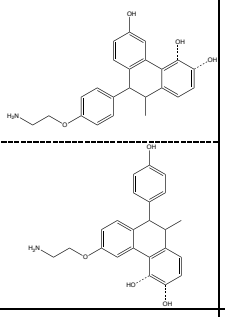	1.21	$C_{23}H_{23}NO_4$	378.1705	378.1696	2.38
PB8	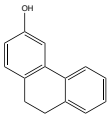	0.75	$C_{14}H_{12}O$	196.0888	196.0877	3.4

Photodegradation of (E)- and (Z)-endoxifen by natural sunlight generated eight PBPs through two different photodegradation pathways (Figures 28 and 29). Hydroxylation and dehydroxylation of benzene nucleus, aromatization by molecular deprotonation, and demethylation were the main chemical reactions occurring during the photodegradation reactions. Similar results were observed by Gros et al. (2015), where photolysis experiments with amisulpride by natural sunlight in wastewater resulted in eight phototransformation by-products generated mainly by hydroxylation and dehydroxilation of aromatic rings and molecular cleavage of small fragments.

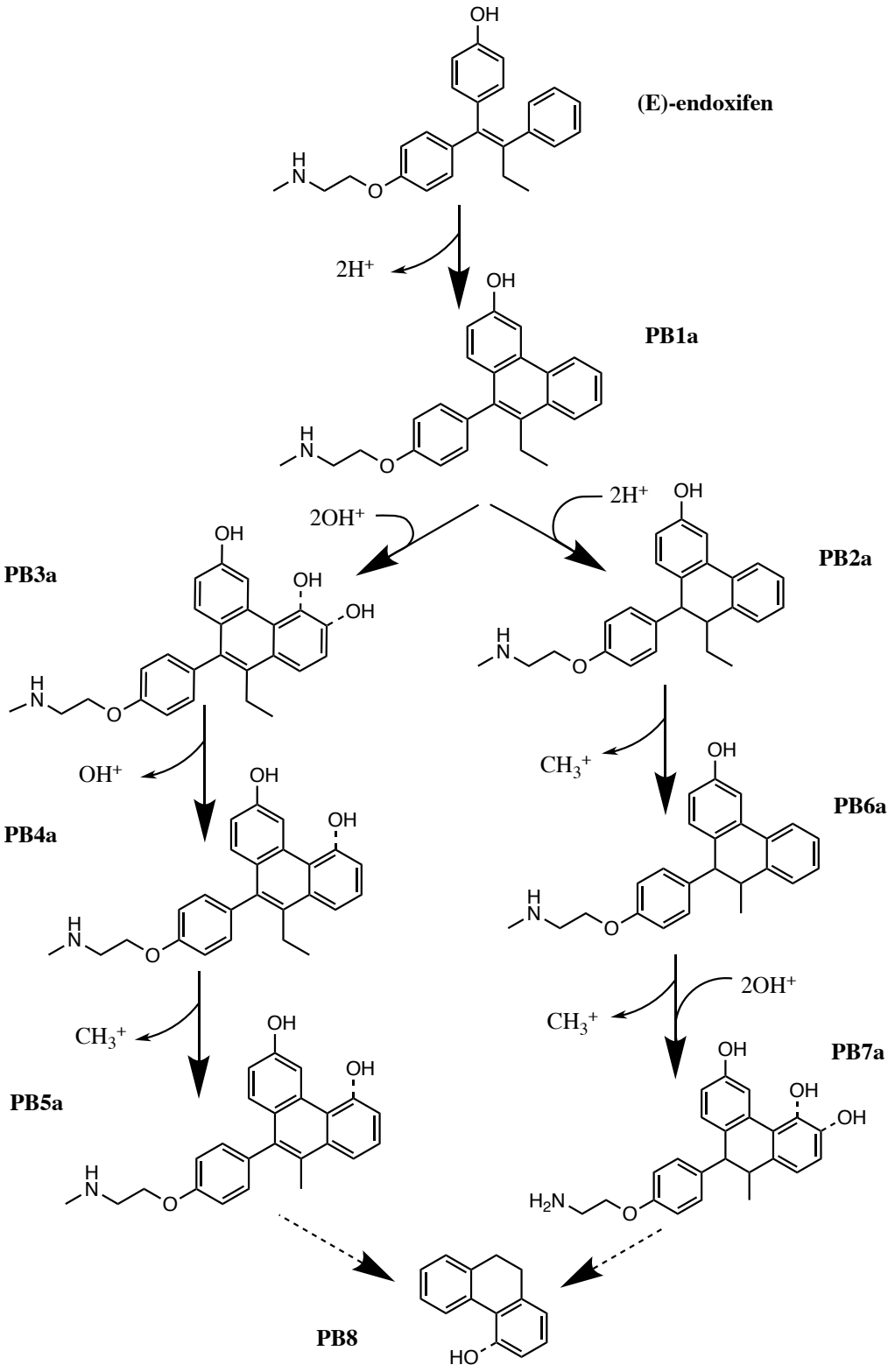

Figure 28. Proposed photodegradation pathway of (E)-endoxifen irradiated with natural sunlight for 9 hours.

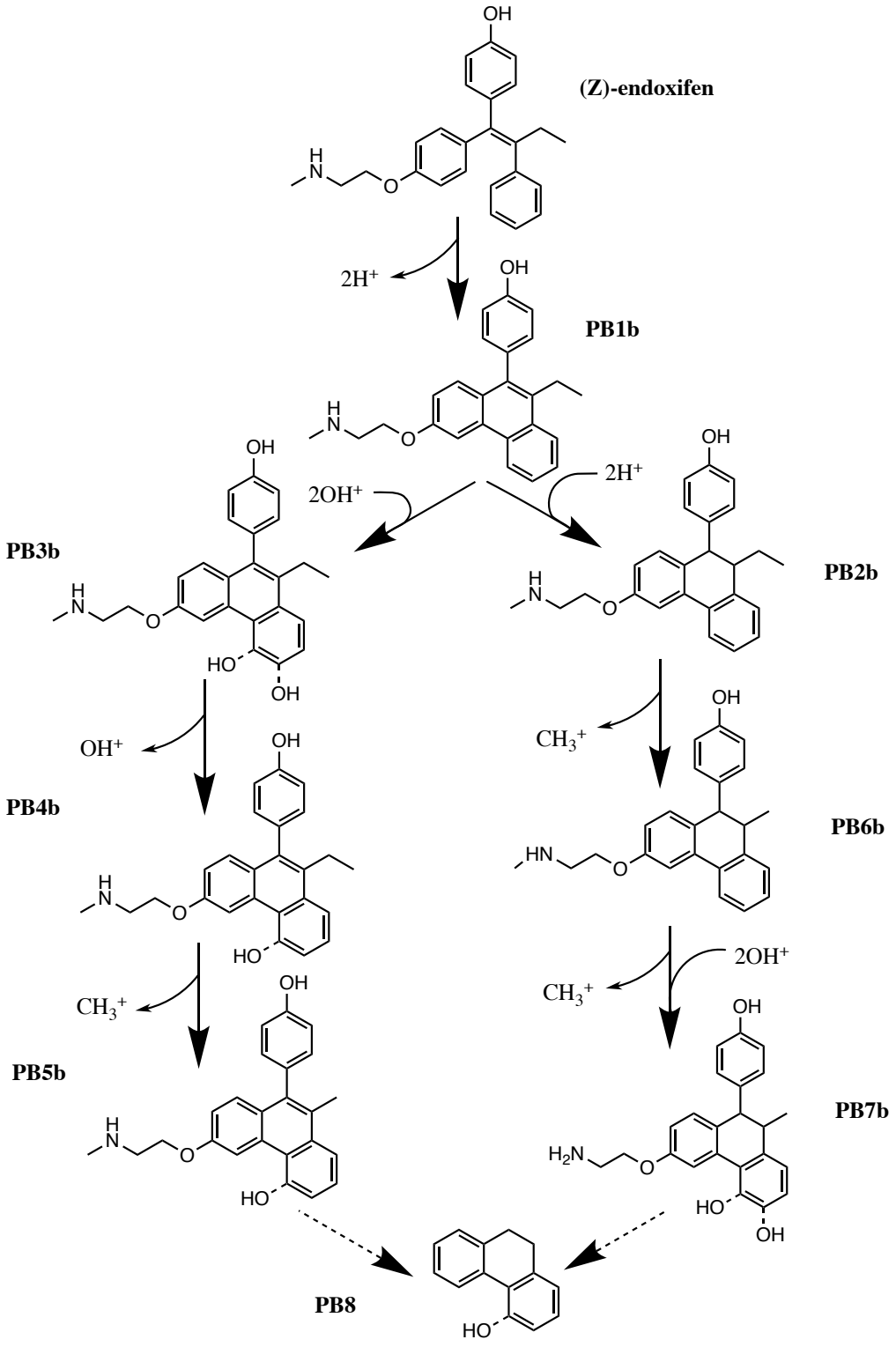

Figure 29. Proposed photodegradation pathway of (Z)-endoxifen irradiated with natural sunlight for 9 hours.

4.3. Toxicity study

4.3.1. Toxicity Assessment of (E)- and (Z)-endoxifen and its PBPs

There has been only one study by Borgatta et al. (2015) that examined the aquatic toxicity of endoxifen. There are no toxicity assessments on the potential effects of endoxifen in the aquatic environment (Borgatta et al., 2015). This lack of information on the toxicity of endoxifen has led to a proposal to use the same PNEC as tamoxifen (Government of Canada, 2015). Endoxifen is 100-folds more potent than tamoxifen (Borgatta et al., 2015). Therefore, the toxicity of (E)- and (Z)-endoxifen and their photodegradation by-products (PBs) should be assessed.

The toxicity of (E)-endoxifen, (Z)-endoxifen, and their eight previously identified PBPs were assessed using TEST (USEPA, 2016). Among different options offered by TEST, the 50% Lethal Concentration (LC_{50}) acute end-points of a crustacean *Daphnia magna* (48h) and a fish fathead minnow (96 h) were selected because they are more suitable for aquatic toxicity assessments (Negreira et al., 2014). Furthermore, LC_{50} predictions for *D. magna* and fathead minnow for endoxifen PBPs were based on coefficients of similarities greater than 0.5 between the molecular structures of PBPs and those of analytes used by the software confirming the reliability of the modeling results. It should be noted that predictions by TEST rely on experimental toxicity results of compounds/analytes (available through database) that have molecular structures similar to compounds of interest. The more molecular structure similarity, the more reliable the prediction. TEST also offers the calculation of the 50% impairment growth concentration (IGC_{50}) of the protozoa *Tetrahymena pyriformis* which is widely used for aquatic toxicology (Sauvant et al., 1999). However, for this study, predicted *T. pyriformis* IGC_{50} was unreliable due to low similarity between the molecular structures of endoxifen PBPs and those of the analytes used by

TEST (the observed similarity coefficients were < 0.5 suggesting unreliable modeling results). The rest of the indicators and conditions offered by TEST is not relevant to aquatic toxicology.

The acute toxicity LC_{50} (48-h) of *D. magna* was lower for (E)- and (Z)-endoxifen (1.45 μg mL^{-1}) than seven of their PBPs ($PB1_{(a,b)}$ to $PB7_{(a,b)}$) with the values ranging from 0.21 μg mL^{-1} to 0.36 μg mL^{-1} (Figure 30). These modeling results suggest that $PB1_{(a,b)}$, $PB2_{(a,b)}$, $PB3_{(a,b)}$, $PB4_{(a,b)}$, $PB5_{(a,b)}$, $PB6_{(a,b)}$ and $PB7_{(a,b)}$ are more toxic than (E)- and (Z)-endoxifen. Further photodegradation of $PB5_{(a,b)}$ and $PB7_{(a,b)}$ led to the formation of PB8 which showed lower toxicity than (E)-and (Z)-endoxifen (LC_{50} for *D. magna* of 2.25 μg mL^{-1}). The results for fathead minnow showed the same trend as those for *D. magna*. Therefore, photodegradation of (E)- and (Z)-endoxifen by UV light resulted in two photodegradation by-products ($PB1_{(a,b)}$ and $PB2_{(a,b)}$) with more toxicity than endoxifen while photodegradation with natural sunlight resulted in 7 PBPs ($PB1_{(a,b)}$ to $PB7_{(a,b)}$) with more toxicity and only one PBP (PB8) with less toxicity than (E)-and (Z)-endoxifen. According to the European Commission Regulation (EC) No 1272 (2008), substances with acute toxicity LC_{50} for *D. magna* and fathead minnow ≤ 1 μg mL^{-1} are considered hazardous to the aquatic environment. However, further experimental work is needed to confirm the modeling results although QSAR predictions are known to be reliable if the molecular structures of the compounds used for the analyses are sufficiently similar to the analytes of interest (He and Jurs, 2005).

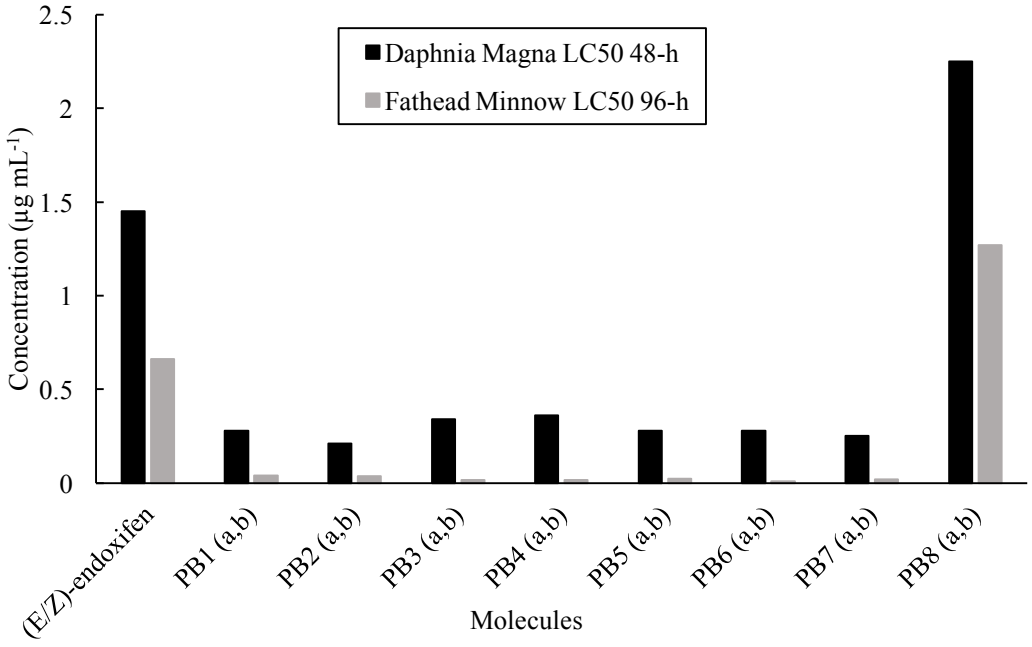

Figure 30. Toxicity data obtained through TEST QSAR assessment.

Photodegradation of (E)- and (Z)-endoxifen resulted in PBPs that are less toxic than products generated from chlorination of endoxifen observed by Negreira et al. (2015). Chlorination of endoxifen potentially generated five DBPs through hydroxylation, chlorination and aromatization (Figure 31). The toxicity assessment of these DBPs by TEST (US EPA, 2016) showed acute toxicity LC_{50} values for *D. magna* from 0.008 to 0.130 µg mL^{-1} (Negreira et al., 2015). According to Larson and Berenbaum (1988), UV light disinfection process in WWTPs should produce less toxic DPBs than chlorination process. Likewise, photodegradation of (E)- and (Z)-endoxifen by UV light in this study resulted in products that are less toxic than DBPs from chlorination of endoxifen. Photodegradation by natural-sunlight also resulted in photodegradation by-products less toxic than chlorination DPBs. Therefore, UV light disinfection process and photodegradation by natural sunlight in WWTP with lagoon system seems a better option to treat wastewater containing (E)- and (Z)-endoxifen than chlorination process. However, all three

processes (UV light, sunlight, and chlorination) provided by-products that are more toxic than the parent compounds.

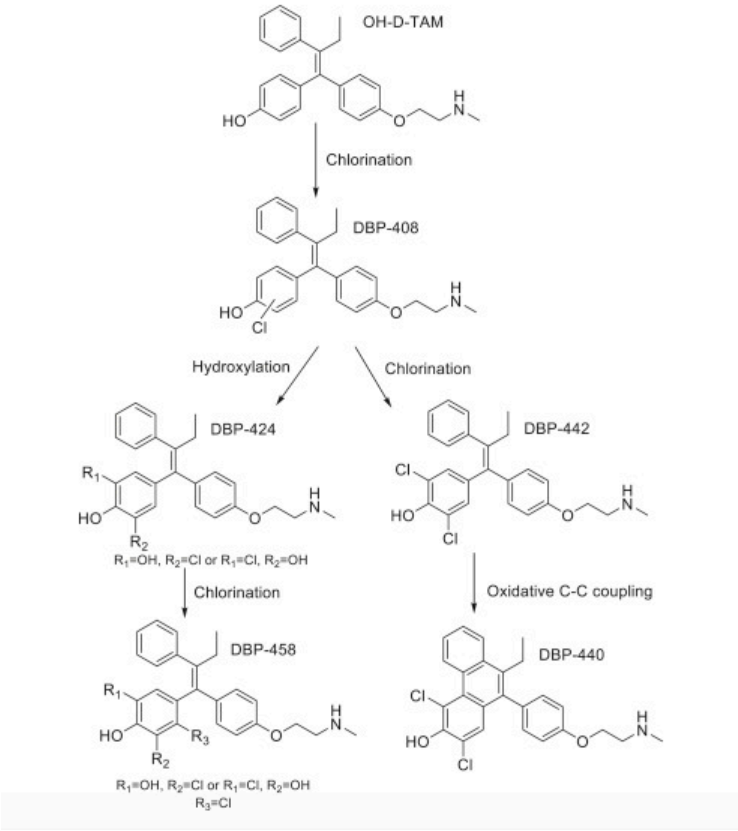

Figure 31. By-products generated from chlorination of endoxifen (Negreira et al., 2015).

4.3.2. Acute toxicity test

Toxicity based on sensitivity of the crustacean D. *magna* has been widely used in water quality monitoring programs in order to evaluate the acute toxicity of chemical compounds released to the water environment (Martins et al., 2007). In the present work, the acute ecotoxicity of (E)- and (Z)-endoxifen is evaluated by measuring the mortality of *D. magna* exposed for 48 hours to five different concentrations of endoxifen: 11.60, 5.80, 2.90, 1.45, and 0.73 μg mL^{-1}. These concentrations were selected based on previous TEST modeling results where the LC_{50} (48 h) of *D. magna* was 1.45 μg mL^{-1}. However, modelling analyses performed in the present study

(section 4.3.1) showed lower LC_{50} values for *D. magna* than the calculated in vivo (Figure 32). A linear regression analysis based on the in vivo acute toxicity test of *D. magna* showed a LC_{50} (48 h) value of 4.96±0.84 μg mL^{-1}.According to Blaauboer et al. (2006), biokinetics of the target compound could play and important role during in vivo analyses. The distribution of the target compound in the solution could be uneven due to absorption, metabolism or elimination by the target organ ending up in lower or higher concentrations (Blaauboer et al., 2006). Therefore, it is difficult to extrapolate a toxic dose from modelling analysis to in vivo assays (Blaauboer et al., 2006).

The available information to compare the acute ecotoxicity result is very limited Borgatta et al. (2015) performed a two-generation study in vivo where the effect of endoxifen on reproduction and growth was determined for *Daphnia pulex*. They reported a 100% mortality of *D. pulex* exposed to endoxifen at 0.2 μg mL^{-1} for 4 days, which was the higher tested concentration. In the present work, the LC_{50} value was higher than that reported by Borgatta et al. (2015). It could be explained by the shorter exposure time of *D. magna* to endoxifen (2 days versus 4 days for Borgatta's study) and the established mortality measurement at 50% of the population instead of 100%.

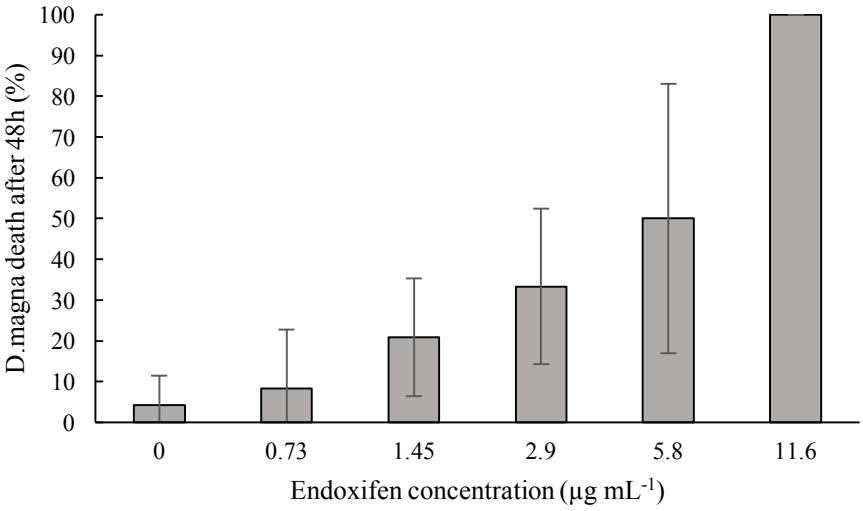

Figure 32. Effect of endoxifen concentration (µg mL^{-1}) on *D. magna* by percentage of population death after 48 hours of exposure.

CHAPTER 5. CONCLUSIONS AND RECOMMENDATIONS FOR FUTURE WORK

5.1. Conclusions

Photodegradation process based on monochromatic UV light irradiation at 253.7 nm is an efficient process for removing (E)- and (Z)-endoxifen from water. The irradiation resulted in ≥ 99.1% elimination of (E)- and (Z)-endoxifen at a light dose of 513 mJ/cm^2. The use of higher emission light intensities provided greater photodegradation rates. The initial concentrations of (E)- and (Z)-endoxifen impacted the photodegradation rates. A linear relationship was observed between the initial concentration and the photodegradation rates of (E)- and (Z)-endoxifen. This observation suggests that collisions of (E)- and (Z)-endoxifen molecules during the excited state could play an important role in the photodegradation. On the contrary, the solution pH (5 to 9) was not a meaningful parameter for the photodegradation. Limited pH reduction after the photodegradation in alkaline, neutral and slightly acidic solutions indicates that (E)- and (Z)-endoxifen become more acidic during the lowest excitation state due to their acid-base property. In addition, the irradiation of (E)-and (Z)-endoxifen with UV light at 244 W cm^{-1} s^{-1}for 120 minutes resulted in mineralization of endoxifen in water at 73.4%.

Natural sunlight also photodegraded endoxifen in water. An effective elimination of (E)- and (Z)-endoxifen in water was observed after 180 minutes of solar radiation reducing the concentration by 90 and 93%, respectively. Unlike photodegradation experiments with UV light, the photodegradation rate of endoxifen was higher in pure water than in wastewater and surface water. The presence of dissolved organic matter in wastewater and surface water likely caused a photoinhibition of endoxifen when irradiated with natural sunlight. It is well known that the composition of DOM plays a role in higher or lower photodegradation due to its ability to act as a photosensitizer or photoinhibitor. (E)- and (Z)-endoxifen in wastewater were photodegraded by

natural sunlight at 85 and 83%, respectively while in receiving surface water both of them were degraded 62%.

Although UV and natural sunlight photodegradation is a promising process for degrading (E)- and (Z)-endoxifen in water, seven PBPs, potentially more toxic than (E)- and (Z)-endoxifen, were observed along the photodegradation time course. During UV light photodegradation experiments, two PBPs from aromatization of (E)- and (Z)-endoxifen (PB1a and PB1b) were identified. Further hydrogenation of PB1a and PB1b provided the third PBP which by modeling is a highly toxic compound. PB1a and PB1b were also observed during the photodegradation of (E)- and (Z)-endoxifen in wastewater with UV light doses similar to those applied at WWTPs. Therefore, highly toxic compounds are potentially generated at WWTPs during UV disinfection process if (E)- and (Z)-endoxifen are present in the treated wastewater. In addition to the three aforementioned PBPs, five more PBPs were observed during sunlight photodegradation experiments. By modeling, four of these PBPs (PB4, PB5, PB6 and PB7) were more toxic than the parent compound and only one PBP (PB8), observed after 9 hours of photodegradation reaction, was less toxic than endoxifen itself. The in vivo acute toxicity test of endoxifen with *D. magna* provided higher LC_{50} (48h) than the modeling result (1.45 μg mL^{-1} for modeling versus 4.98 μg mL^{-1} for vivo).

Natural sunlight experiments revealed that endoxifen photodegradation follows a zero order reaction in water and receiving surface water while a first order model was observed in wastewater. These results suggest that photodegradation of endoxifen by natural sunlight occurs through direct photolysis and the degradation rate relies on the intensity of the solar radiation. A first order reaction was also observed for endoxifen in water during UV light experiments while a second order kinetics model was the case for wastewater. The presence of organic and inorganic

molecules in wastewater that absorb UV light could lead to sensitized photodegradation of (E)- and (Z)-endoxifen resulting in higher photodegradation rates and consequently greater generation of PBPs. The presence of these PBPs in the water environment could bring negative effects to aquatic lives.

5.2. Recommendations for future works

Endoxifen is a relatively new contaminant. More studies on their fate and transport, treatment, and toxicology are needed and therefore recommended as follows.

- Modelled physical and chemical properties of endoxifen should be confirmed experimentally to better understand the fate of endoxifen in the environment.
- Limits of detection and quantification of HPLC methods should be improved to identify actual and exact concentrations of endoxifen in engineered and natural systems and to determine photodegradability of (E)- and (Z)-endoxifen in WWTPs at ppb concentrations.
- Environmental risk assessments and in vivo toxicity studies of endoxifen and its PBPs in the aquatic environment are needed.
- Advanced oxidation processes using UV and other oxidants such as ozone and peroxide should be evaluated as methods to drive the endoxifen degradation pathway completely beyond its toxic PBPs.

REFERENCES

Ahmad, A., Ali, S.M., Ahmad, M.U., Sheikh, S., Ahmad, I. (2010). Orally administered endoxifen is a new therapeutic agent for breast cancer. Breast Cancer Research Treatment, 122 (2), 579–84.

Andreozzi, R., Raffaele, M., Nicklas, P. (2003). Pharmaceuticals in STP effluents and their solar photodegradation in aquatic environment. Chemosphere, 50, 1319–1330.

Antunes, M.V., Raymundo, S., de Oliveira, V., Staudt, D.E., Gössling, G., Peteffi, G.P., Biazús, J.V., Cavalheiro, J.A., Tre-Hardy, M., Capron, A., Haufroid, V., Wallemacq, P., Schwartsmann, G., Linden, R. (2015). Ultra-high performance liquid chromatography tandem mass spectrometric method for the determination of tamoxifen, N-desmethyltamoxifen, 4-hydroxytamoxifen and endoxifen in dried blood spots--development, validation and clinical application during breast cancer adjuvant therapy. Talanta, 132, 775–784.

Aranda, E.O., Esteve-Romero, J., Rambla-Alegre, M., Peris-Vicente, J., Bose, D. (2011). Development of a methodology to quantify tamoxifen and endoxifen in breast cancer patients by micellar liquid chromatography and validation according to the ICH guidelines. Talanta, 84(2), 314–318.

Ashton, D., Hilton, M., Thomas, K. V. (2004). Investigating the environmental transport of human pharmaceuticals to streams in the United Kingdom. Science of the Total Environment, 333 (1-3), 167–84.

Besse, J.P., Latour, J.F., Garric, J., (2012). Anticancer drugs in surface waters. What can we say about the occurrence and environmental significance of cytotoxic, cytostatic and endocrine therapy drugs? Environmental International, 39(1), 73–86.

BestUV. (2011). bestUV. http://www.bestuv.com (Accessed 6.20.17).

Binkhorst, L., Mathijssen, R.H.J., Ghobadi Moghaddam-Helmantel, I.M., de Bruijn, P., van Gelder, T., Wiemer, E.A.C., Loos, W.J. (2011). Quantification of tamoxifen and three of its phase-I metabolites in human plasma by liquid chromatography/triple-quadrupole mass spectrometry. Journal of Pharmaceutical Biomedical Analysis, 56(5), 1016–1023.

Blaauboer, B.J., Hermens, J., van Eijkeren, J. (2006). Estimating acute toxicity based on in vitro cytotoxicity: role of biokinetic modelling. ALTEX Alternativen zu Tierexperimenten, 23, 250–253.

Bolton, J.R., Stefan, M.I., Shaw, P.-S., Lykke, K.R. (2011). Determination of the quantum yields of the potassium ferrioxalate and potassium iodide–iodate actinometers and a method for the calibration of radiometer detectors. Journal of Photochemistry and Photobiology A: Chemistry, 222, 166–169.

Boreen, A.L., Arnold, W.A., McNeill, K. (2004). Photochemical fate of sulfa drugs in the aquatic environment: sulfa drugs containing five-membered heterocyclic groups. Science of the Total Environment, 38, 3933–40.

Borgatta, M., Decosterd, L.-A., Waridel, P., Buclin, T., Chèvre, N. (2015). The anticancer drug metabolites endoxifen and 4-hydroxy-tamoxifen induce toxic effects on Daphnia pulex in a two-generation study. Science of the Total Environment, 520, 232–40.

Challis, J.K., Hanson, M.L., Friesen, K.J., Wong, C.S. (2014). A critical assessment of the photodegradation of pharmaceuticals in aquatic environments: defining our current understanding and identifying knowledge gaps Environmental impact. Environmental Science: Process Impacts, 16(4), 672–696.

Chiou, C.-H., Juang, R.-S. (2007). Photocatalytic degradation of phenol in aqueous solutions by Pr-doped TiO2 nanoparticles. Journal of Hazardous Materials, 149(1), 1–7.

Chowdhury, P., Athapaththu, S., Elkamel, A., Ray, A.K. (2017). Visible-solar-light-driven photo-reduction and removal of cadmium ion with Eosin Y-sensitized TiO2 in aqueous solution of triethanolamine. Purifiying Technology, 174, 109-115.

Clara, M., Gans, O., Windhofer, G., Krenn, U., Hartl, W., Braun, K., Scharf, S., Scheffknecht, C. (2011). Occurrence of polycyclic musks in wastewater and receiving water bodies and fate during wastewater treatment. Chemosphere, 82, 1116–1123.

Coetsier, C.M., Spinelli, S., Lin, L., Roig, B., Touraud, E. (2009). Discharge of pharmaceutical products (PPs) through a conventional biological sewage treatment plant: MECs vs PECs? Environment International 35, 787–792.

Cory, R.M., Harrold, K.H., Neilson, B.T., Kling, G.W. (2015). Controls on dissolved organic matter (DOM) degradation in a headwater stream: The influence of photochemical and hydrological conditions in determining light-limitation or substrate-limitation of photo-degradation. Biogeosciences 12, 6669–6685.

Darby, J.L., Snider, K.E., Tchobanoglous, G. (1993). Ultraviolet disinfection for wastewater reclamation and reuse subject to restrictive standards. Water Environmental Research, 65, 169–180.

Dobrović, S., Juretić, H., Ružinski, N., Dobrovi, S., Jureti, H. (2017). Photodegradation of natural organic matter in water with UV irradiation at 185 and 254 nm: importance of hydrodynamic conditions on the decomposition rate. Separation Science and Technology, 42, 1421–1432.

Drooger, J.C., Jager, A., Lam, M.-H., den Boer, M.D., Sleijfer, S., Mathijssen, R.H.J., de Bruijn, P. (2015). Development and validation of an UPLC–MS/MS method for the quantification of tamoxifen and its main metabolites in human scalp hair. Journal of Pharmaceutical and Biomedical Analysis, 114, 416–425.

Elkins, P., Coleman, D., Burgess, J., Gardner, M., Hines, J., Scott, B., Kroenke, M., Larson, J., Lightner, M., Turner, G., White, J., Liu, P. (2014). Characterization of the isomeric configuration and impurities of (Z)-endoxifen by 2D NMR, high resolution LC-MS, and quantitative HPLC analysis. Journal of Pharmaceutical and Biomedical Analysis, 88, 174–9.

Elmorsi, T.M., Riyad, Y.M., Mohamed, Z.H., Abd El Bary, H.M.H. (2010). Decolorization of mordant red 73 azo dye in water using H2O2/UV and photo-fenton treatment. Journal of Hazardous Materials, 174, 352–358.

EPA. (2002). Wastewater Technology Fact Sheet - Disinfection for small systems. Water Technology.

European Commission Regulation (EC) No 1272, 2008. Notification of new chemical substances in accordance with directive 67/548/EEC on the classification, packaging, and labelling of dangerous substances : no-longer polymers list. Office for Official Publications of the European Communities.

Evgenidou, E.N., Konstantinou, I.K., Lambropoulou, D.A. (2015). Occurrence and removal of transformation products of PPCPs and illicit drugs in wastewaters: a review. Science of the Total Environment, 505, 905–26.

Fatta-Kassinos, D., Vasquez, M.I., Kümmerer, K. (2011). Transformation products of pharmaceuticals in surface waters and wastewater formed during photolysis and

advanced oxidation processes – Degradation, elucidation of byproducts and assessment of their biological potency. Chemosphere, 85, 693–709.

Fauq, A.H., Maharvi, G.M., Sinha, D., (2010). A convenient synthesis of (Z)-4-hydroxy-N-desmethyltamoxifen (endoxifen). Bioorganic & Medicinal Chemistry Letters, 20(10), 3036–3038.

Ferrando-Climent, L., Rodriguez-Mozaz, S., Barceló, D. (2013). Development of a UPLC-MS/MS method for the determination of ten anticancer drugs in hospital and urban wastewaters, and its application for the screening of human metabolites assisted by information-dependent acquisition tool (IDA) in sewage samples. Analytical and Bioanalytical Chemistry, 405(18), 5937–5952.

Fisher, B., Costantino, J.P., Wickerham, D.L., Cecchini, R.S., Cronin, W.M., Robidoux, A., Bevers, T.B., Kavanah, M.T., Atkins, J.N., Margolese, R.G., Runowicz, C.D., James, J.M., Ford, L.G., Wolmark, N. (2005). Tamoxifen for the prevention of breast cancer: Current status of the national surgical adjuvant breast and bowel project P-1 Study. Journal of the National Cancer Institute, 97, 1652–1662.

Franquet-Griell, H., Medina, A., Sans, C., Lacorte, S. (2017). Biological and photochemical degradation of cytostatic drugs under laboratory conditions. Journal of Hazardous Materials, 323, 319–328.

Fujishima, A., Rao, T.N., Tryk, D.., 2000. TiO2 photocatalysts and diamond electrodes. Electrochimica Acta, 45, 4683–4690.

Garcia-Rodríguez, A., Matamoros, V., Fontàs, C., Salvadó, V. (2014). The ability of biologically based wastewater treatment systems to remove emerging organic contaminants—a review. Environmental Science and Pollution Research, 21, 11708–11728.

Goverment of Canada. (2015). Screening assessment - Ethanamine, 2-[4[(1Z)-1,2-diphenyl-1-butenyl]phenoxy]-N, N-dimethyl- (Tamoxifen): Chemical Abstracts Service registry number 10540-29-1.

Gros, M., Williams, M., Llorca, M., Rodriguez-Mozaz, S., Barceló, D., Kookana, R.S. (2015). Photolysis of the antidepressants amisulpride and desipramine in wastewaters: Identification of transformation products formed and their fate. Science of the Total Environment, 530–531, 434–444.

Gruchlik, Y., Linge, K., Joll, C. (2018). Removal of organic micropollutants in waste stabilisation ponds: A review. Journal of Environmental Management, 206, 202–214.

Guerard, J.J., Chin, Y.P. (2012). Photodegradation of ormetoprim in aquaculture and stream-derived dissolved organic matter. Journal of Agricultural and Food Chemistry, 60, 9801–9806.

Guo, M., Hu, H., Bolton, J.R., El-Din, M.G. (2009). Comparison of low- and medium-pressure ultraviolet lamps: Photoreactivation of Escherichia coli and total coliforms in secondary effluents of municipal wastewater treatment plants. Water Research, 43, 815–821.

He, L., Jurs, P.C. (2005). Assessing the reliability of a QSAR model's predictions. Journal of Molecular Graphic and Modelling, 23, 503–523.

Heath, E., Česen, M., Negreira, N., de Alda, M.L., Ferrando-Climent, L., Blahova, L., Nguyen, T.V., Adahchour, M., Ruebel, A., Llewellyn, N., Ščančar, J., Novaković, S., Mislej, V., Stražar, M., Barceló, D., Kosjek, T. (2016). First inter-laboratory comparison exercise for the determination of anticancer drugs in aqueous samples. Environmental Science and Pollution Research, 23, 14692–14704.

Heberer, T. (2002). Occurrence, fate, and removal of pharmaceutical residues in the aquatic environment: a review of recent research data. Toxicology Letter, 131, 5–17.

Heberer, T., Reddersen, K., Mechlinski, A. (2002). From municipal sewage to drinking water: fate and removal of pharmaceutical residues in the aquatic environment in urban areas. Water Science and Technology, 46, 81–8.

Helland, T., Gjerde, J., Dankel, S., Fenne, I.S., Skartveit, L., Drangevåg, A., Bozickovic, O., Flågeng, M.H., Søiland, H., Mellgren, G., Lien, E.A. (2015). The active tamoxifen metabolite endoxifen (4OHNDtam) strongly down-regulates cytokeratin 6 (CK6) in MCF-7 breast cancer cells. PLoS One 10(4), 1-19.

Hoque, M.E., Cloutier, F., Arcieri, C., McInnes, M., Sultana, T., Murray, C., Vanrolleghem, P.A., Metcalfe, C.D. (2014). Removal of selected pharmaceuticals, personal care products and artificial sweetener in an aerated sewage lagoon. Science of the Total Environment, 487, 801–12.

Hoskins, J.M., Carey, L.A., McLeod, H.L. (2009). CYP2D6 and tamoxifen: DNA matters in breast cancer. Nature Review Cancer, 9(8), 576–86.

Hu, X.-L., Bao, Y.-F., Hu, J.-J., Liu, Y.-Y., Yin, D.-Q. (2017). Occurrence of 25 pharmaceuticals in Taihu Lake and their removal from two urban drinking water treatment plants and a constructed wetland. Environmental Science and Pollution Research, 24, 14889–14902.

ICH. (2005). Guideline on validation of analytical procedures: Methodology developed to complement the parent guideline. ICH Harmonised Tripartite Guideline Validation of Analytical Procedures, Text and Methodology, Q2 (R1).

Jager, N.G.L., Rosing, H., Linn, S.C., Schellens, J.H.M., Beijnen, J.H. (2012). Importance of highly selective LC-MS/MS analysis for the accurate quantification of tamoxifen and its

metabolites: focus on endoxifen and 4-hydroxytamoxifen. Breast Cancer Research and Treatment, 133(2), 793–8.

Jaremko, M., Kasai, Y., Barginear, M.F., Raptis, G., Desnick, R.J., Yu, C. (2010). Tamoxifen metabolite isomer separation and quantification by liquid chromatography-tandem mass spectrometry. Analytical Chemistry, 82(24), 10186–10193.

Jin, X., Xu, H., Qiu, S., Jia, M., Wang, F., Zhang, A., Jiang, X. (2017). Direct photolysis of oxytetracycline: Influence of initial concentration, pH and temperature. Journal of Photochemistry and Photobiology, 332, 224–231.

Jo, W.-K., Kumar, S., Isaacs, M.A., Lee, A.F., Karthikeyan, S. (2017). Cobalt promoted TiO_2/GO for the photocatalytic degradation of oxytetracycline and congo red. Applied Catalysis, 201, 159–168.

Johnson, A.C., Oldenkamp, R., Dumont, E., Sumpter, J.P. (2013). Predicting concentrations of the cytostatic drugs cyclophosphamide, carboplatin, 5-fluorouracil, and capecitabine throughout the sewage effluents and surface waters of europe. Environmental and Toxicology Chemistry, 32(9), 1954–1961.

Johnson, M.D., Zuo, H., Lee, K.-H., Trebley, J.P., Rae, J.M., Weatherman, R. V, Desta, Z., Flockhart, D.A., Skaar, T.C. (2004). Pharmacological characterization of 4-hydroxy-N-desmethyl tamoxifen, a novel active metabolite of tamoxifen. Breast Cancer Research and Treatment, 85(2), 151–9.

Kisanga, E.R., Mellgren, G., Lien, E.A. (2005). Excretion of hydroxylated metabolites of tamoxifen in human bile and urine. Anticancer Research, 25(6C), 4487–4492.

Knacker, T., Boettcher, M., Frische, T., Rufli, H., Stolzenberg, H.-C., Teigeler, M., Zok, S., Braunbeck, T., Schäfers, C. (2010). Environmental effect assessment for sexual

endocrine-disrupting chemicals: Fish testing strategy. Integrated Environmental Assessment and Management, 6(4), 653–662.

Kopec, R.E., Schweiggert, R.M., Riedl, K.M., Carle, R., Schwartz, S.J. (2013). Comparison of high-performance liquid chromatography/tandem mass spectrometry and high-performance liquid chromatography/photo-diode array detection for the quantitation of carotenoids, retinyl esters, α-tocopherol and phylloquinone in chylomicron-rich fractions of human plasma. Rapid Communication in Mass Spectrometry, 27, 1393–402.

Koumaki, E., Mamais, D., Noutsopoulos, C., Nika, M.C., Bletsou, A.A., Thomaidis, N.S., Eftaxias, A., Stratogianni, G. (2015). Degradation of emerging contaminants from water under natural sunlight: The effect of season, pH, humic acids and nitrate and identification of photodegradation by-products. Chemosphere, 138, 675–681.

Kovalova, L., Siegrist, H., Singer, H., Wittmer, A., McArdell, C.S. (2012). Hospital wastewater treatment by membrane bioreactor: performance and efficiency for organic micropollutant elimination. Environmental Science and Technology, 46(3), 1536–45.

Lam, M.W., Mabury, S.A. (2005). Photodegradation of the pharmaceuticals atorvastatin, carbamazepine, levofloxacin, and sulfamethoxazole in natural waters. Aquatic Sciences, 67, 177–188.

Lara-Martín, P.A., González-Mazo, E., Petrovic, M., Barceló, D., Brownawell, B.J. (2014). Occurrence, distribution and partitioning of nonionic surfactants and pharmaceuticals in the urbanized Long Island Sound Estuary (NY). Marine Pollution Bulletin, 85(2), 710–719.

Larson, R.A., Berenbaum, M.R. (1988). Environmental phototoxicity solar ultraviolet radiation affects the toxicity of natural and man-made chemicals. Environmental Science and Technology, 22(4), 354–360.

Lawrence, M., Marzzacco, C.J., Morton, C., Schwab, C., Halpern, A.M. (1991). Excited-state deprotonation of 2-naphthol by anions. Journal of Physical Chemistry, 95, 10294–10299.

Li, X., Zheng, W., Kelly, W.R. (2013). Occurrence and removal of pharmaceutical and hormone contaminants in rural wastewater treatment lagoons. Science of the Total Environment, 445–446, 22–8.

Lin, A.Y.-C., Reinhard, M. (2005). Photodegradation of common environmental pharmaceuticals and estrogens in river water. Environmental and Toxicology Chemistry, 24, 1303–9.

Liu, Z.H., Zhang, Y. G., Wang, D.S. (2010). Studies on feminization, sex determination, and differentiation of the Southern catfish, Silurus meridionalis-a review. Fish Physiology Biochemistry, 36(2), 223-235.

Luo, Y., Guo, W., Ngo, H.H., Nghiem, L.D., Hai, F.I., Zhang, J., Liang, S., Wang, X.C. (2014). A review on the occurrence of micropollutants in the aquatic environment and their fate and removal during wastewater treatment. Science of the Total Environment, 473–474, 619–641.

Maradonna, F., Batti, S., Marino, M., Mita, D.G., Carnevali, O. (2009). Tamoxifen as an emerging endocrine disruptor: Effects on fish reproduction and detoxification target genes. Annuals of the New York Academy of Sciences, 1163(1), 457–459.

Martins, J., Oliva Teles, L., Vasconcelos, V. (2007). Assays with Daphnia magna and Danio rerio as alert systems in aquatic toxicology. Environment International, 33, 414–425.

Mathon, B., Choubert, J.M., Miege, C., Coquery, M. (2016). A review of the photodegradability and transformation products of 13 pharmaceuticals and pesticides relevant to sewage polishing treatment. Science of the Total Environment, 551–552, 712–724.

Mayo Foundation for Medical Education and Research. (2014). Endoxifen shows promise as breast cancer treatment - Mayo Clinic Cancer Center's Online Magazine - Mayo Clinic Research.

Mendenhall, D.W., Kobayashi, A., Mel, F., Shih, L., Sternson, L.A., Fabian, C. (1978). Clinical analysis of tamoxifen, an anti-neoplastic agent, in plasma. Clinical Chemistry, 24, 1518–1524.

Miller, J.S., Olejnik, D. (2001). Photolysis of polycyclic aromatic hydrocarbons in water. Water Research, 35, 233–243.

Mumbo, J., Deyerling, D., Henkelmann, B., Pfister, G., Schramm, K.-W. (2017). Photodegradative fate and potential phototoxic products of bromocarbazoles and chlorocarbazoles in water. Environment Science and Pollution Research Intitute, 24, 27525–27538.

National Institute of Health. (2015). Tamoxifen citrate or Z-endoxifen hydrochloride in treating patients with locally advanced or metastatic, estrogen receptor-positive, HER2-Negative breast cancer.

Negreira, N., de Alda, M.L., Barceló, D. (2014). Cytostatic drugs and metabolites in municipal and hospital wastewaters in Spain: filtration, occurrence, and environmental risk. Science of the Total Environment, 497–498, 68–77.

Negreira, N., Regueiro, J., Lopez de Alda, M., Barcelo, D. (2015). Transformation of tamoxifen and its major metabolites during water chlorination: Identification and in silico toxicity assessment of their disinfection byproducts. Water Research, 85, 199–207.

Oppenländer, T. (2003). Photochemical purification of water and air: Advanced oxidation processes (AOPs)-Principles, reaction mechanisms, reactor concepts. Wiley-VCH.

Peng, J., Sengupta, S., Jordan, V. (2009). Potential of selective estrogen receptor modulators as treatments and preventives of breast cancer. Anticancer Agents in Medicinal Chemistry, 9(5), 481–499.

Pereira, V.J., Linden, K.G., Weinberg, H.S. (2007). Evaluation of UV irradiation for photolytic and oxidative degradation of pharmaceutical compounds in water. Water Research, 41, 4413–4423.

Prados-Joya, G., Sanchez-Polo, M., Rivera-Utrilla, J., Ferro-garcia, M. (2011). Photodegradation of the antibiotics nitroimidazoles in aqueous solution by ultraviolet radiation. Water Research, 45, 393–403.

Pragst, F., Herzler, M., Erxleben, B.-T. (2004). Systematic toxicological analysis by high-performance liquid chromatography with diode array detection (HPLC-DAD). Clinical Chemistry and Laboratory Medicine, 42(11), 1325-1340.

Radjenović, J., Petrović, M., Barceló, D. (2009). Fate and distribution of pharmaceuticals in wastewater and sewage sludge of the conventional activated sludge (CAS) and advanced membrane bioreactor (MBR) treatment. Water Research, 43, 831–841.

Rivas, J., Gimeno, O., Borralho, T., Carbajo, M. (2010). UV-C photolysis of endocrine disruptors. The influence of inorganic peroxides. Journal of Hazardous Materials, 174(1-3), 393–397.

Rivera-Utrilla, J., Sánchez-Polo, M., Ferro-García, M.Á., Prados-Joya, G., Ocampo-Pérez, R. (2013). Pharmaceuticals as emerging contaminants and their removal from water. A review. Chemosphere, 93, 1268–1287.

Roberts, P.H., Thomas, K. V. (2006). The occurrence of selected pharmaceuticals in wastewater effluent and surface waters of the lower Tyne catchment. Science of the Total Environment, 356, 143–53.

Sauvant, M.P., Pepin, D., Piccinni, E. (1999). Tetrahymena pyriformis: a tool for toxicological studies. A review. Chemosphere, 38, 1631–69.

Shemer, H., Kunukcu, Y.K., Linden, K.G. (2006). Degradation of the pharmaceutical Metronidazole via UV, Fenton and photo-Fenton processes. Chemosphere, 63, 269–276.

Shin, G.A., Linden, K.G., Arrowood, M.J., Sobsey, M.D. (2001). Low-pressure UV inactivation and DNA repair potential of Cryptosporidium parvum oocysts. Applied Environmental Microbiology, 67, 3029–32.

Singh, A.K. (2013). Introduction of modern endocrine techniques for the production of monosex population of fishes. General and Comparative Endocrinology, 181, 146–155.

Southern New England Ultraviolet Company, n.d. Rayonet-Reactors. https://rayonet.org (Accessed 6.7.17).

Steiner, A.Z., Terplan, M., Paulson, R.J. (2005). Comparison of tamoxifen and clomiphene citrate for ovulation induction: a meta-analysis. Human Reproduction, 20(6), 1511–5.

Teunissen, S.F., Rosing, H., Schinkel, A.H., Schellens, J.H.M., Beijnen, J.H. (2010). Bioanalytical methods for determination of tamoxifen and its phase I metabolites: A review. Analitycal Chim Acta, 683, 21–37.

Thomas, K. V, Hilton, M.J. (2004). The occurrence of selected human pharmaceutical compounds in UK estuaries. Marine Pollution Bulletin, 49, 436–44.

Tønnesen, H.H. (2004). Photostability of drugs and drug products. Boca Raton, Florida: CRC-Press.

Trawiński, J., Skibiński, R. (2017). Studies on photodegradation process of psychotropic drugs: a review. Environment Science and Pollution Research, 24, 1152–1199.

TRC. (2016). Trc-canada. https://www.trc-canada.com/ (Accessed 2.8.18).

Udom, I., Myers, P.D., Ram, M.K., Hepp, A.F., Archibong, E., Stefanakos, E.K., Yogi Goswami, D. (2014). Optimization of photocatalytic degradation of phenol using simple photocatalytic reactor. American Journal of Analytical Chemistry, 5, 743–750.

Urbatzka, R., Bottero, S., Mandich, A., Lutz, I., Kloas, W. (2007). Endocrine disrupters with (anti)estrogenic and (anti)androgenic modes of action affecting reproductive biology of Xenopus laevis: Effects on sex steroid levels and biomarker expression. Comparative Biochemistry and Physiology Toxicology Pharmacology, 144(4), 310–318.

USEPA. (2016). User's Guide for T.E.S.T. (version 4.2) (Toxicity Estimation Software Tool): A program to estimate toxicity from molecular structure.

USEPA (2003). Ultraviolet disinfection guidance manual.

Van der Ven, L.T.M., van den Brandhof, E.-J., Vos, J.H., Wester, P.W. (2007). Effects of the estrogen agonist 17beta-estradiol and antagonist tamoxifen in a partial life-cycle assay with zebrafish (Danio rerio). Environmental Toxicology and Chemistry, 26(1), 92–99.

Wang, J., Wang, S. (2016). Removal of pharmaceuticals and personal care products (PPCPs) from wastewater: A review. Journal of Environmental Management, 182, 620–640.

Wang, M., Wang, H., Zhang, R., Ma, M., Mei, K., Fang, F., Wang, X. (2015). Photolysis of low-brominated diphenyl ethers and their reactive oxygen species-related reaction mechanisms in an aqueous system. PLoSOne 10, 1–14.

Wang, Y., Roddick, F.A., Fan, L. (2017). Direct and indirect photolysis of seven micropollutants in secondary effluent from a wastewater lagoon. Chemosphere, 185, 297–308.

Weller, A. (1961). Fast reaction of excited molecules. Progess Reaction Kinetics 1(187), 189-214.

Wu, X., Hawse, J.R., Subramaniam, M., Goetz, M.P., Ingle, J.N., Spelsberg, T.C. (2009). The tamoxifen metabolite, endoxifen, is a potent antiestrogen that targets estrogen receptor alpha for degradation in breast cancer cells. Cancer Research, 69(5), 1722–1727.

Wu, Y.-S., Huang, H.-C., Shen, J.-Y., Tseng, H.-W., Ho, J.-W., Chen, Y.-H., Chou, P.-T. (2015). Water-catalyzed excited-state proton-transfer reactions in 7-Azaindole and its analogues. Journal of Physical Chemistry B, 119, 2302–2309.

Yamamoto, H., Nakamura, Y., Moriguchi, S., Nakamura, Y., Honda, Y., Tamura, I., Hirata, Y., Hayashi, A., Sekizawa, J. (2009). Persistence and partitioning of eight selected pharmaceuticals in the aquatic environment: Laboratory photolysis, biodegradation, and sorption experiments. Water Research, 43, 351–362.

Yassine, M., Fuster, L., Dévier, M.H., Geneste, E., Pardon, P., Grélard, A., Dufourc, E., Al Iskandarani, M., Aït-Aïssa, S., Garric, J., Budzinski, H., Mazellier, P., Trivella, A.S. (2018). Photodegradation of novel oral anticoagulants under sunlight irradiation in aqueous matrices. Chemosphere, 193, 329–336.

Yazdanbakhsh, A., Eslami, A., Moussavi, G., Rafiee, M., Sheikhmohammadi, A. (2018). Photo-assisted degradation of 2, 4, 6-trichlorophenol by an advanced reduction process based on

sulfite anion radical: Degradation, dechlorination and mineralization. Chemosphere, 191, 156–165.

Zepp ', R.G., Cline, D.M. (1977). Rates of direct photolysis in aquatic environment. Environmental Science and Technology, 11, 359–366.

Zhang, C., Zhong, Q., Zhang, Q., Zheng, S., Miele, L., Wang, G. (2015). Boronic produg of endoxifen as an effective hormone theraphy for breast cancer. Breast Cancer Research and Treatment, 152(2), 283-291.

Zhang, Y., Zhang, J., Xiao, Y., Chang, V.W.C., Lim, T.-T. (2017). Direct and indirect photodegradation pathways of cytostatic drugs under UV germicidal irradiation: Process kinetics and influences of water matrix species and oxidant dosing. Journal of Hazardous Materials, 324, 481–488.

APPENDIX A. HPLC-DAD METHOD OPTIMIZATION AND VALIDATION

A.1. Chromatography parameters optimization

A.1.1. Absorbance wavelength selection

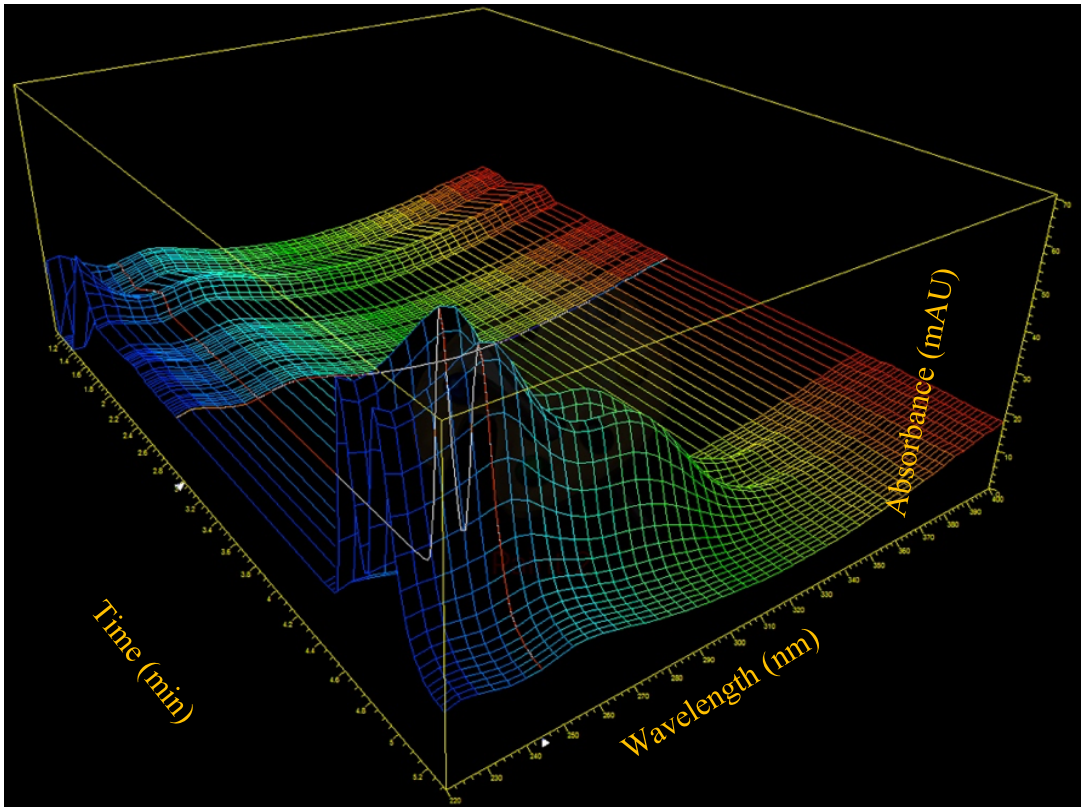

Figure A1. Absorbance 3D plot for (E)- and (Z)-endoxifen in the wavelength range of 190 to 390 nm. The maximum absorbance is indicated with a red line crossing the spectrum. (E)- and (Z)-endoxifen isomers showed a maximum isoabsorbance at 244 nm. Spectral coloring indicates an increase in the length of the wavelength starting with blue color for the shorter wavelengths (220 nm) and red color for the longer wavelengths (400 nm).

A.2. HPLC-DAD method validation

A.2.1. Selectivity

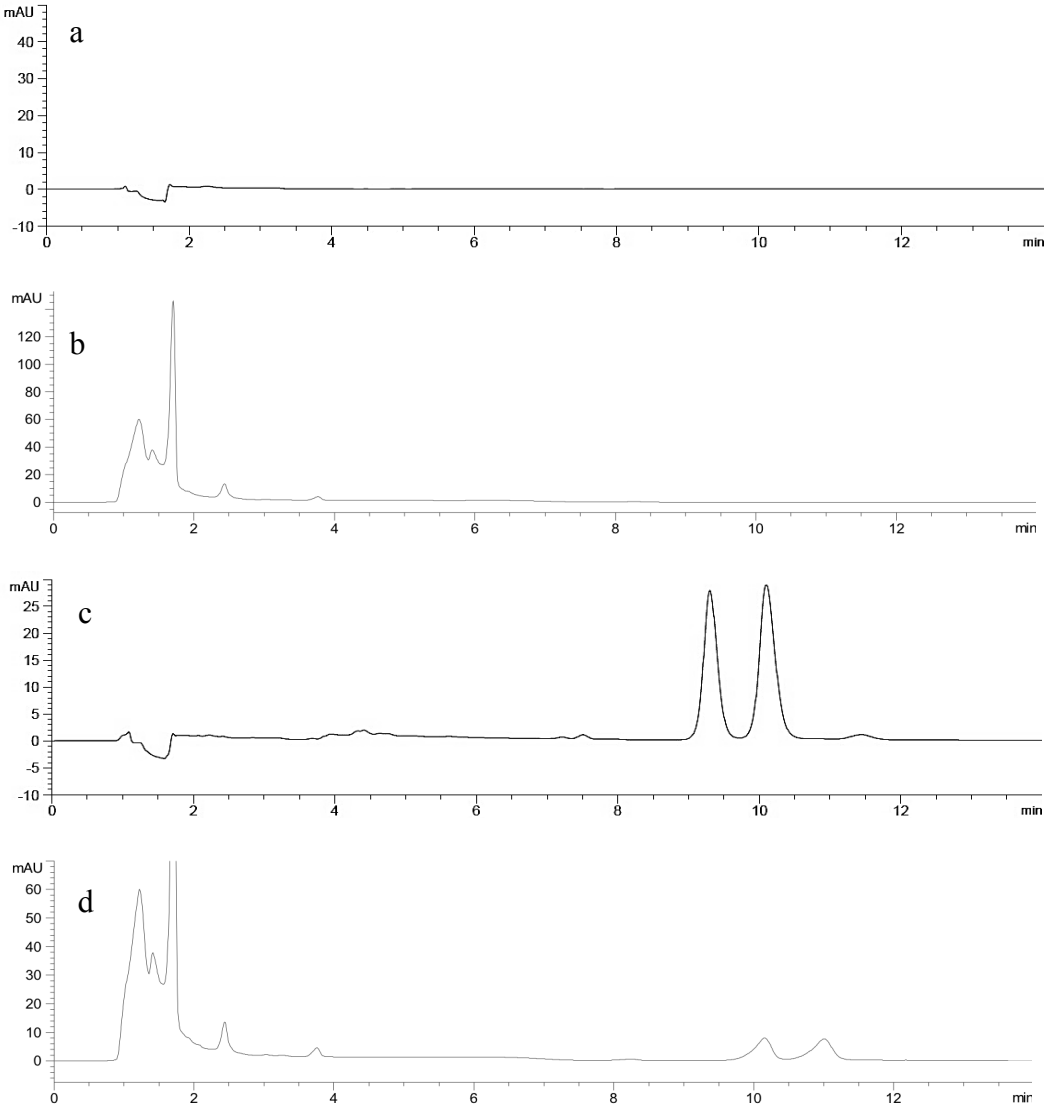

Figure A2. HPLC-DAD chromatograms obtained by the proposed method: (a) blank water sample, (b) blank wastewater; (c) water sample spiked with 1μg mL^{-1} of (E)-endoxifen and 1μg mL^{-1} of (Z)-endoxifen; (d) wastewater sample spiked with 1μg mL^{-1} of (E)-endoxifen and 1μg mL^{-1} of (Z)-endoxifen.

A.2.2. Isomer Identification

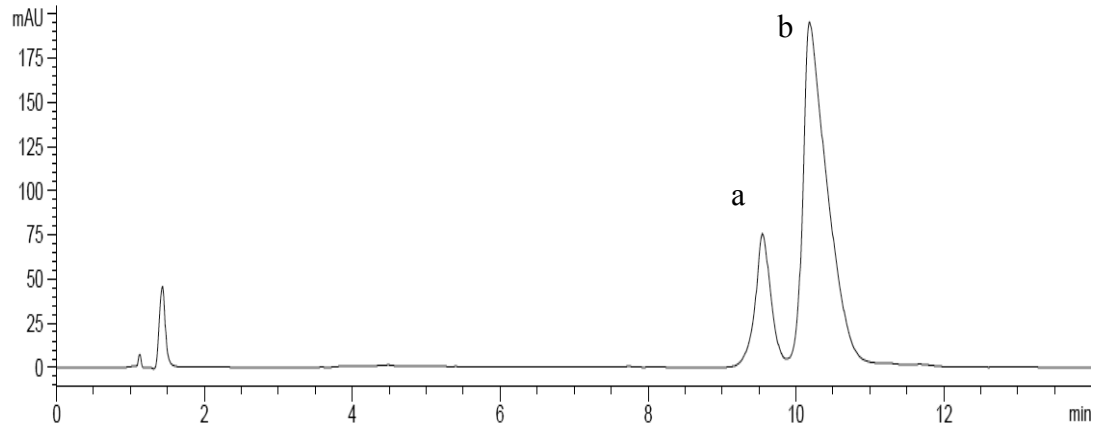

Figure A3. HPLC-DAD chromatogram monitored at 244 nm of (Z)-endoxifen isomer in aqueous solution (0.5 mg mL^{-1}): (1) (E)-endoxifen impurity with a chromatograph area percentage of 19.2% of the total chromatogram area and a retention time of 9.55 minutes, (2) (Z)-endoxifen with a chromatogram area percentage of 75.5 % of the total chromatogram area and a retention time of 10.12 minutes.

A.2.3. Linearity and Sensitivity

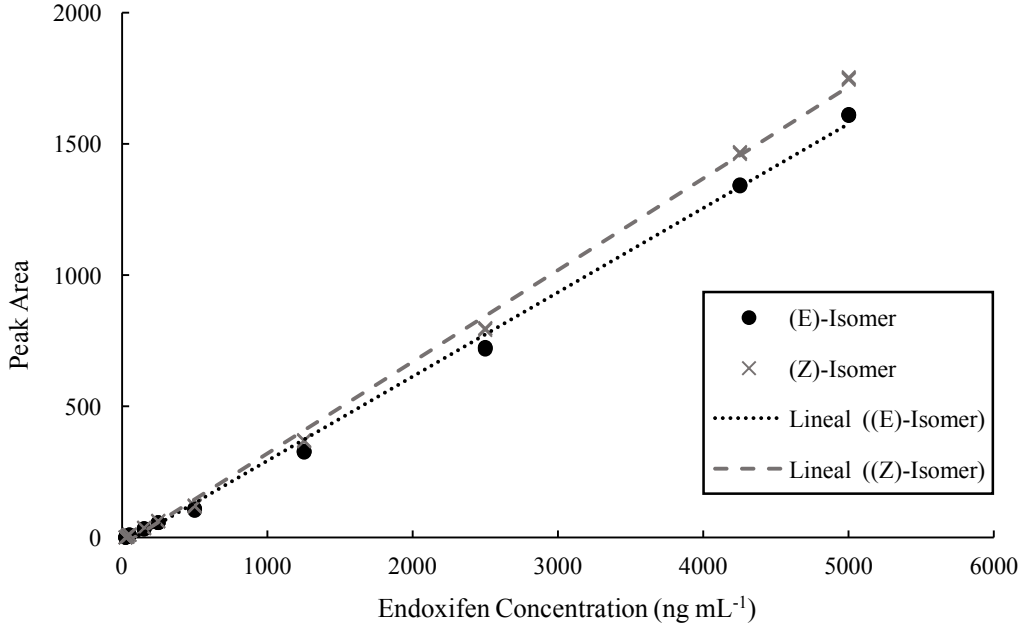

Figure A4. Linear calibration curve with the response peak areas as a function of (E)- and (Z)-endoxifen conentration.

Table A1. R^2, linear equation, LOD and LOQ of (E)- and (Z)-endoxifen by the proposed HPLC-DAD method.

Analyte	R^2	Linear Equation	LOD (ng mL^{-1})	LOQ (ng mL^{-1})
(E)-endoxifen	0.9975	y=0.3493x-27.931	12.66	38.35
(Z)-endoxifen	0.9981	y=0.3208x-28.440	12.12	36.74

A.2.4. Accuracy and Precision

Table A2. Method validation for accuracy and precision in intra-day assay; QCL: Quality control low (n=5); QCM: quality control medium (n=5); QCH: Quality control High (n=5).

Analyte	Standard Quality Control	Nominal Concentration (ng mL^{-1})	Theoretical Concentration (ng mL^{-1})	Accuracy (%)	Precision RSD (%)
(E)-endoxifen	QCL	100	95.5±1.32	4.5±1.32	1.38
	QCM	350	354.1±10.50	2.8±0.98	2.97
	QCH	700	685.1±14.76	2.6±1.62	2.15
(Z)-endoxifen	QCL	100	87.2±1.31	12.8±1.31	1.51
	QCM	350	367.1±11.15	4.9±3.19	3.04
	QCH	700	717.0±15.08	2.5±2.04	2.10

Table A3. Method validation for accuracy and precision in inter-day assay; QCL: Quality control low (n=5); QCM: quality control medium (n=5); QCH: Quality control High (n=5).

Analyte	Standard Quality Control	Nominal Concentration (ng mL^{-1})	Theoretical Concentration (ng mL^{-1})	Accuracy (%)	Precision RSD (%)
(E)-endoxifen	QCL	100	93.2±1.06	6.8±1.06	1.14
	QCM	350	349.1±11.06	1.7±4.17	4.60
	QCH	700	640.3±34.67	8.5±4.22	5.41
(Z)-endoxifen	QCL	100	84.8±0.80	15.2±0.80	0.95
	QCM	350	358.4±13.34	3.3±2.81	3.72
	QCH	700	666.2±45.93	5.8±5.52	6.90

A.3. 3D-Plot Fluorescence emission of (E)- and (Z)-endoxifen

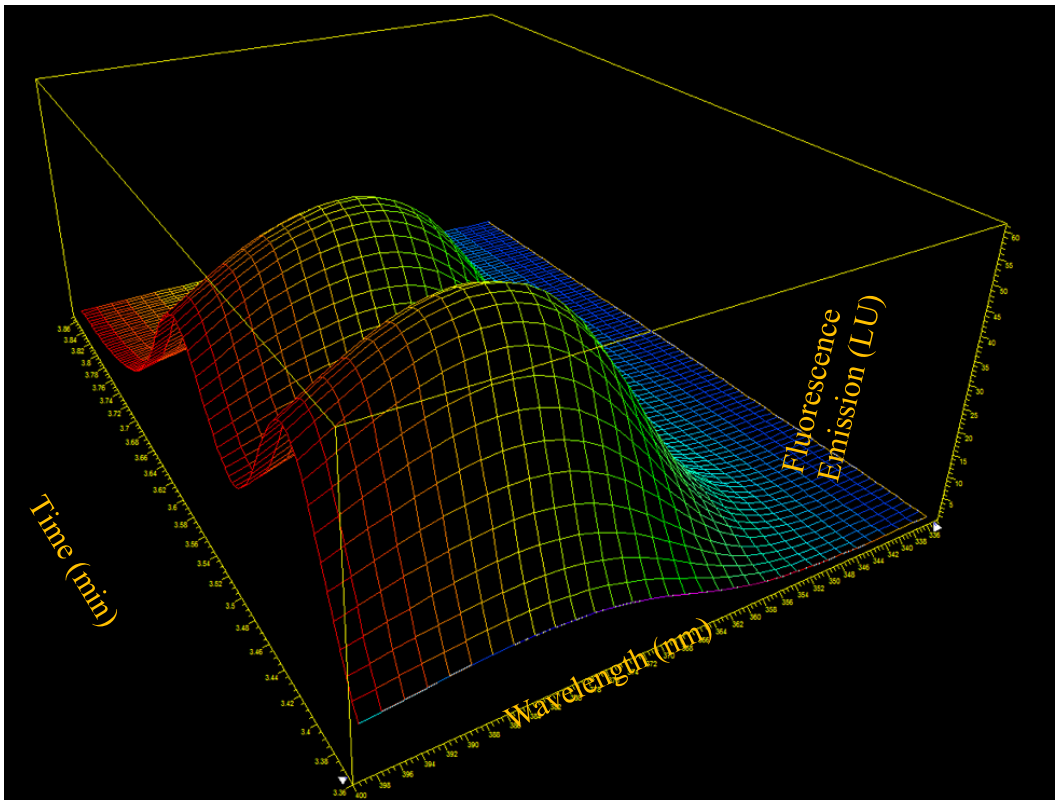

Figure A5. Fluorescence emission 3D plot for (E)- and (Z)-endoxifen in a wavelength range of 335 to 400 nm. (E)- and (Z)-endoxifen isomers showed a maximum fluorescence emission at 382 nm. Spectral coloring indicates a decrease in the length of the wavelength starting with red color for the longer wavelength (400 nm) and blue color for the shorter wavelength (335 nm).

APPENDIX B. PHOTODEGRADATION IN WATER WITH UV-LIGHT

B.1. Photodegradation kinetic of (E)- and (Z)-endoxifen in water

Table B1. R^2, linear equations (first order), and rate constants (k) (first order) of (E)- and (Z)-endoxifen based on a first order kinetic model for five emission light intensities.

Analyte	UV Light Intensity ($W\ s^{-1}\ cm^{-2}$)	Zero Order R^2	First Order R^2	Second Order R^2	Linear Equation (First Oder)	k ($\mu M\ s^{-1}$) (First Order)
(E)-endoxifen	28	0.918	0.996	0.968	y = -0.0177x - 0.056	17.7±1.0
	56	0.840	0.987	0.952	y = -0.0382x - 0.1364	38.2±1.7
	112	0.852	0.992	0.949	y = -0.0467x - 0.1287	46.7±2.5
	168	0.865	0.975	0.888	y = -0.0575x - 0.1114	57.5±3.7
	224	0.840	0.988	0.941	y = -0.0771x - 0.1153	77.1±5.4
(Z)-endoxifen	28	0.955	0.980	0.934	y = -0.0144x - 0.0454	14.5±1.0
	56	0.858	0.992	0.942	y = -0.0400x - 0.0943	40.0±2.8
	112	0.923	0.995	0.915	y = -0.0500x - 0.0039	50.0±2.9
	168	0.929	0.976	0.839	y = -0.0612x - 0.0083	61.2±4.9
	224	0.883	0.990	0.929	y = -0.0825x - 0.0295	82.5±5.6

B.2. Effects of UV light intensity, initial pH and initial concentration of (E)- and (Z)-endoxifen on photodegradation kinetics.

B.2.1. Effect of light intensity on photodegradation rate constant

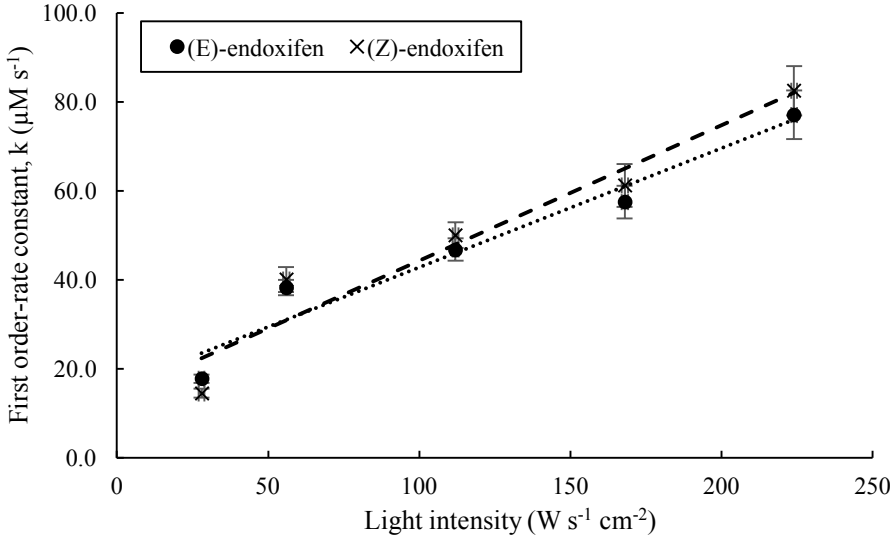

Figure B1. Effect of light intensity (W s-1 cm-2) on photodegradation rate constant (k) in aqueous solution spiked with (E)- and (Z)-endoxifen isomers (2 µg mL^{-1}, pH 7, and 22.4 °C)

B.2.2. Change of pH before and after UV irradiation in water

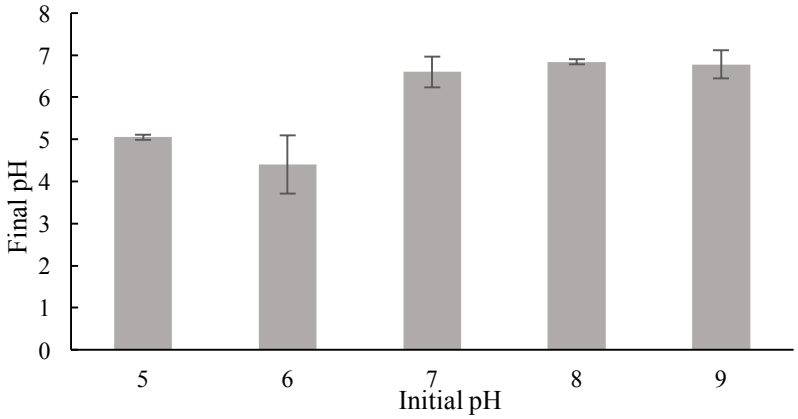

Figure B2. pH variations after photodegradation reaction on aqueous solution spiked with (E)- and (Z)-endoxifen isomers (2 µg mL-1) (22.4 °C) and irradiated with an emission light intensity of 28 W s^{-1} cm^{-2} for 80 seconds

B.2.3. Effect of initial (E)- and (Z)-endoxifen concentration on photodegradation rate constant

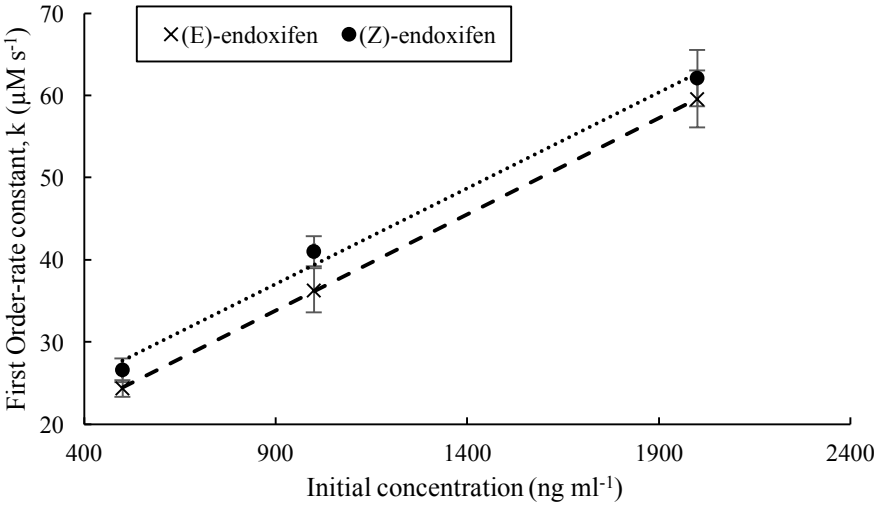

Figure B3. Effect of initial concentration of (E)- and (Z)-endoxifen (µg mL^{-1}) on photodegradation rate constant (k) in aqueous solution spiked with (E)- and (Z)-endoxifen isomers (pH 7, and 22.4°C) and irradiated with an emission light intensity of 244 W s^{-1} cm^{-2}.

APPENDIX C. MOLAR EXTINCTION COEFFICIENT AND QUANTUM YIELD

C.1. Molar extinction coefficient of (E/Z)-endoxifen at 253.7 nm

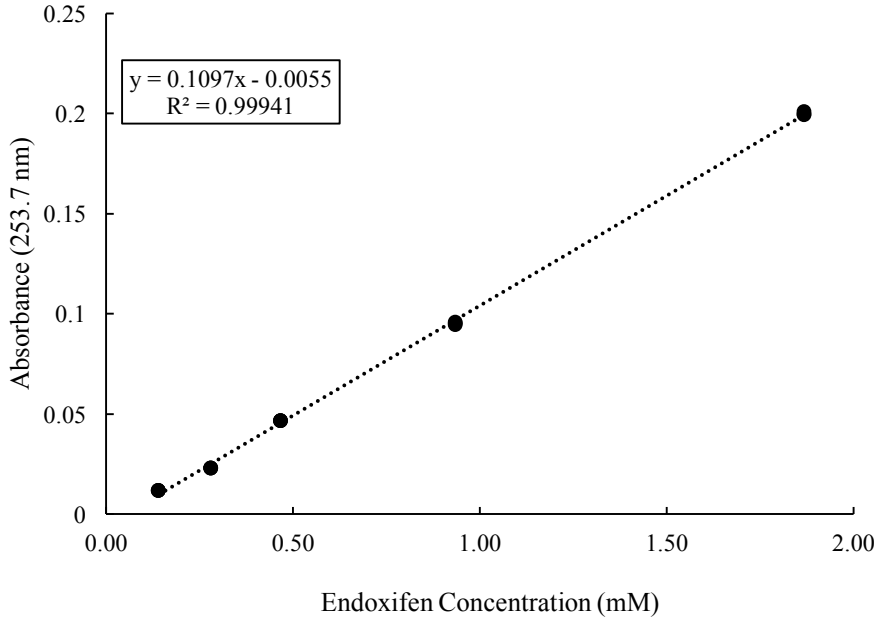

Figure C1. Absorbance of (E/Z)-endoxifen (1:1, w/w) at 253.7 nm at five concentrations ranging from 0.375 to 5 mg L^{-1}. The slope (0.1097 mM^{-1} cm^{-1}) indicates the molar extintion coefficient of (E/Z)-endoxifen. (R^2>0.999).

C.2. Absorption spectra (510 nm) of Iron (III) solution after UV irradiation

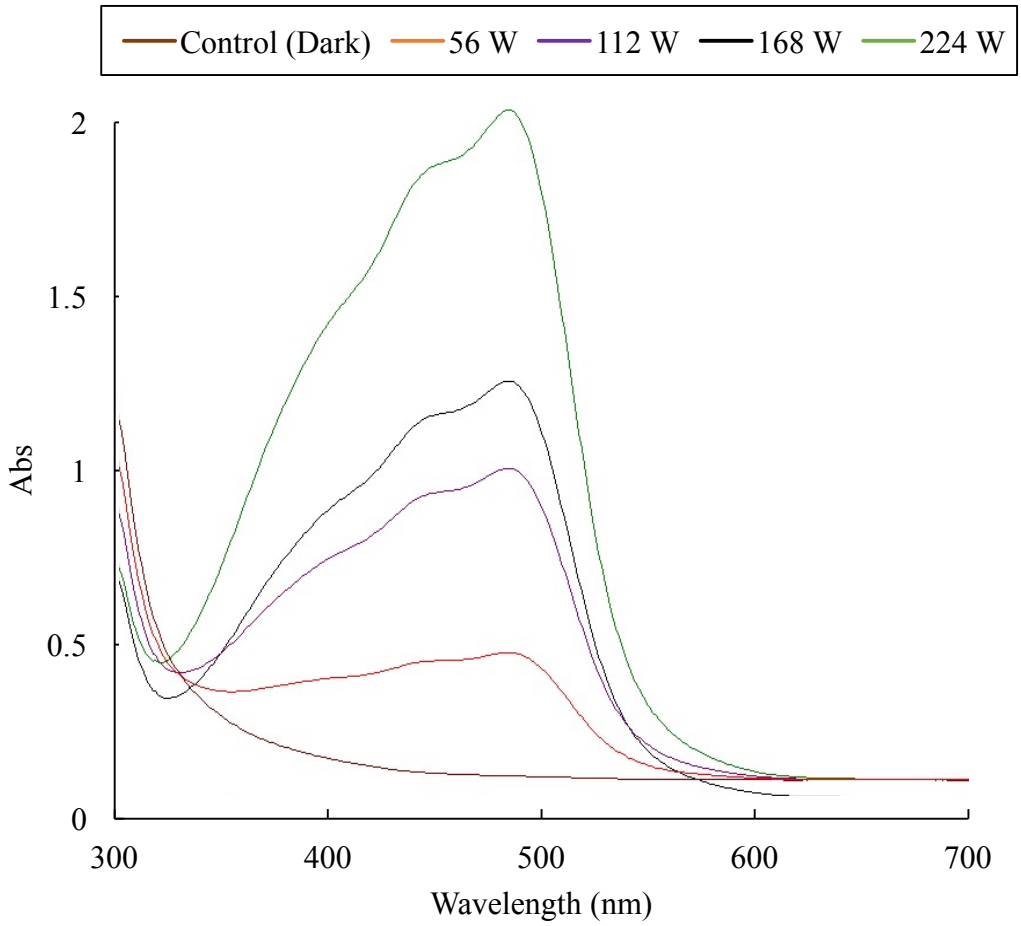

Figure C2. Absorbance spectrum (300-700 nm) of Iron(III) sulfate solution after 1 minute irradiation with UV light at four emission light intensities (56, 112, 168, and 224 W s^{-1} cm^{-2}).

APPENDIX D. DETECTION AND IDENTIFICATION OF UV LIGHT PBPs

D.1. HPLC-DAD chromatograms of (E)- and (Z)-endoxifen during UV irradiation

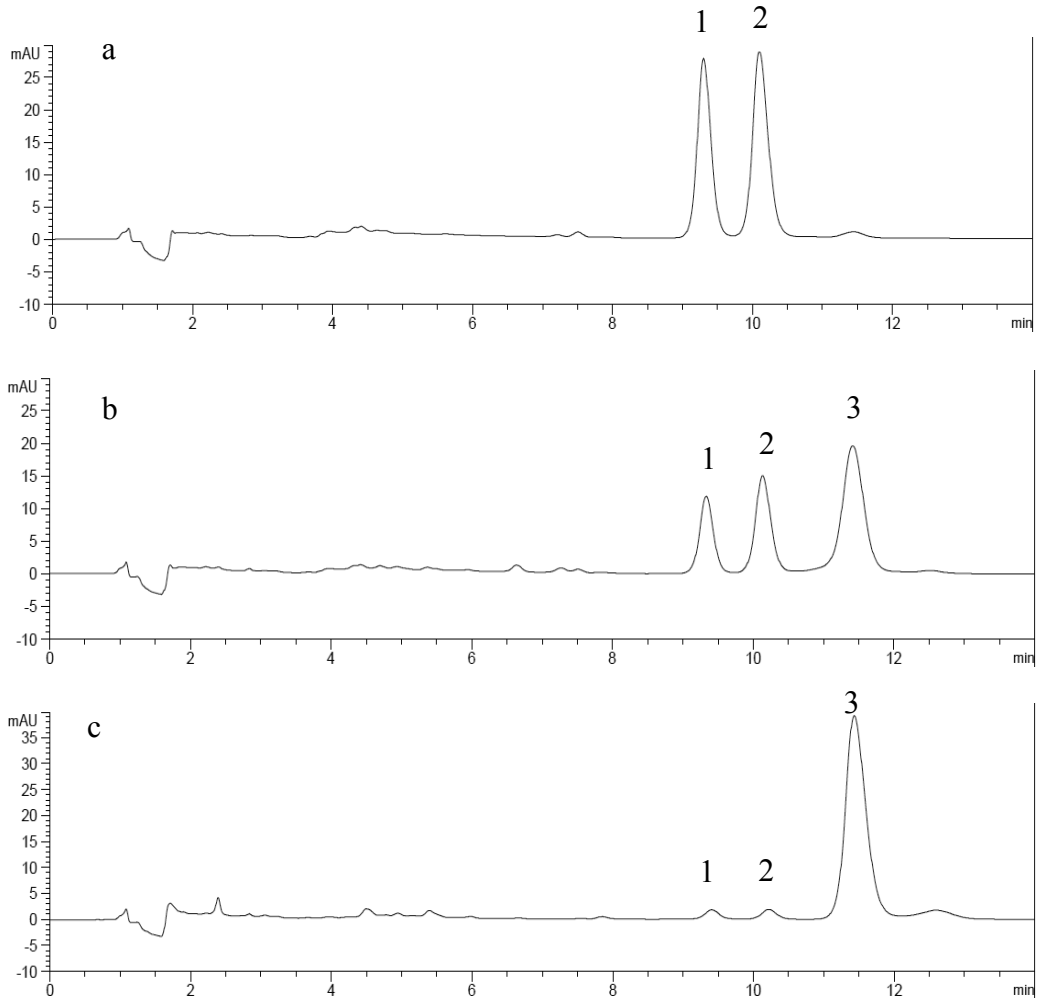

Figure D1. HPLC-DAD chromatogram of (E)-endoxifen (1; Rt = 9.55 minutes) and (Z)-endoxifen (2; Rt = 10.12 minutes) (2 μg mL^{-1}, pH 7, 22.4°C, and emission light intensity of 224 W s^{-1} cm^{-2}) and the detection of a photodegradation by-product (3; Rt = 11.43 minutes): (a) before photodegradation reaction; (b) after 5 seconds of photodegradation reaction; (c) after 30 seconds of photodegradation reaction.

D.2. (E)- and (Z)-endoxifen detection by UHPLC-MS/MS

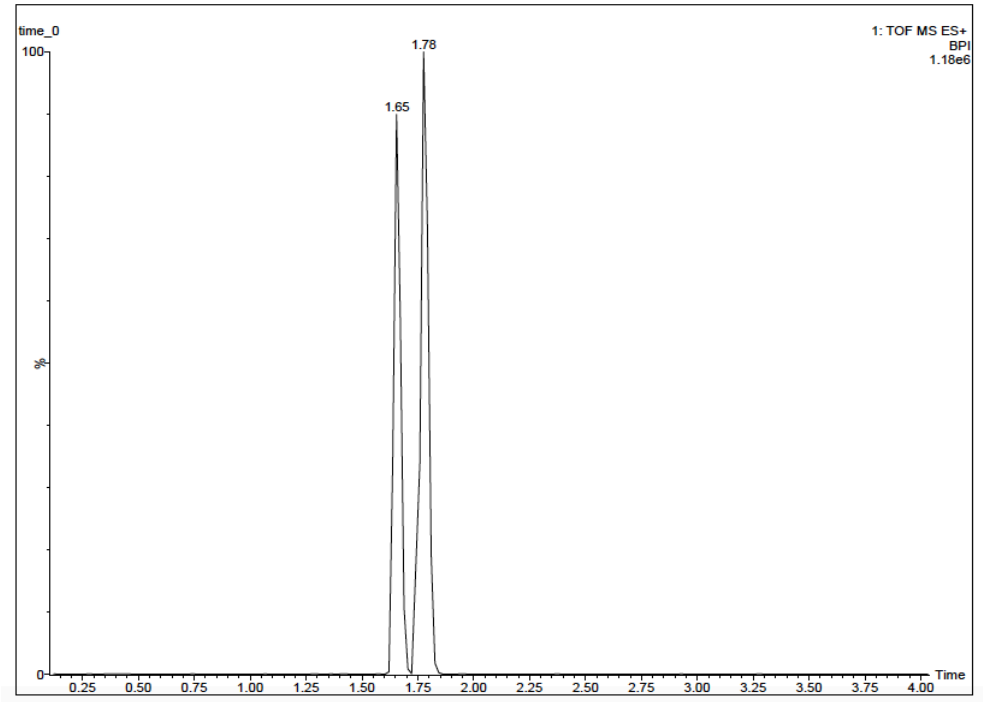

Figure D2. Chromatograph of (E)-endoxifen (Rt = 1.65 minutes) and (Z)-endoxifen (Rt = 1.78 minutes) in aqueous solution at 1 μg mL^{-1} prior to photodegradation reaction.

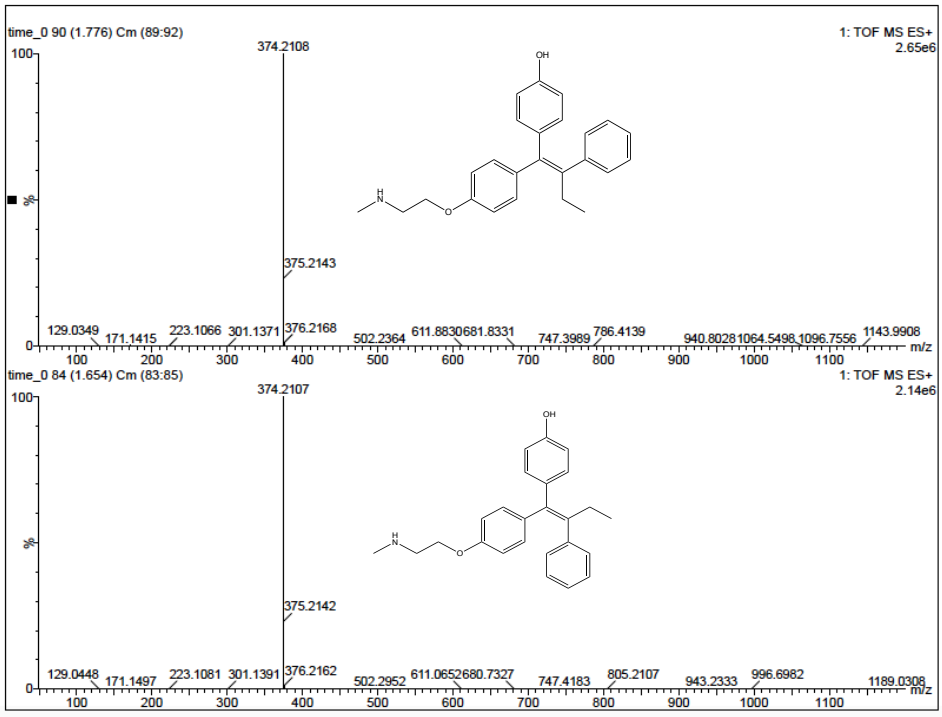

Figure D3. Mass spectrometry of (E)- and (Z)-endoxifen isomers: (a) ion-m/z (374.2108) of (Z)-endoxifen isomer with a retention time of 1.78 minutes; (b) ion-m/z (374.2107) of (E)-endoxifen isomer with a retention time of 1.65 minutes.

D.3. PBPs detection by UPLC-MS/MS

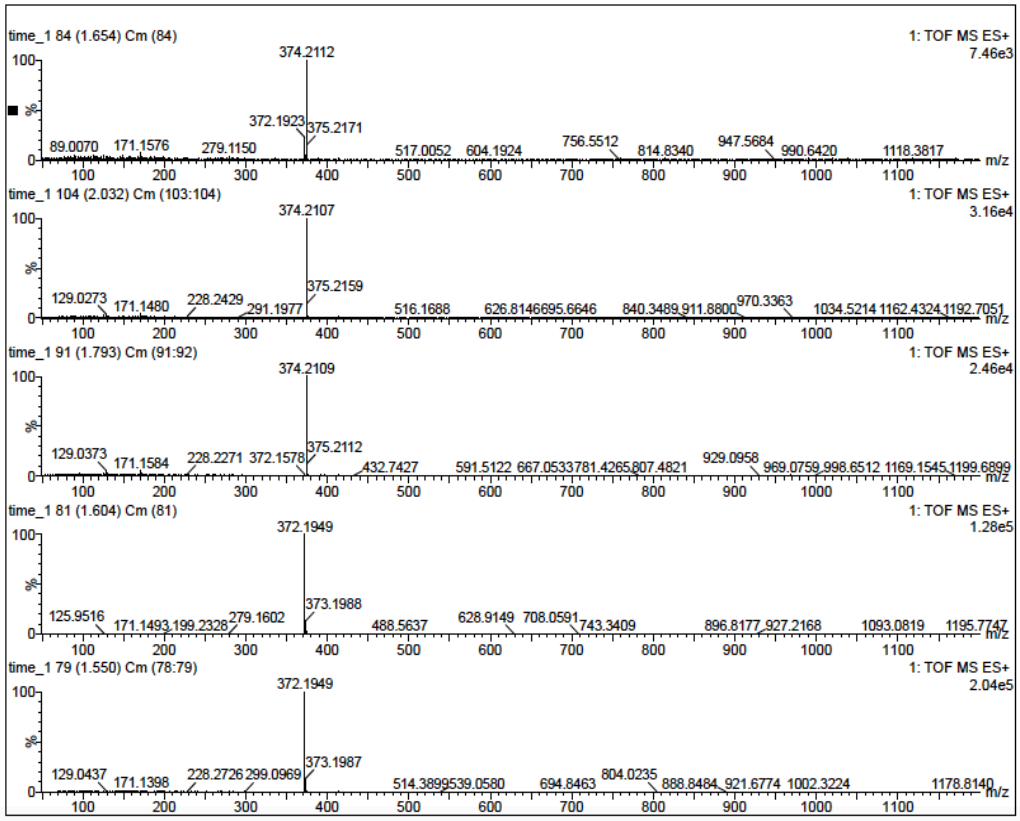

Figure D4. Mass spectrometry of the five peaks observed at chromatogram after 35 seconds of UV light irradiation: (a) ion-*m/z* of (E)-endoxifen isomer with retention time of 1.65 minutes; (b) ion-*m/z* of PB2 with retention time of 2.03 minutes; (c) ion-*m/z* of (Z)-endoxifen isomer with retention time of 1.79 minutes; (d) ion-*m/z* of PB1b with retention time of 1.60 minutes; and (e) ion-*m/z* of Pb1a with retention time of 1.55 minutes.

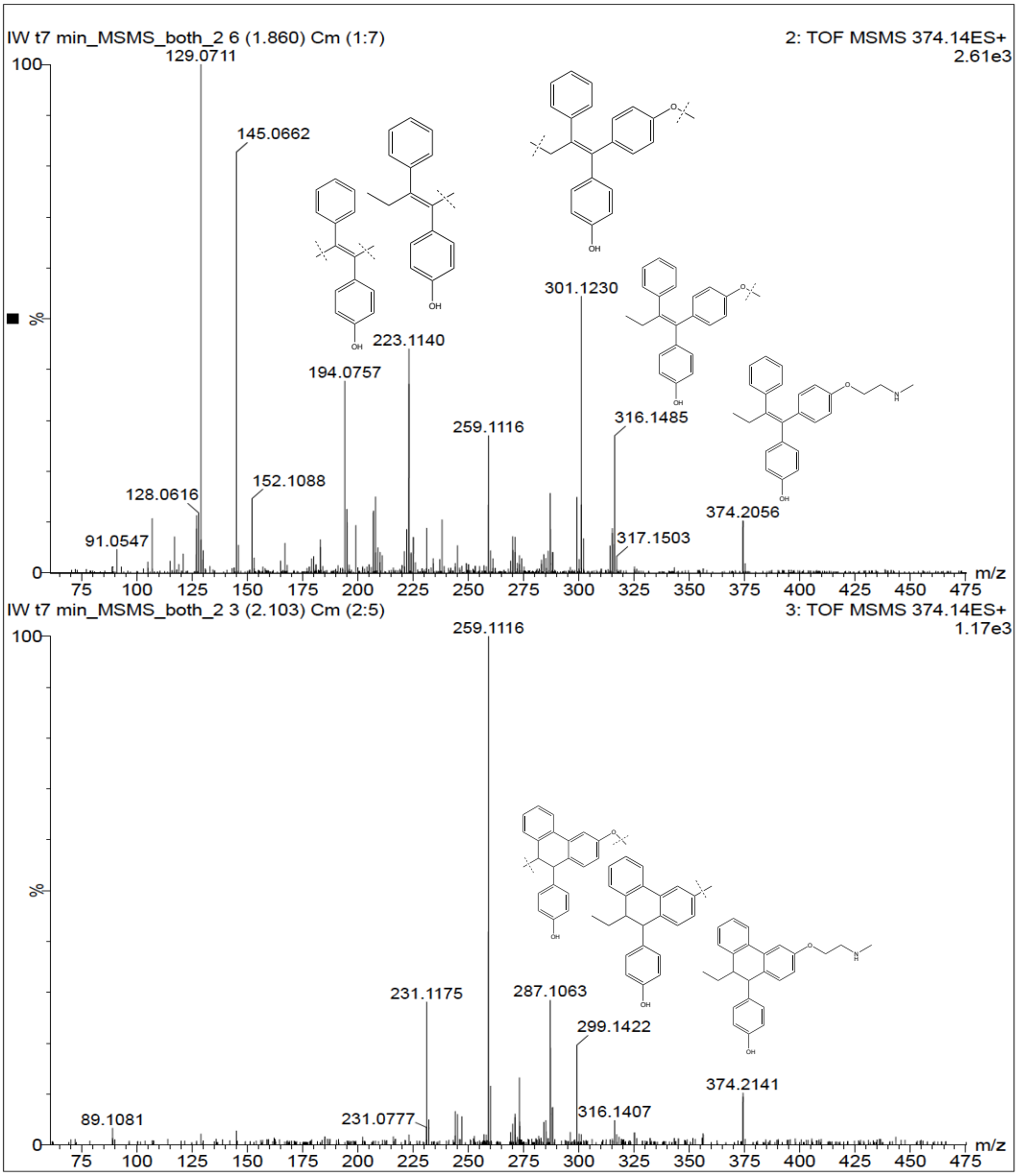

Figure D5. MS/MS analyses of ion-m/z = 374.21 with the proposed molecular fragments: (a) fragmentation formed products ions of (E/Z)-endoxifen; (b) fragmentation formed products ions of PB2.

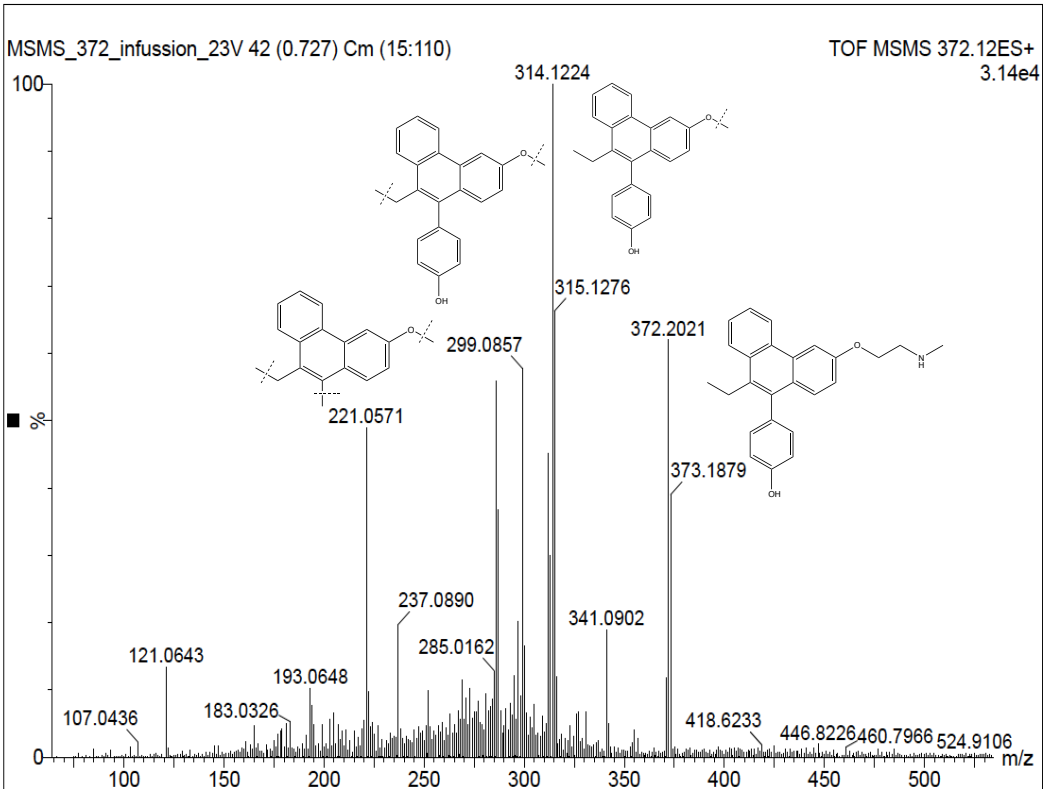

Figure D6. MS/MS analyses of ion-m/z = 372.19 with the proposed molecular fragments for the fragmentation formed products ions of PB1(a, b)

D.4. Photodegradation in wastewater by UV light

D.4.1. Correlation coefficients for zero, first and second order models

Table D1. Correlation coefficients for zero, first, and second order fits on (E)-and (Z)-endoxifen photodegradation with UV light in wastewater

Analyte	R^2		
	Zero Order	First Order	Second Order
(E)-endoxifen	0.854	0.972	0.996
(Z)-endoxifen	0.845	0.970	0.991

D.4.2. Mass spectrometry of (E)- and (Z)-endoxifen in wastewater by UPLC-MS/MS

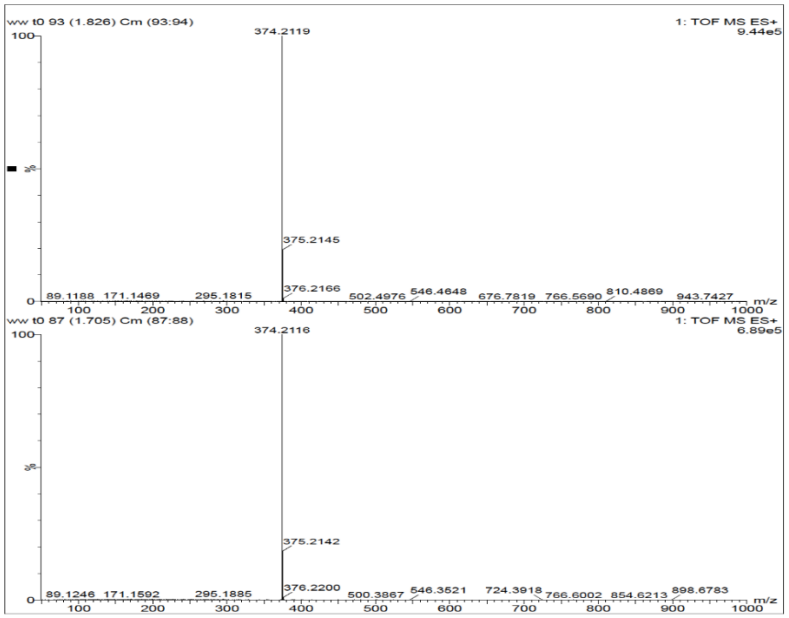

Figure D7. MS of the wastewater sample spiked with (E)- and (Z)-endoxifen (1µg mL^{-1}) before irradiation with UV light (emission light intensity = 56 W s^{-1} cm^{-2}): (a) (Z)-endoxifen (Rt = 1.83 minutes, ion-m/z = 374.2119); (b) (E)-endoxifen (Rt = 1.71 minutes, ion--m/z = 374.2116)

D.4.3. Second-order fits for photodegradation of (E)- and (Z)-endoxifen in wastewater

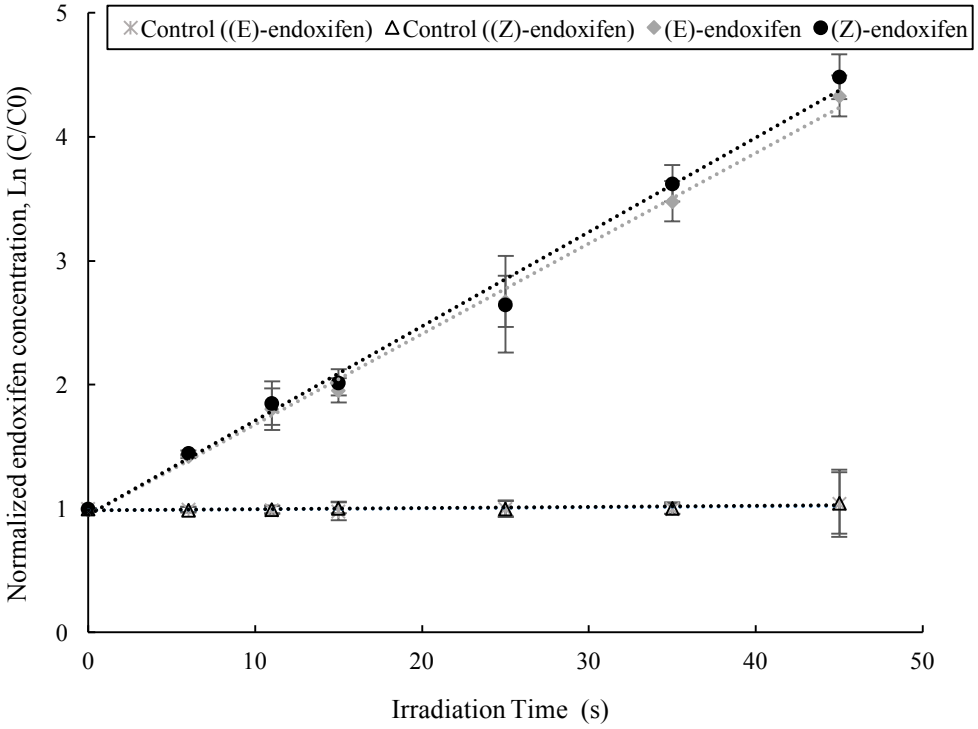

Figure D8. Second order fits for (E)- and (Z)-endoxifen photodegradation in wastewater at 1 μg mL^{-1} (emission light intensity = 224 W s^{-1} cm^{-2}). Control samples ran in dark condition.

D.4.4. Tandem mass spectrometry of PB1 (a, b) in wastewater by UPLC-MS/MS

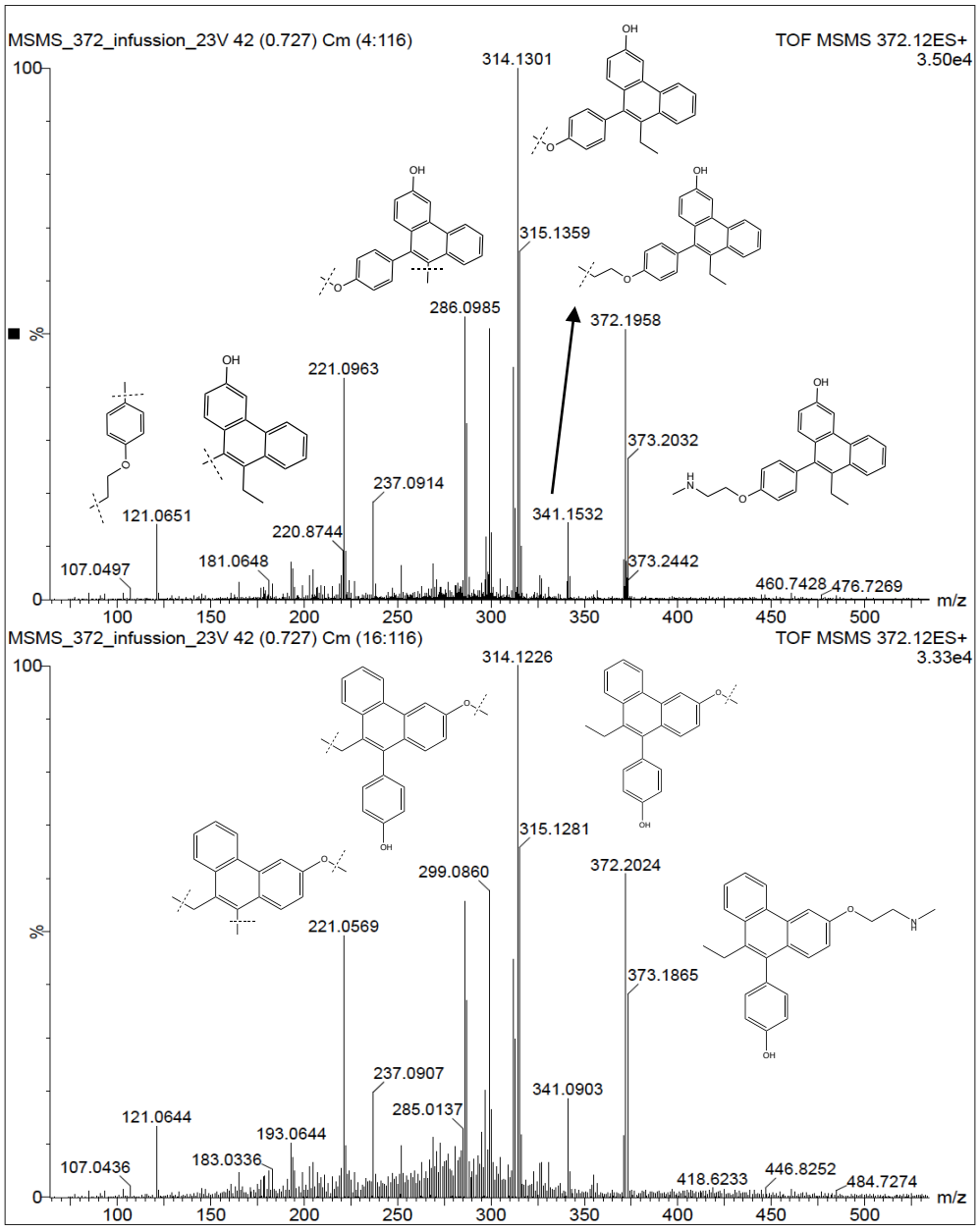

Figure D9. MS/MS analyses at ion-m/z = 372.19 with the proposed molecular fragments for wastewater sample after 45 seconds of irradiation with UV light (emission light intensity = 56 W s^{-1} cm^{-2}): (a) fragmentation formed products ions of PB1a; (b) fragmentation f formed products ions of PB1a; (b) fragmentation formed products ions of PB1

APPENDIX E. PHOTODEGRADATION WITH NATURAL SUNLIGHT

E.1. Determination coefficients for zero, first and second order models in water

Table E1. R^2 for zero, first and second order fits, linear equation (zero order), and rate constants (k) (zero order) on (E)- and (Z)-endoxifen photodegradation with natural sunlight.

Analyte	Zero Order R^2	First Order R^2	Second Order R^2	Linear Equation (Zero Order)	k (µM min-1) (Zero Order)
(E)-endoxifen	0.970	0.917	0.805	y=-0.0052x+0.946	5.0±0.1
(Z)-endoxifen	0.965	0.908	0.765	y=-0.005x+0.9296	5.2±0.1

E.2. Determination coefficients for zero, first and second order models in wastewater and receiving surface water

Table E2. R^2 of (E)- and (Z)-endoxifen based on a zero, first and second order kinetic modeling wastewater and receiving surface water samples.

Solution	Analyte	R^2		
		Zero Order	First Order	Second Order
Wastewater	(E)-endoxifen	0.886	0.966	0.955
	(Z)-endoxifen	0.870	0.972	0.909
Receiving surface water	(E)-endoxifen	0.874	0.837	0.775
	(Z)-endoxifen	0.851	0.816	0.754

E.3. Tandem mass spectrometry of (E)- and (Z)-endoxifen PBPs in water by UPLC-MS/MS

Table E3. MS/MS analyses of (E)-and (Z)-endoxifen PBPs generated through natural sunlight photodegradation with the proposed molecular fragments for the fragmentation formed products ions.

Compound	Measured mass ion-*m/z*	Molecular formular	Theoretical ion-*m/z*	Precursor ion/product ion	|ppm|
PB1a	372.1945	$C_{25}H_{26}NO_2$	372.1964	$[M+H]^+$	1.9
	341.1535	$C_{24}H_{21}O_2$	341.1542	$[M+H\text{-}CH_5N]^+$	0.7
	314.1268	$C_{22}H_{18}O_2$	314.1307	$[M+H\text{-}C_3H_8N]^+$	3.9
	299.1052	$C_{21}H_{15}O_2$	299.1072	$[M+H\text{-}C_4H_{11}N]^+$	2.0
	286.0966	$C_{20}H_{14}O_2$	286.0994	$[M+H_2\text{-}C_5H_{12}N]^+$	2.8
	220.0852	$C_{16}H_{12}O$	220.0888	$[M+H\text{-}C_9H_{14}NO]^+$	3.0
	194.0675	$C_{14}H_{10}O$	194.0732	$[M+H_3\text{-}C_{11}H_{16}NO]^+$	5.7
PB1b	372.1945	$C_{25}H_{26}NO_2$	372.1964	$[M+H]^+$	1.9
	342.1555	$C_{23}H_{20}NO_2$	342.1494	$[M+H\text{-}C_2H_6]^+$	6.1
	315.1352	$C_{22}H_{19}O_2$	315.1385	$[M+H_2\text{-}C_3H_7N]^+$	3.3
	312.1132	$C_{22}H_{16}O_2$	312.1150	$[M+H\text{-}C_3H_{10}N]^+$	1.8
	299.1052	$C_{21}H_{15}O_2$	299.1072	$[M+H\text{-}C_4H_{11}N]^+$	2.0
	286.0966	$C_{20}H_{14}O_2$	286.0994	$[M+H_2\text{-}C_5H_{12}N]^+$	2.8
	220.0852	$C_{16}H_{12}O$	220.0888	$[M+H\text{-}C_9H_{14}NO]^+$	3.6
	194.0675	$C_{14}H_{10}O$	194.0732	$[M+H_3\text{-}C_{11}H_{16}NO]^+$	5.7
PB2a	374.2099	$C_{25}H_{28}NO_2$	374.2120	$[M+H]^+$	2.1
	356.2088	$C_{25}H_{26}NO_2$	342.1494	$[M+H\text{-}H_2O]^+$	0.6
	299.1399	$C_{21}H_{19}O$	299.1436	$[M+H\text{-}C_3H_9NO]^+$	3.7
	287.1050	$C_{20}H_{15}O_2$	287.1072	$[M+H\text{-}C_5H_{13}N]^+$	2.2
	273.1257	$C_{20}H_{17}O$	273.1279	$[M+H_3\text{-}C_5H_{11}NO]^+$	2.2
PB2b	374.2096	$C_{25}H_{28}NO_2$	374.2120	$[M+H]^+$	2.4
	356.1985	$C_{25}H_{26}NO_2$	342.1494	$[M+H\text{-}H_2O]^+$	2.9
	299.1414	$C_{21}H_{19}O$	299.1436	$[M+H\text{-}C_3H_9NO]^+$	2.2
	287.1047	$C_{20}H_{15}O_2$	287.1072	$[M+H\text{-}C_5H_{13}N]^+$	2.5
	273.1263	$C_{20}H_{17}O$	273.1279	$[M+H_3\text{-}C_5H_{11}NO]^+$	1.6
PB3a	404.1823	$C_{25}H_{26}NO_4$	404.1862	$[M+H]^+$	3.9
	345.1110	$C_{22}H_{17}O_4$	345.1127	$[M+H\text{-}C_3H_9N]^+$	1.7
	235.0720	$C_{16}H_{11}O_2$	235.0759	$[M+H\text{-}C_9H_{15}NO_2]^+$	3.9
	121.0190	$C_6H_3NO_2$	121.0164	$[M+H\text{-}C_{19}H_{22}O_2]^+$	2.6
PB3b	404.1822	$C_{25}H_{26}NO_4$	404.1862	$[M+H]^+$	4.0
	345.1111	$C_{22}H_{17}O_4$	345.1127	$[M+H\text{-}C_3H_9N]^+$	1.6
	235.0722	$C_{16}H_{11}O_2$	235.0759	$[M+H\text{-}C_9H_{15}NO_2]^+$	3.7
	152.0996	$C_9H_{14}NO$	152.0996	$[M+H\text{-}C_{16}H_{12}O_3]^+$	7.9
PB4a	359.1515	$C_{23}H_{21}NO_3$	359.1521	$[M+H\text{-}C_2H_5]^+$	0.6
	302.0940	$C_{20}H_{14}O_3$	302.0943	$[M+H_2\text{-}C_5H_{12}N]^+$	0.3
	237.0877	$C_{16}H_{13}O_2$	237.0916	$[M+H\text{-}C_9H_{13}NO]^+$	3.9
	209.0920	$C_{15}H_{13}O$	209.0966	$[M+H\text{-}C_{15}H_{13}O]^+$	4.6

Table E3. MS/MS analyses of (E)-and (Z)-endoxifen PBPs generated through natural sunlight photodegradation with the proposed molecular fragments for the fragmentation formed products ions (continued).

Compound	Measured mass ion-*m/z*	Molecular formular	Theoretical ion-*m/z*	Precursor ion/product ion	|ppm|
PB4b	388.1920	$C_{25}H_{26}NO_3$	388.1913	$[M+H]^+$	0.7
	359.1521	$C_{23}H_{21}NO_3$	359.1521	$[M+H-C_2H_5]^+$	0.0
	302.0929	$C_{20}H_{14}O_3$	302.0943	$[M+H_2-C_5H_{12}N]^+$	1.4
	237.0876	$C_{16}H_{13}O_2$	237.0916	$[M+H-C_9H_{13}NO]^+$	4.0
	209.0920	$C_{15}H_{13}O$	209.0966	$[M+H-C_{15}H_{13}O]^+$	4.6
PB5a	374.1769	$C_{24}H_{24}NO_3$	374.1756	$[M+H]^+$	1.3
	357.1456	$C_{23}H_{19}NO_3$	357.1456	$[M+H-CH_5]^+$	9.1
	301.1197	$C_{21}H_7O_2$	301.1229	$[M+H_2-C_3H_7NO]^+$	3.2
	245.0818	$C_{17}H_{11}NO$	245.0841	$[M+H-C_7H_{13}O_2]^+$	2.3
PB5b	374.1774	$C_{24}H_{24}NO_3$	374.1756	$[M+H]^+$	1.8
	343.1352	$C_{23}H_{19}O_3$	343.1334	$[M+H-CH_5N]^+$	1.8
	301.1233	$C_{21}H_7O_2$	301.1229	$[M+H_2-C_3H_7NO]^+$	0.4
	299.1047	$C_{21}H_{15}O_2$	299.1072	$[M+H-C_3H_9NO]^+$	2.5
PB6a	360.1929	$C_{24}H_{26}NO_2$	360.1964	$[M+H]^+$	3.5
	329.1518	$C_{23}H_{21}O_2$	329.1542	$[M+H-CH_5N]^+$	2.4
	314.1293	$C_{22}H_{18}O_2$	314.1307	$[M+H-C_2H_8N]^+$	1.4
	299.1069	$C_{21}H_{15}O_2$	299.1072	$[M+H-C_3H_{11}N]^+$	0.3
	287.1039	$C_{20}H_{15}O_2$	287.1072	$[M+H-C_4H_{11}N]^+$	3.3
PB6b	360.1948	$C_{24}H_{26}NO_2$	360.1964	$[M+H]^+$	1.6
	329.1518	$C_{23}H_{21}O_2$	329.1542	$[M+H-CH_5N]^+$	2.4
	314.1294	$C_{22}H_{18}O_2$	314.1307	$[M+H-C_2H_8N]^+$	1.4
	299.1072	$C_{21}H_{15}O_2$	299.1072	$[M+H-C_3H_{11}N]^+$	0.0
	287.1047	$C_{20}H_{15}O_2$	287.1072	$[M+H-C_4H_{11}N]^+$	3.1
PB7(a,b)	378.1705	$C_{23}H_{21}NO_4$	378.1705	$[M+H]^+$	2.4
	312.1126	$C_{22}H_{16}O_2$	312.1150	$[M+H-CH_4NO_2]^+$	2.4
	297.1277	$C_{22}H_{17}O$	297.1279	$[M+H-CH_3NO_3]^+$	0.2
	272.1169	$C_{20}H_{16}O$	272.1201	$[M+H_2-C_3H_5NO_3]^+$	3.2
PB8	178.0749	$C_{24}H_{10}$	178.0783	$[M+H-H_3O]^+$	3.4
	168.0575	$C_{12}H_8O$	168.0575	$[M+H-C_2H_5]^+$	1.1
	152.0627	$C_{12}H_8$	152.0626	$[M+H-C_2H_5O]^+$	0.1
	107.0465	C_7H_7O	107.0497	$[M+H-C_7H_6]^+$	3.2